Use of GENOPT and BIGBOSOR4 to obtain optimum designs of an axially compressed cylindrical shell with a composite truss-core sandwich wall

David Bushnell[1]
775 Northampton Drive, Palo Alto, CA 94303

Charles Rankin[2]
Rhombus Consultants Group, Inc.
Suite B100, 1121 San Antonio Rd., Palo Alto, CA 94303

GENOPT/BIGBOSOR4 is applied to the problem of an axially compressed perfect elastic cylindrical shell the wall of which is a composite truss-core sandwich. The truss-core sandwich is constructed of trapezoidal core tubes that are sandwiched between two face sheets. At the junction of the core webs and the face sheets are "noodle" regions that are filled with unidirectional composite material. The design constraints are local buckling, general buckling, and five stress constraints for each material. Local and general buckling are computed from BIGBOSOR4 models in which the "huge torus" prismatic representation of the cylindrical shell is employed. In both the local and general buckling models the "huge torus" representation of the cylindrical shell consists of a number of identical modules of the cross section of the truss-core sandwich wall that are strung together along the curved meridian of the "huge torus". The rather elaborate 22-segment module used for local buckling includes small curved and straight segments that occur at the corners of the trapezoidal tool around which the truss-core is wrapped during the fabrication process. The presence of "noodles" that fill the prismatic triangular-like gaps between adjacent trapezoids is accounted for. BIGBOSOR4 models are included that determine approximately the effect on local buckling of support by each noodle of the little shell segments that enclose it. The six-segment module used in the general buckling is much simpler than the 22-segment module used for local buckling. It consists of six shell segments analogous to those used in the truss-core sandwich model employed in PANDA2. The effect of the "noodles" is accounted for, however, which is not possible in the PANDA2 model. Also, the GENOPT/

BIGBOSOR4 general buckling model retains both face sheets and truss-core webs as flexible shell segments. Therefore, the general buckling model exhibits the correct global transverse shear deformation (t.s.d.) characteristics, whereas in PANDA2 the effect of t.s.d. is simulated approximately by a knockdown factor. The number of modules used in the model for general buckling is determined by the largest circumferential arc that subtends the maximum number of shell segments permitted by BIGBOSOR4: 295 segments. Stress constraints are computed in a way completely analogous to that used in PANDA2 for composite laminates, but calculations are simpler because the pre-buckled state of the "huge torus" is a uniform membrane state whereas local bending due to initial imperfections is permitted in the PANDA2 model. The effect of thermal curing is included in the model. The decision variables for optimization are the width of a single module, the width of the crown of one trapezoid, the height of the trapezoid, two distinct corner radii of the trapezoidal core tube, and lamina thicknesses. Optimum designs are obtained via SUPEROPT. The objective is the weight per unit area of the cylindrical shell. Predictions from GENOPT/ BIGBOSOR4 are compared with those from PANDA2. Local and general finite element models for processing by STAGS are automatically produced by GENOPT/BIGBOSOR4 for the truss-core sandwich configurations previously optimized by GENOPT/BIGBOSOR4.

SECTION 1 INTRODUCTION AND SUMMARY

Motivation and Previous work done

The effort that resulted in this paper was motivated by work currently being performed at the NASA Langley Reaearch Center (LaRC) on the buckling behavior of cylindrical shells with a truss-core sandwich wall fabricated from laminated composite material [1, 21]. A capability to analyze and efficiently to optimize such a shell has been needed. This paper reports results from a continuation of the work documented in [2] and [3]. Reference [2], derived from a case called "**nasatruss2**", reports results from the use of PANDA2 [4, 13] and BIGBOSOR4 [5]. Reference [3], derived from a generic case called "**trusscomp**" and a specific case called "**test**", reports results from the use of GENOPT [6] and BIGBOSOR4 [5]. A brief overview of the GENOPT program [6] is given here. Extensive details about how to use GENOPT in connection with BIGBOSOR4 are presented in [7] and [8] and will not be repeated here. The GENOPT/BIGBOSOR4 capability has been used to optimize axially compressed cylindrical shells with a number of axially oriented Tee-stiffened weld lands [8] and a ring-stiffened cylindrical shell with a "wavy" wall [5].

The work reported in [3] and [8] is based on "huge torus" models [9] of cylindrical shells. Figure 1a, created by Robert P. Thornburgh [8], demonstrates the concept of the "huge torus" model. The results from GENOPT/BIGBOSOR4 reported in this paper are based on a version of BIGBOSOR4 in which cylindrical shells are modeled as true prismatic assemblages of shell segments [8,10]. Descriptions of the "huge torus" model and of the "true prismatic shell" model are given in [8]. A brief summary is provided in this paper.

American Institute of Aeronautics and Astronautics

Both the PANDA2 [4, 13] and the GENOPT [6] computer programs perform optimization with the use of a gradient-based optimizer called "ADS", created many years ago by Vanderplaats and his colleagues [11,12]. In [2 - 8] ADS is "hard wired" in a "modified-method-of-steepest-descent" (1-5-7) mode. In PANDA2 and GENOPT a matrix of behavior constraint gradients is computed from finite differences of the behavior constraints for the perturbed design minus the behavior constraints for the current design in which the decision variables are perturbed one at a time by a certain percentage, usually five per cent. By "behavior" is meant buckling, stress, displacement, vibration frequency, clearance, and any other phenomena that may affect the evolution of a design during optimization cycles.

Purposes of this paper and some geometry

This paper is analogous to [8]. The main purpose of the work reported here is to produce a "quick and dirty" way of optimizing uniformly axially compressed cylindrical shells with a composite truss-core sandwich wall in which the truss-core webs run in the axial direction. An auxiliary purpose of this paper is to provide enough detail so that the reader, with the use of [3], [6], [7] and [8], can employ GENOPT/BIGBOSOR4 [6,5] to optimize other shell structures and can subsequently use STAGS [15-18] or some other general-purpose finite element computer program to evaluate those optimized designs. The name given to the generic case is "**trusscomp**". The specific cases discussed in this paper are called "**nasatruss2**" and "**nasatruss3**". Additional information on these specific cases and on two additional specific cases, "**isotruss**" and "**isotruss2**", that are also members of the generic class, "**trusscomp**", is contained in the supplemental (unpublished) reports listed in [23].

Figure 1a, produced by Dr. Robert P. Thornburgh for [8], demonstrates the "huge torus" concept. The cylindrical shell that is part of the huge torus has a wall with a truss-core sandwich configuration. The minimum weight per surface area of the axially compressed cylindrical shell is sought. The decision variables of the optimization problem include the height and pitch of the truss-core sandwich, the ply thicknesses in the composite laminates that form the webs and face sheets, and the "corner" radii adjacent to the "noodle gaps" indicated in Fig. 1c.

Figures 1b – 1f show various models used by GENOPT/BIGOBOSR4 for the generic case, "**trusscomp**". Figure 1b shows the first few modules of the model used for the prediction of general buckling by GENOPT/BIGBOSOR4. The truss-core sandwich cross section is discretized, and variation of the general buckling mode in the direction normal to the plane of the paper is trigonometric. Figures 1c -1f show various models used for the prediction of local buckling. The uniformly axially compressed pre-buckled state of the truss-core sandwich wall is demonstrated by the STAGS model displayed in Fig. 1g. (NOTE: Fig. 1g is included here only to emphasize that the pre-buckled state in the GENOPT/BIGBOSOR4 model is a membrane state (no pre-buckling bending). STAGS and predictions from STAGS are NOT used in the GENOPT/ BIGBOSOR4 optimization loop.)

Figures 2 and 3 present end views of an optimized configuration with **local** buckling modes corresponding to a model consisting of a single module (Fig. 2a,b) and local buckling models

American Institute of Aeronautics and Astronautics

consisting of three modules (Fig.3a) and five modules (Fig. 3b). The user of GENOPT/BIGBOSOR4 decides how many modules to use in the local buckling model.

In GENOPT/BIGBOSOR4 models the cross section of a single repeating module of the truss-core sandwich wall of the cylindrical shell is divided into a number of shell segments. Figure 4 shows the BIGBOSOR4 segment numbering scheme, direction of "travel" along each segment, and dimensions used for a single module of the **local** buckling models such as those depicted in Figs. 1c-1f, 2a,b, and 3a,b. Figure 5 shows the critical **general** buckling mode of the optimized configuration. Figure 6 (top) shows the segment numbering scheme and direction of "travel" along each segment used for a single module of the **general** buckling multi-module model such as that depicted in Figs. 1b and 5.

Figure 6 (bottom portion) and Fig. 7 focus on a typical "noodle gap" and "noodle" cross-section area. Typically, a "noodle" is formed by filling the noodle gap with epoxy/adhesive or by inserting unidirectional fibrous composite material with all fibers oriented along the axis of the cylindrical shell. In this paper it is assumed that each noodle consists of unidirectional fibrous composite material with the same properties as those of a single ply oriented at zero degrees, that is, with the composite fibers oriented along the axis of the cylindrical shell. There are four noodle gaps in the single-module cross-sections shown in Figs. 1c, 1e, 1f, 2a,b, and 4.

Figure 8 shows the composite layup used in [3], which is different from that used in this paper, but which represents a typical selection of decision variables for the optimization process in a specific case that is a member of the generic class called "**trusscomp**". In [3] the specific case is called "**test**". In this paper the specific cases are called "**nasatruss2**" and "**nasatruss3**".

The starting design for the specific case, "**nasatruss2**" is listed in Table 3. The cylindrical shell has an inner surface radius of 78.15 inches, is 109 inches long, is simply supported, and is subjected to a total load, 2535000 lb axial compression. The properties of a single ply and the stress allowables are listed in Table 3. In Table 3 the curing "delta-temperature", TEMCUR, is listed as zero because most of the results in this paper pertain to cases in which there is no thermal curing effect. The results listed in Table 6 were obtained with TEMCUR = 200 degrees.

In the laminated composite truss-core wall segments shown in Fig. 4 there are four different layer "types". Each layer "type" has a bundle of three properties: thickness, layup angle, and material type. The layer thicknesses for the four layer "types" are called THICK(1), THICK(2), THICK(3), and THICK(4). These are all decision variable candidates. The corresponding layer layup angles are called ANGLE(1), ANGLE(2), ANGLE(3), and ANGLE(4). These are not decision variable candidates in the formulation used for the production of this paper. The four layup angles are fixed at ANGLE(1) = +45 degrees, ANGLE(2) = -45 degrees, ANGLE(3) = 0 degrees, and ANGLE(4) = 90 degrees, as listed in Table 3 in the section entitled "PARAMETERS WHICH ARE ALWAYS FIXED…". Zero degrees corresponds to the fibers of a unidirectional ply oriented along the axis of the cylindrical shell. Note that in the specific case called "**nasatruss2**" the three decision variable candidates, THICK(2), THICK(3), and THICK(4), are all linked to THICK(1), as seen near the top of Table 3. Hence, in "**nasatruss2**" there is only one independent thickness decision variable in this particular application, THICK(1). [However, note that in the specific case for which results are listed in Table 5

("**nasatruss3**") there are two independent thickness decision variables, THICK(1) and THICK(4)].

THICK(1) is the thickness of the +45-degree ply in both the laminates, NLAYRC and NLAYRF, two quantities that are defined in Fig. 8; THICK(2) is the thickness of the –45-degree ply in both the laminates, NLAYRC and NLAYRF; THICK(3) is the thickness of a 0-degree ply in the laminate, NLAYRF; and THICK(4) is the thickness of each 90-degree ply in the laminate, NLAYRF. The meanings of NLAYRC and NLAYRF are demonstrated in Fig. 8, which applies to the specific case called "**test**" in [3]. In the specific cases, "**nasatruss2**" and "**nasatruss3**", on which the results of this paper are based, NLAYRC has only two layers, [+45, -45], and NLAYRF has only six layers, [0, 90, 90, 0, -45, +45] (bottom face sheet) or [-45, +45, 0, 90, 90, 0] (top face sheet). The two-layered laminate, NLAYRC, is the laminate that is wrapped around each trapezoidal mandrel during the fabrication process. Two adjacent wrapped trapezoidal mandrels, one with its crown down and the other with its crown up, produce a non-symmetric anisotropic slanted truss-core web with four layers, [+45, -45, +45, -45].

A single 22-segment module of the fabricated truss-core sandwich shell wall, such as that displayed in Fig. 4, has the following laminated segments:

face sheet segments not at the "noodle gaps" (Segments 1, 6, 15 in Fig. 4):
[+45, -45, 0, 90, 90, 0, -45, +45]total

face sheet segment not at the "noodle gaps" (Segment 18 in Fig. 4):
[-45, +45, 0, 90, 90, 0, +45, -45]total

slanted truss-core webs (Segments 7 and 12 in Fig. 4):
[+45, -45, +45, -45]total

curved and short straight segments in Fig. 4 that enclose the "noodle gaps" except the face sheets:
[+45, -45]total

two bottom face sheet segments at the "noodle gaps" (Segments 3 and 8 in Fig. 4):
[0, 90, 90, 0, -45, +45]total

two top face sheet segments at the "noodle gaps" (Segments 17 and 22 in Fig. 4):
[-45, +45, 0, 90, 90, 0]total

Summary of this paper

The objective of the optimization is to minimize the weight per area of the axially compressed composite truss-core sandwich wall subjected to a set of specified requirements (behavior constraints). Next and in SECTIONS 2 and 3 descriptions are given of the "quick and dirty" models of a cylindrical shell with a truss-core sandwich wall. A brief description of GENOPT [6] appears in SECTION 4. SECTION 5 describes how GENOPT is used to produce a user-friendly

capability to optimize any cylindrical shell with a truss-core sandwich wall that consists of isotropic or laminated composite segments (the generic class called "**trusscomp**"). Section 6 discusses numerical results relating to two specific members, "**nasatruss2**" and "**nasatruss3**", of the generic class, "**trusscomp**". Section 7 demonstrates the effect of thermal curing on the design margins for the specific case, "**nasatruss2**". In Section 8 predictions from GENOPT/ BIGBOSOR4 and from PANDA2 are compared for cases in which thermal curing is neglected and included in the model. Section 9 demonstrates the construction of detailed finite element models for local and general buckling from which predictions from a general-purpose computer program such as STAGS [15-18] can be compared with those from GENOPT/BIGBOSOR4 [1]. Section 10 describes the effect on local buckling of support afforded by each noodle to the little shell segments that enclose it. Section 11 shows results from a design sensitivity analysis of the previously optimized specific case, "**nasatruss3**".

Models used

The models used in this paper are much simpler than those constructed for processing by general-purpose finite-element computer programs such as STAGS [15-18, Fig. 1g]. Naturally, the GENOPT/BIGBOSOR4 models used here are approximate. For example, the pre-buckled state is assumed to be a membrane state: there is no pre-buckling bending of the axially compressed cylindrical shell with the composite truss-core sandwich wall. The axial compression, N_x, in the various segments of the model, such as those displayed in Figs. 1b-1f and $2 - 6$, is distributed in proportion to the membrane axial stiffness of those segments. This distribution of N_x is prismatic, that is, it does not vary along the axis of the cylindrical shell. There is no axially varying "boundary layer", that is, there is no axisymmetric pre-buckling nonuniformity of radial displacement w in the neighborhoods of the two ends of the axially compressed cylindrical shell caused by restriction of induced Poisson ratio radial expansion there. The pre-buckled state is a uniform membrane state, as if uniform end shortening were applied and the shell were free to expand axisymmetrically and uniformly radially along its entire length. Fig. 1g, which is generated from a STAGS model that consists of three modules of the type shown in Fig. 4, demonstrates the prismatic pre-buckled membrane state that exists in the GENOPT/BIGBOSOR4 models that are used for optimization. (NOTE: A finite element model such as that shown in Fig. 1g is NOT used for optimization. Figure 1g is included here only to demonstrate the membrane pre-buckled state that is assumed to exist in the much simpler GENOPT/BIGBOSOR4 generic "**trusscomp**" model.)

The models used here for the optimization of the composite truss-core sandwich wall are BIGBOSOR4 models [5,19]. Therefore, the discretization is one-dimensional (strip method), which causes solution times on the computer to be much less than for the usual two-dimensionally discretized finite-element models such as that displayed in Fig. 1g. This property of one-dimensional discretization leads to efficient optimization.
.

SECTION 2 MODELING A CYLINDRICAL SHELL AS A HUGE TORUS

The cylindrical shell is modeled as a huge torus [9]. This concept is displayed in Fig. 1a. More

precisely, part of the cylindrical shell (180 degrees or less of its circumference) is modeled as part of a huge torus.

Modeling a cylindrical shell or a sector of a cylindrical shell as a part of a huge toroidal shell is a "trick" that permits, for example, the detailed modeling of a cylindrical shell with an axially oriented truss-core sandwich wall while working within the restriction that BIGBOSOR4 only handles shells of revolution. See Figs. 1a – 1f, 2, 3, 5, and 9 - 14 for examples.

With the "huge torus" model [3,8,9] the shell coordinates are exchanged: what was the axial coordinate of the cylindrical shell modeled in the usual way becomes the circumferential coordinate of the "huge torus" model, and what was the circumferential coordinate of the cylindrical shell modeled in the usual way becomes the meridional coordinate of the "huge torus" model. In the "huge torus" model of a stiffened cylindrical shell what were stringers become rings, and what were rings become stringers. What were axial half waves in the buckling mode of the cylindrical shell become circumferential half waves in the "huge torus" model of that cylindrical shell, and what were circumferential waves in the buckling mode of the cylindrical shell become meridional waves in the "huge torus" model of that cylindrical shell.

If the radius (RBIG in Fig. 1a) from the axis of revolution to the center of meridional curvature of the huge torus is large enough, then under certain circumstances the behavior of the huge torus or a segment of the huge torus should be close to that of the cylindrical shell that the "huge torus" model simulates. The "certain circumstances" are:

Item 1: The cylindrical shell must be simply supported at its ends. In the "huge torus" model of a cylindrical shell meridionally oriented buckling nodal lines, two of which are shown in Fig. 1a, occur at buckling modal half-wavelength intervals around the circumference of the huge torus. The conditions at a buckling nodal line are identical to simple support (antisymmetry of the buckling modal displacement components, u, v, w, and shell wall rotation). In the "huge torus" model of a cylindrical shell the BIGBOSOR4 user must choose the circumferential wave numbers, N0B, NMINB, NMAXB, INCRB, such that buckling nodal lines will always fall at intervals around the circumference of the huge torus that correspond to an integral number of half waves over the circumferential length of the huge torus that is equal to the axial length of the cylindrical shell that is being simulated by the "huge torus" model.

Item 2: The pre-buckled state must be a membrane state [3,8], that is, there is no pre-buckling bending. In terms of input data, the BIGBOSOR4 user must choose INDIC = 4 (linear buckling) and IPRE = 0 (membrane pre-buckling state to be specified by the BIGBOSOR4 user rather than being calculated by BIGBOSOR4). This implies that the shell must be perfect. The effect of the sensitivity of local and general buckling loads to initial imperfections can be accounted for in the "huge torus" model only by the use of appropriate factors of safety.

Item 3: The radius, RBIG in Fig. 1a must be much larger than the meridional radius of curvature, RADIUS.

In **Items 1** and **2** reference is made to "the BIGBOSOR4 user". In the GENOPT/BIGBOSOR4 optimization context there is no "BIGBOSOR4 user". The requirements just stipulated are

satisfied automatically, except that the GENOPT user must establish names and definitions for numbers of axial half-waves (in Table 1, MLOWL, MHIGHL for local buckling and MLOWG, MHIGHG for general buckling), and the end user must specify ranges of wave numbers that must be covered in the searches for the critical (smallest) buckling load factors that correspond to local buckling (MLOWL = 1, MHIGHL = 9 axial half-waves over the axial length, FACLEN x LENGTH, for example) and that correspond to general buckling (MLOWG = 1, MHIGHG = 5 axial half-waves over the axial length, LENGTH, for example).

In the "huge torus" model, as in any shell-of-revolution model, the meridional coordinate is discretized and variation of the buckling mode in the circumferential coordinate direction (normal to the plane of the paper in Figs. 3 and 5, for examples) is trigonometric with n (or N) circumferential waves around the huge circumference of the torus. There is a relationship between the axial length of the cylindrical shell and the smallest "huge torus" circumferential wave number that corresponds to one half wavelength spanning that axial length. As mentioned above, simple support end conditions on the cylindrical shell are implied because simple support (antisymmetry) is what naturally occurs along the meridionally oriented buckling nodal lines in the "huge torus" model of the cylindrical shell.

In the discussion above it is implied that the "huge torus" model only applies to circular cylindrical shells. However, this is not so. The "huge torus" model can be used for shells or panels of any cross section, such as the "oval-shaped" cylindrical shells and corrugated panels discussed in [9]. The same holds for true prismatic shells and for true prismatic assemblages of shells to be described in the next section.

For more details of the "huge torus" model, see [8] and [9].

SECTION 3 TRUE PRISMATIC SHELLS

In principle, predictions for a "huge torus" model of a cylindrical shell should approach those for a true prismatic shell as the radius from the axis of revolution of the center of meridional curvature (RBIG in Fig. 1a) approaches infinity. Reference [8] describes modifications that were made to BIGBOSOR4 [5] in order to generate a valid model of buckling of a truly prismatic, segmented shell, not just a "huge torus" approximation of a prismatic structure. All the GENOPT/BIGBOSOR4 results in this paper were generated with use of the new "true prismatic shell" formulation in BIGBOSOR4 [8,10]. In the "true prismatic shell" formulation n or N is the number of axial half-waves over the length, FACLEN x LENGTH for local buckling and over the length, LENGTH, for general buckling, not the number of full waves around the circumference of a huge torus.

SECTION 4 ABOUT GENOPT

GENOPT [6] is a system by means of which one can convert any analysis into a user-friendly analysis and into an optimization capability. GENOPT is not limited to the field of structural mechanics [20]. In the GENOPT "universe" there are considered to be two types of user: 1. **the**

American Institute of Aeronautics and Astronautics

"GENOPT user", and 2. **the "end user"**. The GENOPT user creates the user-friendly analysis and optimization capability for a class of problems with a generic name ("**trusscomp**" in this paper), and the end user uses that capability to find optimum designs for a member of that class with a specific name ("**test**" in [3] and "**nasatruss2**" or "**nasatruss3**" in this paper). For the work reported here the GENOPT user and the end user are the same person: the first author.

References [3] and [5-8] provide examples in which GENOPT is used to optimize shell structures. References [3,5,7,8] and this paper provide examples in which GENOPT is used with BIGBOSOR4 to find optimum designs of complex cylindrical and ellipsoidal shells. Many details are given in Ref. [7] about what GENOPT does and how to use it. These details will not be repeated here.

It is the duty of **the GENOPT user** to create user-friendly names, one-line definitions, and "help" paragraphs for the variables to be used in the analysis or analyses. The GENOPT user must also supply software (subroutines and/or FORTRAN statements) that perform the analysis or analyses that generate the behavior constraints, such as buckling, stress, vibration, etc. The GENOPT user must decide what behaviors will constrain the design during optimization cycles, behaviors such as general buckling, local buckling, stress, vibration, etc. [5]. While identifying each variable to be used in the generic case, the GENOPT user must decide which of seven roles each of these variables plays. The seven possible roles are:

1. decision variable candidate (such as a structural dimension)
2. parameter that is not a decision variable candidate (such as a material property)
3. environmental variable (such as a load)
4. behavioral variable (such as a stress)
5. allowable variable (such as a maximum allowable effective stress)
6. factor of safety (such as a factor of safety for stress)
7. objective (such as weight)

It is the duty of **the end user** to provide, for a specific case, a starting design, loads, and material properties, to choose decision variables, lower and upper bounds, equality constraints, and inequality constraints, and to choose whether to optimize or simply to analyze an existing design or both.

Please read [6] first, followed by the first part of [7], which contains many details about how to use GENOPT. Also read [8], which is analogous to this paper. For additional information on the generic case, "**trusscomp**", and on several specific cases, see [23].

SECTION 5 PRODUCTION OF THE PROGRAM SYSTEM TO OPTIMIZE A TRUSS-CORE SANDWICH SHELL WALL

The generic case is called "**trusscomp**".

Table 8 in [3] and Table 4 in [8] list typical run streams for obtaining optimum designs for configurations in which GENOPT [6] is used in connection with BIGBOSOR4 [5]. Table 8 in [3]

lists the run stream used to obtain results analogous to those presented here. The results are different in this paper from those listed in [3] because:

1. The specific cases, called "**nasatruss2**" and "**nasatruss3**" in this paper, have different properties from those of the specific case called "**test**" in [3].

2. The results of this paper are based on the "true prismatic shell" model [8,10] that did not exist when [3] was produced.

3. Since [3] was written extensive modifications have been made to the computer code that generates the behavioral constraints, especially to the computer code that generates the local and general buckling load factors.

The long Table 8 in [3] (18 pages long) first gives the run stream used to produce the generic "**trusscomp**" system of computer programs (pages 1-5 of Table 8 of [3]), then lists the run streams to employ the generic "**trusscomp**" system to obtain optimum designs for the specific case called "**test**" (pages 5-6 and 9-10 and 12-13 and 14-15 and 17 of Table 8 of [3]), then lists the run streams for executing BIGBOSOR4 outside the GENOPT context in order to produce plots such as those in Figs. 2, 3, and 5 (pages 6-9 and 10-12 and 13-14 and 14-15 and 17-18 of Table 8 of [3]), and then lists a run stream for executing PANDA2 (pages 15-17 of Table 8 of [3]). The specific case in this paper called "**nasatruss2**" is analogous to the specific case called "**test**" in [3].

The GENOPT user first provides input during the long GENTEXT interactive session as listed in Table 9 of [3] (the trusscomp.INP file, 14 pages long). During the interactive GENTEXT session, GENOPT automatically produces the files trusscomp.DEF and trusscomp.PRO. Table 1 of this paper contains a small part of the trusscomp.DEF file: a glossary of the GENOPT user's variable names, one-line definitions, the role of each variable, and other properties of each variable. Table 2 of this paper lists the entire trusscomp.PRO file for the generic case, "**trusscomp**". The trusscomp.PRO file contains the prompts and "help" paragraphs, created by the GENOPT user. These prompts and "help" paragraphs will be seen by the end user. The program system created by GENOPT for the "**trusscomp**" generic case will be end-user friendly if the one-line prompting phrases and "help" paragraphs created by the GENOPT user, such as the following (taken from Table 2) are written clearly by the GENOPT user and are reasonably free of jargon with which the end user might not be familiar:

```
60.1 local radius from side to crown of trapezoidal tool: ROBTUS   |one-line
                                                                    |prompt
60.2
     ROBTUS is the radius that fairs each side wall of the          | "help"
     trapezoidal tool into the crown of the trapezoidal             |paragraph
     tool. The trapezoidal tool is the object around which          |
     the core laminate is laid up. ROBTUS is the radius             |
     that spans the obtuse angle from trapezoid crown to            |
     trapezoid sloping sides. ROBTUS is similar                     |
     to the dimension called "R2" in Fig. 4.                        |
     (R2 = ROBTUS + total thickness of shell segment 2 in Fig.4)    |
```

American Institute of Aeronautics and Astronautics

Although it is very long, Table 2 is included here because the "help" paragraphs will help the reader better to understand the generic "**trusscomp**" model.

GENTEXT also produces FORTRAN fragments, trusscomp.*, analogous to the weldland.* files listed on page 1 of Table 4 of [8**b**] and described on pages 2 and 3 of Table 6 of [8**b**]. GENOPT automatically assembles these FORTRAN fragments into various programs (BEGIN.NEW, STOGET.NEW, STRUCT.NEW, BEHAVIOR.NEW, CHANGE.NEW) described on page 2 of Table 6 of [8**b**]. BEGIN.NEW, STOGET.NEW, and CHANGE.NEW are complete programs and subroutines, created automatically entirely by GENOPT. The GENOPT user does not have to be concerned about them at all.

It is a different matter in the case of STRUCT.NEW and BEHAVIOR.NEW. These are "**skeletal**" subroutine libraries either or both of which must be "fleshed out" by the GENOPT user. In this particular application the GENOPT user adds merely three statements to the version of STRUCT.NEW automatically created by GENOPT. (See page 2 of Table 8 of [3]). In this particular application the GENOPT user does more to "flesh out" the BEHAVIOR.NEW library. (See Table 12 of [3] for an early version of BEHAVIOR.NEW, and see the file, /home/progs/genopt/case/trusscomp/behavior.trusscomp, for the latest version).

In preparing for the GENTEXT interactive session the GENOPT user here decided to introduce four behaviors:

1. local buckling (LOCBUK in Table 1)
2. general buckling (GENBUK in Table 1)
3. a maximum of six stress components in material number 1 (STRM1 in Table 1)
4. a maximum of six stress components in material number 2 (STRM2 in Table 1)
(STRM2 is present but not listed in Tables 3 - 5 because the specific cases, "**nasatruss2**" and "**nasatruss3**", are fabricated of only one material.)

Corresponding to these four behaviors, GENTEXT automatically creates four **skeletal** "behavioral" subroutines, SUBROUTINE BEHX1 (local buckling), SUBROUTINE BEHX2 (general buckling), SUBROUTINE BEHX3 (up to six components of stress in material no. 1), and SUBROUTINE BEHX4 (up to six components of stress in material no. 2). The GENOPT user has to "flesh out" each of these four "behavioral" subroutines, as listed in Table 12 of [3]. The GENOPT user also has to "flesh out" the subroutine that computes the objective, SUBROUTINE OBJECT in Table 12 of [3]. NOTE: SUBROUTINEs BEHX1, BEHX2, BEHX3, BEHX4, and OBJECT have been extensively changed since [3] was written. See the latest versions on which this paper is based in the file:
 /home/progs/genopt/case/trusscomp/behavior.trusscomp.

In the "fleshed out" versions of SUBROUTINE BEHX1 and SUBROUTINE BEHX2 there are calls to SUBROUTINE BOSDEC. SUBROUTINE BOSDEC must be written by the GENOPT user. SUBROUTINE BOSDEC ("BOSorDECk") creates a valid input file for BIGBOSOR4. A general guideline on how to go about creating SUBROUTINE BOSDEC is provided in the file associated with the GENOPT sample case called "cylinder":
/home/progs/genopt/case/cylinder/howto.bosdec.

For the present application an early version of SUBROUTINE BOSDEC is listed in Tables 13a and 13b of [3]. {SUBROUTINE BOSDEC has been extensively changed since [3] was written. See the latest version of SUBROUTINE BOSDEC (on which this paper is based) in the file, /home/progs/genopt/case/trusscomp/bosdec.trusscomp.} In the generic case, **trusscomp**, SUBROUTINE BOSDEC now not only creates input files for BIGBOSOR4, but also creates two input files for STAGS [15 -18], one for local buckling (*.inp) and the other for general buckling (*.inp2), in which "*" represents the end-user-selected name for the specific case, such as "**nasatruss2**" or "**nasatruss3**".

SECTION 6 NUMERICAL RESULTS

Figures 2, 3, 5, and 9-17 and Tables 3-5 display and list results from the specific cases called "**nasatruss2**" and "**nasatruss3**". The starting design has the properties of the test section of the composite truss-core sandwich cylindrical shell analyzed by Lovejoy [1]. Figures 9 – 14 and Table 3 pertain to this starting design. The results presented in this section were obtained neglecting thermal curing (TEMCUR = 0.0) and neglecting any support that a noodle may afford the little shell segments that enclose it (ILINKS = 0).

Figure 15 shows the evolution of the objective during an execution of SUPEROPT. Figures 2, 3, and 5 and Table 4 pertain to the optimum design found as a result of the execution of SUPEROPT.

SUPEROPT is a script by means of which an attempt is made to find a "global" optimum design [4D]. "Global" is in quotes because SUPEROPT does not actually find a global optimum, but attempts to find nearly a global optimum by executing repeated optimizations from different starting points in design space. The different starting points are determined randomly but mostly consistent with linking and inequality conditions [4D,4L]. Each "spike" in the plot in Fig. 15 corresponds to a new "starting" design. Each new "starting" design is automatically generated by a GENOPT processor called "AUTOCHANGE".

Comments about the numerical results for the specific case called "nasatruss2":

1. The plot of objective versus design iterations during the SUPEROPT execution (Fig. 15) implies that the same optimum design is generated over and over again. In other generic/specific cases, plots of this kind often exhibit several different "minimum" weights during a single execution of SUPEROPT, demonstrating that SUPEROPT is finding several different "optimum" designs, each corresponding to a local minimum in design space, not a global minimum design. The specific case, "**nasatruss2**", appears to be especially well behaved in this respect. See Fig. 11 of [4I] and Fig. 3 of [13] for examples of less well behaved cases.

2. The optimum design listed in Table 4 corresponds to the thickness of each ply reaching and staying at its lower bound. A lighter design would have evolved if a lower bound less than the 0.0057 inches specified in Table 3 had been used for the decision variable called THICK(1).

American Institute of Aeronautics and Astronautics

Alternatively, the lower bound of the thickness, THICK(4), of the 90-degree layer type could be set to half the ply thickness of 0.0057 inches provided that THICK(4) is not linked to THICK(1) but instead is made an independent decision variable. This can be done because the two 90-degree plies always occur next to each other and therefore could, during fabrication, be replaced by a single 90-degree layer of ply thickness equal to 0.0057 inches. See the sub-section entitled, "**Comments about the numerical results for the specific case called "nasatruss3"**", for results from a model in which this is done.

3. The beneficial effect of the "noodles" is significant. The "noodles" absorb some of the axial load and the "noodle gaps" effectively decrease the segment width over which local buckling occurs. Compare Fig. 9, from the model in which "noodles" and "noodle gaps" are present, with Fig. 10, from the model in which "noodles" and "noodle gaps" are absent. The local buckling load factor (eigenvalue) is increased by more than 60 per cent because of the presence of the "noodles" and "noodle gaps": eigenvalue=0.9840 in Fig. 10 (no noodles or noodle gaps) versus 1.6075 in Fig. 9 (yes noodles and yes noodle gaps).

4. Figure 12 is derived from a multi-module model in which the "noodles" are present but the "noodle gaps" are absent. The number of modules of the type shown at the top of Fig. 6 is 46. Forty-six modules generate a BIGBOSOR4 buckling model with 276 little shell segments, close to the maximum number of shell segments presently permitted by BIGBOSOR4. This multi-module model is generated from the single module displayed in Fig. 6, which is ordinarily used only for the prediction of general buckling. However, local buckling as well as general buckling can be predicted from this multi-module model. In order to predict local buckling from this general buckling model, one simply specifies a range of number of axial half-waves that includes the critical local buckling axial half-wavelength. For example, the critical local buckling axial half-wavelength corresponding to the local buckling mode depicted in Fig. 12 is LENGTH/N = 109/94 inches. This local buckling mode derived from the multi-module general buckling model is similar to that displayed in Fig. 10 for a three-module model of the same type (Fig. 6, top) but with no noodles.

5. Compare the local buckling eigenvalues given in Figs. 9, 10, 11, and 12. The local buckling eigenvalue (load factor) in Fig. 9, eigenvalue=1.6075, is from a model in which both "noodles" and "noodle gaps" are present. The local buckling eigenvalue in Fig. 12, eigenvalue=1.5330, is from a model in which the "noodles" are present but the "noodle gaps" are absent. The local buckling eigenvalues in Figs. 10 and 11, eigenvalues=0.98399 and 0.94632, respectively, are from models in which both the "noodles" and the "noodle gaps" are absent. Two items are revealed by this comparison:

Item a. The presence of "noodles" only (no "noodle gaps") raises the local buckling load factor by about 50 per cent (from approximately 1.0 in Figs. 10 and 11 to approximately 1.5 in Fig. 12), and the addition of "noodle gaps" raises the local buckling load factor by another approximately 5 per cent (from approximately 1.53 in Fig. 12 to approximately 1.61 in Fig. 9).

Item b. The model shown in Fig. 11 yields a buckling load factor (eigenvalue) that is fairly close to that given in Fig. 10. Therefore, the multi-module model in Fig. 11 is essentially as good at predicting local buckling as that in Fig. 10. This result implies that the multi-module model in

American Institute of Aeronautics and Astronautics

Fig. 12 is essentially as good at predicting local buckling as that in Fig. 9. It therefore appears to be revealed with reasonable accuracy that there is an approximately **5-percent effect** of neglecting (Fig. 12) or including (Fig. 9) "noodle gaps" in two models that both include "noodles". NOTE: The local buckling load factor in Fig. 9 is obtained from a model in which the "noodle support" index, ILINKS = 0, that is, each noodle provides no support to the little shell segments that enclose it. Therefore, the "**5-percent effect**" is a very conservative estimate. See Section 10 for a discussion pertaining to the noodles supporting the noodle gap shell segments. In Section 10 it is shown that if the noodles support the shell segments that enclosed them, the local buckling load factor increases from 1.6075 (Fig. 9, "noodle support" index, ILINKS = 0) to 2.36 (Fig. 23e, "noodle support" index, ILINKS = 2) or to 2.34 (Fig. 24f, ILINKS = 1).

6. Compare Figs. 13 and 14. These two figures reveal the effect of including (Fig. 13) and neglecting (Fig. 14) the "noodles" in a general buckling analysis. The "noodles" raise the general buckling load factor by about 11 per cent, from 0.79071 in Fig. 14 to 0.88751 in Fig. 13. Note from Fig. 1b that the noodle centroids do not coincide with the face sheet reference surface, but lie slightly inside the core. This small difference acts to decrease the general buckling load factor by about 7 per cent.

7. The general buckling load factors listed in Tables 3 and 4 under the heading, "GENERAL BUCKLING LOAD FACTORS AND MODES (BEHX2)" are relatively insensitive to the number of axial half-waves in the buckling mode. This is especially true for the optimized configuration (Table 4).

8. For the optimum design the following most critical margins are listed near the end of Table 4:

```
Margin   Margin      Definition of the margin
Number   value
  2      7.858E-03   (LOCBUK(1 )/LOCBUKA(1 )) / LOCBUKF(1 )-1; F.S.=  1.30
  3     -8.510E-03   (GENBUK(1 )/GENBUKA(1 )) / GENBUKF(1 )-1; F.S.=  1.00
  5      4.047E-04   (STRM1A(1 ,2 )/STRM1(1 ,2 )) / STRM1F(1 ,2 )-1; F.S.=  1.00
  8      4.686E-02   (STRM1A(1 ,5 )/STRM1(1 ,5 )) / STRM1F(1 ,5 )-1; F.S.=  1.00
```

in which LOCBUK(1) is the local buckling load factor for load set 1; GENBUK(1) is the general buckling load factor for load set 1; STRM1(1,2) is the maximum compressive stress in the fiber direction for material 1 (the "1" in the name STRM1), load set 1 [the "1" in the array element designation, (1,2)]; and STRM1(1,5) is the maximum in-plane shear stress for material 1, load set 1. The variable names, STRM1, STRM1A, STRM1F from which the margin definition is automatically constructed are created by the GENOPT user (Table 1). Those names that end in "A" are allowables, and those names that end in "F" are factors of safety (F.S.). The forms of the definitions of the margins are created automatically by GENOPT from the variable names created by the GENOPT user. These and other variable names created by the GENOPT user are listed in Table 1.

The various components of the array of maximum stress, STRM1(i,j), i =1, and j = 1, 2,...,5, are defined in Tables 3 and 4. From Table 4 (the optimum design), we have the following:

```
Maximum stress components from BEHX3 (Material type 1):
```

```
Stress component no. 1:  0 deg. tension   3.123998E+04
Stress component no. 2:  0 deg. comp.     1.046716E+05
Stress component no. 3: 90 deg. tension   5.257718E+01
Stress component no. 4: 90 deg. comp.     7.407604E+03
Stress component no. 5: in-plane shear    6.008428E+03
```

9. Notice that the factor of safety for general buckling is 1.0. This is not good design practice because small imperfections in the shell geometry will significantly reduce its general buckling capability. To generate a practical optimum design the user would ordinarily use a factor of safety of 1.5 to 2.0 for general instability in order to compensate for the deleterious effect of unknown geometric imperfections. In this paper we use a factor of safety for general instability of 1.0 because we will compare predictions from GENOPT/BIGBOSOR4 with those from a general-purpose finite element program [1]. In the finite element models in [1] the shell is assumed to be perfect.

10. The factor of safety for local buckling, LOCBUKF(1) = 1.3 in Table 3, is set greater than unity in order to compensate for the effects of transverse shear deformation (t.s.d.) and local shell wall anisotropy on local buckling within a given shell segment. **Transverse shear deformation (t.s.d.) and shell wall anisotropy in individual shell segments are not accounted for in BIGBOSOR4 models.** For the prediction of general buckling (Fig. 5, for example) the neglect of local segment t.s.d. and local shell wall anisotropy are not especially important. The overall (global) t.s.d. over the entire truss-core sandwich wall is automatically accounted for in the general buckling model because each part of the truss-core sandwich wall is included as a little flexible shell segment as displayed in Figs. 1b, 5, and 20b; nothing is "smeared out", as is done in the PANDA2 model of general instability to be discussed in SECTION 8 and as is done in some of the general buckling models described in [1].

11. The effect of pre-stress caused by curing the composite truss-core sandwich is not accounted for. See Section 7 for results and a discussion of a **nasatruss2** model in which the effect of thermal curing is included.

Comments about the numerical results for the specific case called "nasatruss3":

Figures 16 and 17 and Table 5 display and list results from the specific case called "**nasatruss3**".

The specific case, "**nasatruss3**" is the same as "**nasatruss2**" except that the lower bound of the thickness of the 90-degree plies in the face sheets is set equal to 0.00285 inches rather than 0.0057 inches, and the decision variable candidate, THICK(4), is no longer linked to THICK(1) but is an independent decision variable. The 90-degree plies always occur in adjacent pairs. Hence, if at the optimum design of "**nasatruss3**" the thickness of each 90-degree ply reaches this new lower bound, the optimized truss-core sandwich wall can be fabricated with the adjacent pair of 90-degree plies of thickness 0.00285 inches each replaced with a single 90-degree ply of thickness 0.0057 inches.

Figure 16 shows the evolution of the objective during four executions of the GENOPT processor

called OPTIMIZE [3,6]. Indeed, the new optimum design at Iteration No. 23, listed in Table 5, weighs significantly less than the optimum design listed in Table 4, yet it can be fabricated because the thickness of each 90-degree layer has reached its lower bound of 0.00285 inch. Figure 17 shows the design margins corresponding to the evolution of the objective displayed in Fig. 16. The final optimum design of the specific case, **nasatruss3**, is listed in Table 5.

Comments about the numerical results from the finite element models for the specific case called "nasatruss2":

Predictions from GENOPT/BIGBOSOR4 for the case called "**nasatruss2**" are compared with predictions from the STAGS and/or NASTRAN general purpose finite-element computer programs in [1]. See Section 9 for a description of STAGS models for local and for general buckling that are automatically generated by the GENOPT/BIGBOSOR4 subroutine called SUBROUTINE BOSDEC (/home/progs/genopt/case/trusscomp/bosdec.trusscomp).

SECTION 7 THE SIGNIFICANT EFFECT OF THERMAL CURING

Up to this point the effect of curing the laminated composite truss-core sandwich wall has been neglected. Curing this configuration generates residual stresses that affect both the stress and buckling margins, especially the stress margins. Table 6 lists results from computations in which the effect of thermal curing on the starting design listed in Table 3 is included. Also included in Table 6 is a description of how the effect of thermal curing is calculated.

In this case the effect of thermal curing on local and general buckling margins is insignificant. However, there is a significant effect on the stress margins. In particular, there is one additional critical stress margin listed near the bottom of Table 6:

```
5   -5.938E-01 (STRM1A(1,3)/STRM1(1,3))/STRM1F(1,3)-1; F.S.=1.00
```

The stress component, **STRM1(1,3)** , is the tensile stress normal to the fibers for material no. 1, load case no. 1. (There is only one load case considered throughout this paper.) The quantity, **STRM1A(1,3)** , is the corresponding maximum allowable stress (10560 psi as listed in Table 3), and **STRM1F(1,3)** is the corresponding factor of safety (1.0 as listed in Table 3). As listed in Table 6, this critical stress component, **STRM1(1,3)**, corresponds to SIG2 in the 0-degree plies in shell segments 1, 6, 15, and 18: SIG2 = 25987 psi. (SIG2 is the stress normal to the fibers). However, note from the listing of the in-plane stress components, SIG1, SIG2, and SIG12, near the end of Table 6 that every ply in all of the 22 shell segments shown in Fig. 4 has stress, SIG2, normal to the fibers between 21192 psi and 25987 psi. This stress component is significant and is entirely caused by curing, not by application of the axial load, -2535000 lb.

Unfortunately, optimization will not significantly reduce this critical stress component. If the effect of thermal curing is to be included in the computations during optimization cycles, the best solution is either greatly to increase the stress allowable, **STRM1A(1,3)**, or to perform optimization in which the particular "behavior", **STRM1(1,3)**, is ignored. **The GENOPT**

system allows the user to eliminate from consideration any selected behavior or behaviors. The rationale for neglecting the design margin corresponding to tension normal to the fibers is that cracking normal to the fibers in a laminate usually does not cause failure of a composite structure. However, it might be advisable to reduce the allowable, **STRM1A(1,2)** (compressive stress along the fibers), because if matrix cracking has occurred because of curing these fibers might buckle more easily under compression, leading to early failure of one or more plies that experience compression along the fibers.

The residual thermal stress resultants, FN20T (Table 6), in the shell segments shown in Fig. 4 and the residual thermal forces, FNOOD1T and FNOOD2T (Table 6), in the "noodles" are considered to be "fixed" loads, not "eigenvalue" loads. "Eigenvalue" loads are loads that are to be multiplied by the bifurcation buckling load factor (eigenvalue); "fixed" loads are not to be multiplied by the bifurcation buckling load factor.

In order to incorporate curing effects in the GENOPT/BIGBOSOR4 model of the truss-core sandwich configuration the first author had to modify the BIGBOSOR4 computer program in order to permit the user to provide both "eigenvalue" and "fixed" loads for the particular BIGBOSOR4 analysis branch, INDIC = 4 and IPRE = 0. "INDIC = 4" means "linear bifurcation buckling" and "IPRE = 0" means "the user provides the pre-buckling state of the shell rather than having BIGBOSOR4 calculate the pre-buckling state." In the GENOPT/BIGBOSOR4 context, the "user" who provides the pre-buckling state of the shell is SUBROUTINE BOSDEC.

SECTION 8 COMPARISONS OF PREDICTIONS FROM GENOPT/BIGBOSOR4 AND PANDA2

Predictions of stress margins from GENOPT/BIGBOSOR4 models with no "noodles" or "noodle gaps" including the effect of thermal curing and neglecting that effect agree with the predictions of stress margins from the equivalent PANDA2 models including and neglecting thermal curing. PANDA2 models cannot include "noodles" or "noodle gaps".

Results from a comparison of GENOPT/BIGBOSOR4 predictions and PANDA2 predictions for the starting design of the specific case, "**nasatruss2**" without noodles and without noodle gaps are listed in Table 7. Design margins are listed in Table 7 for cases neglecting curing (Parts 1 – 3) and including curing (Parts 4 and 5). The following comments apply to the results listed in Table 7:

1. The transverse shear deformation (t.s.d.) effect is significant in the PANDA2 model with regard to both local and general buckling, but especially significant with regard to general buckling. That is because in the PANDA2 model for general buckling the truss-core sandwich properties are "smeared out". With t.s.d. neglected none of the sort of local deformation depicted in Fig. 14, for example, is represented in the PANDA2 model of general instability. The general buckling load factor from PANDA2 is therefore unacceptably unconservative if t.s.d. is neglected. With t.s.d. neglected, the local buckling load factor from PANDA2 is somewhat less unacceptably unconservative.

2. There is reasonably good agreement between the GENOPT/BIGBOSOR4 and the PANDA2 models with respect to local and general buckling, both with and without curing, provided that the effect of t.s.d. is included in the PANDA2 model.

3. The t.s.d. effect is accounted for in the GENOPT/BIGBOSOR4 model of local buckling by use of a factor of safety (F.S.) greater that unity. In the **nasatruss2** case the factor of safety for local buckling is 1.3.

4. The stress margins from the GENOPT/BIGBOSOR4 model agree with those from the PANDA2 model for all of the cases listed in Table 7.

5. Neglecting or including the effects of curing have essentially no influence on the local and general buckling margins in this case.

SECTION 9 COMPARISON OF PREDICTIONS FROM GENOPT/BIGBOSOR4 WITH THOSE FROM GENERAL-PURPOSE FINITE ELEMENT CODES

Figure 18 shows a close-up view of part of a finite element model constructed for analysis by the STAGS computer program [15-18]. The STAGS input file, nasatruss2.inp, is created by SUBROUTINE BOSDEC for this and other finite element models of "**trusscomp**" configurations previously optimized by GENOPT/BIGBOSOR4.

Figure 19 displays a STAGS local buckling model that consists of four 22-segment modules of the type shown in Fig. 4 joined together. A much smaller cylindrical shell radius, 7.815 inches, is used in that STAGS model than the 78.15-inch radius of the cylindrical shell that is the subject of the rest of this paper. This is done in order to emphasize that the circumferential curvature of the cylindrical shell is included in all of the local buckling models investigated in this paper.

Figures 20a and 20b show a general buckling model (cylindrical shell radius = 78.15 inches), and Fig. 21 depicts a typical general buckling mode shape. Figures 19-21 were produced from STAGS runs executed with the use of input files generated automatically by the GENOPT/BIGBOSOR4/trusscomp system. In particular, SUBROUTINE BOSDEC, written by the GENOPT user, generates input files for local and general buckling analysis by both BIGBOSOR4 and STAGS. For a list of SUBROUTINE BOSDEC, see the file: /home/progs/genopt/case/trusscomp/bosdec.trusscomp.

Results from STAGS and other general-purpose finite element computer codes applied to the cylindrical shell with the composite truss-core sandwich wall are given and discussed in [1].

SECTION 10 EFFECT OF THE NOODLE PROVIDING SUPPORT FOR THE LITTLE SHELL SEGMENTS THAT ENCLOSE THAT NOODLE

This entire section is concerned only with local buckling. In the local buckling models investigated up to this point it is assumed that a noodle enclosed by the little shell segments that

American Institute of Aeronautics and Astronautics

define a noodle gap (for example, Segments 2 – 5 in Fig. 4) offers no support to those little shell segments. ("noodle support" index, ILINKS = 0). The noodle shares the axial load, but the little shell segments are free to deform locally in the buckling mode as if the noodle gap were filled with air rather than with a noodle. The purpose of this section is to obtain an estimate of how much the local buckling load factor might be increased if support by the noodle to the noodle gap segments were somehow included in the local buckling model. The best way to determine accurately the effect of noodle support would be to construct a finite element model in which solid finite elements with the properties of a noodle fill each of the noodle gaps. In the absence of such a model as of this writing, several alternative approximate models are constructed in order to obtain a rough estimate of the effect of noodle support.

The effect of noodle support is governed by a "noodle support" index, ILINKS, defined in Table 1 and described in some detail at Prompt Number 195 in Table 2.

There are four types of models that pertain to this section:

EFNOOD > 0, ILINKS = 0: This is the "Winkler Foundation" model. The main disadvantage of this model is that the Winkler foundation connects the little noodle gap segments to ground, not to each other. Therefore, this model is unconservative.

EFNOOD = 0, ILINKS = 0: The local buckling single module is as displayed in Fig. 4, and the noodle does NOT provide any support for the little shell segments that enclose it. For example, shell segments 2, 3, 4 and 5 in Fig. 4 receive no support by the noodle that is enclosed in that noodle gap. This is the conservative model on which the results shown in Figs. 1c, 2, 3, and 9 are based.

EFNOOD = 0, ILINKS = 1: The local buckling module does not have any little shell segments that enclose each noodle, such as shown in Fig. 4. Instead, the neighboring "straight" segments (webs and face sheets) have gaps between them, as displayed in Figs 1d and 1e, for example. They are linked to each other by "rigid" links. In the GENOPT/BIGBOSOR4 model displacements at one end of a gap are related to those at the other end of the gap by simple compatibility relationships that involve the radial and axial components of the gap (D1 and D2, respectively, in BIGBOSOR4 jargon; see Fig. A1 on page 52 of [22]). In STAGS models the gaps are spanned by what in STAGS jargon are called E130 finite elements ("fasteners").

EFNOOD = 0, LINKS = 2: "extra" inner and outer layers are added to the little shell segments that enclose each noodle. For example, Segments 2, 3, 4, and 5 in Fig. 4 enclose one of the noodles. "Extra" inner and outer layers are added to those little segments and to the other analogous little segments that enclose the other three noodles in the single-module model displayed in Fig. 4. Figure 1f shows a local buckling mode from a model of this type. The "extra" inner and outer layers applied to these little shell segments have properties established in SUBROUTINE BOSDEC as follows:

```
MAXMAT1 = MAXMAT + 1              (an "extra" material type is introduced)
EMOD1(MAXMAT1) = 10.*EMOD1(1)   (modulus along the fibers of each "extra" ply)
THKSTF =  5.*THICK(1)            (thickness of each "extra" ply)
```

EMOD2(MAXMAT1) = 0.00001   (modulus normal to fibers of each "extra" ply)
G12(MAXMAT1) = 0.00001   (in-plane shear modulus of each "extra" ply)
G13(MAXMAT1) = EMOD1(MAXMAT1)/2.   (transverse shear modulus of each "extra" ply)
G23(MAXMAT1) = G13(MAXMAT1)   (transverse shear modulus of each "extra" ply)
NU(MAXMAT1) = 0.   (Poisson ratio of each "extra" ply)
ALPHA1(MAXMAT1) = 0.   (thermal expansion coefficient of each "extra" ply)
ALPHA2(MAXMAT1) = 0.   (thermal expansion coefficient of each "extra" ply)
TEMCUR(MAXMAT1) = 0.   (curing temperature rise above ambient of each "extra" ply)
DENSTY(MAXMAT1) = 0.   (weight density of each "extra" ply)

In the FORTRAN code just listed the following definitions apply:

EMOD1(1) = modulus along the fibers for material type 1
THICK(1) = thickness of layer type 1

The inner and outer "extra" layers are oriented in the "hoop" direction of the cross section of the truss-core sandwich wall, that is, the fibers run in the plane of this cross section, normal to the direction along the axis of the cylindrical shell. The "extra" inner and outer layers are like unidirectional composite plies laid up in the "hoop" direction, that is, with the fibers running at 90 degrees to the axis of the cylindrical shell. The "extra" inner and outer layers carry no axial load and generate no in-plane shear energy in the buckling mode. These roles are filled by the "real" layers and by the enclosed noodles, which still absorb their share of axial load and which still retain their in-plane shear stiffness and torsional stiffness. The effect of the "extra" inner and outer layers is to give the little shell segments that enclose each noodle high "hoop" extensional and bending stiffnesses. These high "hoop" extensional and bending stiffnesses causes the cross sections of these little shell segments to remain essentially undeformed in the local buckling mode. They can still translate and rotate but cannot deform very much.

Winkler Foundation (EFNOOD > 0, ILINKS = 0)

Figure 22 demonstrates, for the starting design listed in Table 3, the effect of the elastic foundation stiffness, EFNOOD, provided by the noodle on the prediction of local buckling of the truss-core sandwich wall. EFNOOD is the spring stiffness/area of a Winkler foundation. The units of EFNOOD are force/length^3. The Winkler foundation supports the little shell segments that enclose each noodle. Note that a Winkler foundation links each nodal point on the reference surface of a supported shell segment to **ground**. The strain energy per surface area of the Winkler foundation is given by kw^2/2, in which k is the spring stiffness/area (k = EFNOOD) and w is the normal deflection at a nodal point on the reference surface of a spring-supported shell segment. Because the Winkler springs connect the nodal points to ground and not to each other, the elastic foundation concept is not really a valid model in the trusscomp case because it does not account for the fact that each noodle cross section may rotate and translate as a rigid entity. Therefore, the Winkler model is unconservative.

From Fig. 22 it is seen that the convergence with respect to increasing elastic foundation stiffness, EFNOOD, is slow. The local buckling modes obtained with the stiffest foundation

modulus demonstrate that the noodle gaps do not experience any rigid body rotations or translations. Figure 22(a) shows the local buckling prediction with no elastic foundation. With EFNOOD = 0 there is significant deformation of the noodle cross section in the critical buckling mode. EFNOOD = 0, ILINKS = 0 is the model from which Figs. 1c, 2, 3, and 9 are generated. As EFNOOD increases it is clear from Fig. 22 that the noodle gaps become attached to ground, since their cross sections experience no rigid body rotations or translations.

Simulating "rigid" noodle gap segments by greatly increased 90-degree (meridional) bending stiffness of those segments in the 22-segment module model (Fig.4) for local buckling (EFNOOD = 0, ILINKS = 2)

In practice, the noodle material completely fills the noodle gap that encloses it. This noodle material bonds to the shell segments surrounding it. A rigorous model would represent the noodle material as solid finite elements. BIGBOSOR4 cannot handle solid finite elements. One way to simulate approximately the support provided by the noodle material to the surrounding shell segments in a "legal" BIGBOSOR4 model is greatly to increase the meridional bending stiffness of those shell segments without allowing them to absorb any more of the applied axial load than they do with ILINKS = 0. This is done by adding inner and outer layers to Segments 2, 4, 5, 9, 10, 11, 13, 14, 16, 19, 20, and 21 (Fig. 4). These new plies are oriented with the fiber direction at 90 degrees, have thicknesses equal to 5 x 0.0057 inches each, have modulus in the fiber direction equal to 10 x EMOD1(1), have all other moduli except the transverse shear moduli, G_{13} and G_{23}, set very small (0.00001 psi), and have the Poisson ratio and density equal to zero. With these material properties the two new layers have very high bending stiffness in the 90-degree (meridional) direction yet carry none of the applied axial compression. As seen in Fig. 1f, the cross sections of these little reinforced segments do not deform significantly as the overall cross section buckles locally. (Compare Fig. 1f with Fig. 1c).

Figure 23 shows, for the starting design listed in Table 3, critical **local** buckling mode shapes and load factors obtained from BIGBOSOR4 for local buckling models with 1, 3, 5, 7, and 9 modules of 22 segments each (Fig. 4). These local buckling modes have from five to seven axial half-waves along the length, FACLEN x LENGTH = 0.05 x 109 = 5.45 inches. The local buckling load factor converges from above to a value, 2.3583 (Fig. 23e) as the number of modules increases. Compare Fig. 23 with Fig. 22. Notice that in the ILINKS = 2 case (Fig. 23) there are significant rigid body displacements and rotations of those noodle gaps that are adjacent to segments that participate significantly in the critical local buckling mode. The converged local buckling load factor, eigenvalue = 2.3583, is therefore significantly less than the eigenvalues listed in Fig. 22 for EFNOOD > 10^7 lb/in^3, the buckling modes of which exhibit no such rigid body rotations or displacements of the noodle gaps. The converged critical local buckling load factor, 2.3583, from this "rigid segments" (ILINKS = 2) model significantly exceeds that obtained from a multi-module ILINKS = 0 model in which there are no gaps between segments and in which the elastic foundation stiffness, EFNOOD = 0. (See Fig. 9, eigenvalue=1.6075.) Therefore, it would be beneficial to optimize the truss-core sandwich wall with the index, ILINKS, set equal to 2 in order to simulate the support that each noodle gives to the little shell segments that enclose it.

It appears from these results that the "rigid segments" (ILINKS = 2, EFNOOD = 0) model is better than the "elastic foundation" (EFNOOD > 0, ILINKS = 0) model. In order to verify these results, a general-purpose computer program such as STAGS should be executed, with solid finite elements used in the noodle gaps to represent the noodles.

Representation of the noodle gaps as rigid links between shell segments (EFNOOD=0, ILINKS = 1)

Figure 24 shows, for the starting design listed in Table 3, local buckling from BIGBOSOR4 models in which the noodle gaps are replaced by rigid links where gaps occur between segments. Figure 24c demonstrates the model. Each axial noodle stiffener is represented by an "X", which is located at the centroid of its noodle gap. There are discontinuities (gaps) between segments, as displayed in Figs. 1d and 1e. The local buckling load factor converges from above to 2.3369 with respect to the number of modules used in the BIGBOSOR4 model for local buckling.

The predictions from this ILINKS = 1 model are similar to those from the ILINKS = 2 model, results from which appear in Fig. 23. It would be beneficial to obtain an optimum design of the truss-core sandwich wall with ILINKS set equal to 1, simulating the support that each noodle provides to the little shell segments that surround it.

Local buckling load factor versus the "hoop" modulus E of the "extra" inner and outer layers that stiffen the little segments that enclose each noodle when the index, ILINKS = 2

Figure 25 displays the results pertaining to this sub-section. The "hoop" modulus, E, is given by $E = EMOD1(1) \times 10^{exp}$, in which EMOD1(1) is the modulus in the fiber direction of material type 1. The "extra" inner and outer layers are like plies oriented at 90 degrees. Each "extra" layer has thickness equal to 5 x THICK(1) = 5 x 0.0057 inches. E is the modulus of the "extra" layers in the fiber direction of the "extra" layers (90 degrees from the direction of the axis of the cylindrical shell and lying in the plane of the cross section of the truss-core sandwich wall). Figure 25 shows that there is a range of "exp" (0 < exp < 4) for which the local buckling load factor is almost independent of "exp". It is not known why the predictions from BIGBOSOR4 yield increasing local buckling load factors for "exp" > 4. Perhaps round-off error plays a role. Data points corresponding to local buckling models with ILINKS = 0 and ILINKS = 1 are also plotted in Fig. 25. ILINKS = 0 corresponds to "exp" = minus infinity, and ILINKS = 1 corresponds to "exp" = plus infinity.

Optimization in the specific case called "nasatruss3" of the truss-core sandwich cross section with ILINKS = 2 and ILINKS = 1

Figures 26 and 27 and Table 8 pertain to this sub-section. With ILINKS = 0 the optimum weight/area is 0.006456 lb/in^2 (Fig. 16). With ILINKS = 2 the optimum weight/area is 0.006204 lb/in^2 (Fig. 26). With ILINKS = 1 the optimum weight/area is 0.006385 lb/in^2 (Fig. 27). For this particular example, in which all the ply thicknesses have already reached their lower bounds with

the use of the most conservative model, that is, with ILINKS = 0, the maximum decrease in optimized weight is only about 4 per cent (ILINKS=2). The decrease in optimized weight is only 1.1 per cent when ILINKS = 1 is used instead of ILINKS = 0. It is therefore probably best in this particular case to rely on the ILINKS = 0 model rather than take a chance with the possibly unconservative models in which ILINKS = 1 or ILINKS = 2.

The effect of using ILINKS = 1 or ILINKS = 2 rather than ILINKS = 0 is more significant with the starting design (Table 3) than with the optimized designs because the noodle gaps become smaller when the truss-core sandwich wall is optimized.

SECTION 11 DESIGN SENSITIVITY ANALYSIS

One of the three analysis options available in GENOPT is a design sensitivity analysis. Figure 28 contains plots of the most critical margins as functions of the height, HEIGHT, of the truss-core sandwich wall for the specific case called "**nasatruss3**". The design sensitivity analysis is based on the "**nasatruss3**" configuration previously optimized with the "noodle support" index, ILINKS = 0. (See PART 1 of Table 8). The height, HEIGHT, at the optimum is 0.58772 inches. In this case, as with most optimized designs, several of the design margins are zero in the immediate neighborhood of the optimum value of the decision variable being varied in the design sensitivity analysis, in this example in the immediate neighborhood of HEIGHT = 0.58772 inches.

The behavior is smooth in the neighborhood of the optimum design. This smooth behavior is a property that is associated with repeated convergence to the same objective, such as that exhibited in Fig 15 for the specific case, "**nasatruss2**". Optimized thin shells do not always exhibit such smooth behavior in the neighborhood of an optimum design. Figures 20 and 24 of [4K] (axially compressed, imperfect, stiffened cylindrical shell) provide an example in which the design margins are very sensitive to small changes in the decision variables, a characteristic that makes it difficult to find a "global" optimum. The user of GENOPT is urged to conduct design sensitivity studies in order better to understand the behavior of their specific system in the neighborhood of its optimum design.

SECTION 12 CONCLUSIONS

1. The GENOPT/BIGBOSOR4 system can be used to find minimum-weight designs of axially compressed cylindrical shells with composite truss-core sandwich wall construction.

2. Enough detail is presented here and in [3] and [6-8] so that other researchers can use GENOPT to create program systems for the optimization of other shell structures for which local buckling, general buckling, and stress constraints affect the evolution of the design during optimization cycles.

3. For the specific case, **nasatruss2**, which is a member of the generic class, **trusscomp**, the critical design margins at the optimum are local buckling, general buckling, compressive stress

in the direction of the fibers, and in-plane shear stress (thermal curing not included).

4. The cylindrical shell with the composite truss-core sandwich wall is modeled for BIGBOSOR4 as a true prismatic branched shell structure.

5. The effects of "noodles" and "noodle gaps" are significant, especially for local buckling.

6. At the optimum design the general buckling load factor (eigenvalue) is relatively insensitive to the number of axial half-waves in the general buckling mode.

7. Thermal curing has a significant effect on the stress constraints, especially the stress constraint that involves the tensile stress normal to the fibers. Predictions of the effect of thermal curing from PANDA2 agree with those from GENOPT/BIGBOSOR4.

8. At the optimum design in this particular case the layer thicknesses are at their lower bound: the thickness, 0.0057 inch, of a single ply. A significantly lighter optimum design can be obtained by setting the lower bound of a 90-degree ply to half the thickness of a single ply. The optimum design can still be fabricated because the two adjacent 90-degree plies in each laminate of the truss-core sandwich cross section can be replaced by a single 90-degree ply of thickness 0.0057 inch.

9. The STAGS input files, *.inp and *.inp2, are automatically generated by the GENOPT/BIGBOSOR4 system for local buckling and general buckling, respectively. Results for finite element models processed by STAGS and other general-purpose computer programs are given in [1].

10. A factor of safety of 1.3 is used for local buckling in order to compensate for the lack of the capability of BIGBOSOR4 to handle the effects of transverse shear deformation and local shell wall anisotropy.

11. A factor of safety of 1.0 is used for general buckling. This is generally not good practice. It was done here in order to make comparisons easier with predictions from general-purpose finite element codes [1].

12. The "rigid segments" ("noodle support" index, ILINKS = 2) and "rigid links" (ILINKS = 1) BIGBOSOR4 models for local buckling appear to be better than the "elastic foundation" BIGBOSOR4 model used to demonstrate the effect of the support by each noodle of the small shell segments that enclose that noodle. For the "starting" design (Table 3) the ILINKS = 2 and ILINKS = 1 models yield local buckling load factors that are about 45 per cent higher than that obtained from the ILINKS=0 model (1.6075 in Fig. 9 and about 2.34 in Figs. 23e and 24f). A STAGS model with solid finite elements in the noodle gaps should be constructed to verify this finding.

13. For the particular specific case explored here ("**nasatruss3**") the effect on optimum weight/area of optimizing with ILINKS = 2 or ILINKS = 1 rather than with the more conservative ILINKS = 0 is minor. This is because the noodle gaps in the **optimized**

configurations are smaller than those in the **starting** design (Table 8). It is therefore recommended that in similar cases optimizations be carried out with ILINKS = 0. Again, it is emphasized that STAGS finite element models should be set up in which the noodle gaps are filled with solid elements that simulate the presence of the noodles that fill the noodle gaps and support the little shell segments that enclose them.

SECTION 13 ACKNOWLEDGMENT

SECTION 14 REFERENCES

[1] Lovejoy, Andrew E., "Evaluation of Analysis Techniques for Cylinders of Truss-core Sandwich Construction", AIAA Paper 2011-xxxx, 52nd AIAA Structures, Structural Dynamics and Materials Meeting, Denver, Colorado, April 2011.

[2] Bushnell, David, "Optimum designs from PANDA2 of a uniformly axially compressed cylindrical shell with a composite truss-core sandwich wall and verification of the design by BIGBOSOR4", Unpublished report for NASA Langley Research Center, March 16, 2009.

[3] Bushnell, David, "Use of GENOPT and BIGBOSOR4 to obtain optimum designs of a cylindrical shell with a composite truss-core sandwich wall" Unpublished report for NASA Langley Research Center, June 20, 2009

[4] Bushnell, David, et al, **(A)** "PANDA2 - Program for minimum weight design of stiffened, composite, locally buckled panels", Computers and Structures, Vol. 25 (1987) pp. 469-605. See also: **(B)** "Theoretical basis of the PANDA computer program for preliminary design of stiffened panels under combined in-plane loads", Computers and Structures, v. 27, No. 4, pp 541-563, 1987; **(C)** "Optimization of composite, stiffened, imperfect panels under combined loads for service in the postbuckling regime", Computer Methods in Applied Mechanics and Engineering, Vol. 103, pp 43-114, 1993; **(D)** "Recent enhancements to PANDA2", 37th AIAA Structures, Dynamics, and Materials (SDM) Conference, April 1996; **(E)** "Approximate method for the optimum design of ring and stringer stiffened cylindrical panels and shells with local, inter-ring, and general buckling modal imperfections", Computers and Structures, Vol. 59, No. 3, 489-527, 1996, with W. D. Bushnell; **(F)** "Optimum design via PANDA2 of composite sandwich panels with honeycomb or foam cores", AIAA Paper 97-1142, AIAA 38th SDM Conference, April 1997; **(G)** "Additional buckling solutions in PANDA2", AIAA 40th SDM Conference, p 302-345, April 1999, with H. Jiang and N. F. Knight, Jr.; **(H)** "Minimum-weight design of a stiffened panel via PANDA2 and evaluation of the optimized panel via STAGS", Computers and Structures, Vol. 50, 569-602 (1994); **(I)** "Optimization of perfect and imperfect ring and stringer stiffened cylindrical shells with PANDA2 and evaluation of the optimum designs with STAGS", AIAA Paper 2002-1408, pp 1562-1613, Proceedings of the 43rd AIAA SDM Meeting, April, 2002, with C. Rankin; **(J)** "Optimum design of stiffened panels with substiffeners, AIAA Paper

2005-1932, AIAA 46th SDM Conference, April 2005, with C. Rankin; **(K)** "Difficulties in optimization of imperfect stiffened cylindrical shells, AIAA Paper 2006-1943, AIAA 47th SDM Conference, April 2006, with C. Rankin; **(L)**.../panda2/doc/panda2.news, a continually updated file distributed with PANDA2.

[5] Bushnell, David, "Automated optimum design of shells of revolution with application to ring-stiffened cylindrical shells with wavy walls", AIAA paper 2000-1663, 41st AIAA Structures Meeting, Atlanta, GA, April 2000. Also see Lockheed Martin report, same title, LMMS P525674, November 1999

[6] Bushnell, David, "GENOPT--A program that writes user-friendly optimization code", International Journal of Solids and Structures, Vol. 26, No. 9/10, pp. 1173-1210, 1990. The same paper is contained in a bound volume of papers from the International Journal of Solids and Structures published in memory of Professor Charles D. Babcock, formerly with the California Institute of Technology.

[7] Bushnell, David, "Minimum weight design of imperfect isogrid-stiffened ellipsoidal shells under uniform external pressure", AIAA paper 2009-2702, 50th AIAA Structures Meeting, Palm Springs, CA, May 4-7, 2009

[8] **a.** Bushnell, David and Thornburgh, Robert P., "Use of GENOPT and BIGBOSOR4 to optimize weld lands in axially compressed stiffened cylindrical shells and evaluation of the optimized designs by STAGS" AIAA Paper 2010-2927, 51st AIAA Structures, Materials and Dynamics Meeting, Orlando, FL, April, 2010. See also: **b.** Bushnell, David, "Use of GENOPT and a BIGBOSOR4 "huge torus" model to optimize a typical weld land and weld land edge stringers in a previously optimized internally stiffened cylindrical shell without weld lands, unpublished report sent to NASA Langley Research Center, May 15, 2009.

[9] Bushnell, David, "Stress, buckling, and vibration of prismatic shells", AIAA Journal, Vol. 9, No. 10, pp.204-213, October, 1971.

[10] Bushnell, David, "Comparison of a "huge torus" model with a true prismatic model for: 1. an axially compressed simple monocoque cylindrical shell, 2. an axially compressed optimized truss-core sandwich cylindrical shell, and 3. an axially compressed optimized internally ring and stringer stiffened cylindrical shell with a T-stiffened weld land, Unpublished report for NASA Langley Research Center, February 12, 2010 and contained in the file, ...bigbosor4/case/prismatic/prismaticshell.pdf

[11] Vanderplaats, G. N., "ADS--a FORTRAN program for automated design synthesis, Version 2.01", Engineering Design Optimization, Inc, Santa Barbara, CA, January, 1987

[12] Vanderplaats, G. N. and Sugimoto, H., "A general-purpose optimization program for engineering design", Computers and Structures, Vol. 24, pp 13-21, 1986

[13] Bushnell, David, "Optimization of an axially compressed ring and stringer stiffened cylindrical shell with a general buckling modal imperfection", AIAA Paper 2007-2216, AIAA

48th Structures Meeting, Honolulu, Hawaii, May, 2007

[14] Bushnell, David, The file, .../panda2/case/nasacoldbend/coldbending.pdf, included with the PANDA2 documentation. Also, see Item No. 790 in Ref. [4L].

[15] B. O. Almroth, F. A. Brogan, "The STAGS Computer Code", NASA CR-2950, NASA Langley Research Center, Hampton, Va.(1978)

[16] C. C. Rankin, P. Stehlin and F. A. Brogan, "Enhancements to the STAGS computer code", NASA CR 4000, NASA Langley Research Center, Hampton, Va, November 1986

[17] Riks, E., Rankin C. C., Brogan F. A., "On the solution of mode jumping phenomena in thin walled shell structures", First ASCE/ASM/SES Mechanics Conference, Charlottesville, VA, June 6-9, 1993, in: Computer Methods in Applied Mechanics and Engineering, Vol.136, 1996.

[18] G. A. Thurston, F. A. Brogan and P. Stehlin, "Postbuckling analysis using a general purpose code", AIAA Journal, 24, (6) (1986) pp. 1013-1020.

[19] Bushnell, David, "Stress, stability and vibration of complex, branched shells of revolution", Computers & Structures, vol. 4, pp 399-435 (1974)

[20] Bushnell, Bill D., "Using GENOPT to minimize the noise of a two-stage RF amplifier", LMSC Report F318422, Lockheed Missiles & Space Company, March 14, 1991

[21] Jegley, Dawn C., "A Study of the Structural Efficiency of Fluted Core Graphite-Epoxy Panels", NASA TM 101681, January, 1990.

[22] Bushnell, D.: "BOSOR4 – Program for Stress Stability and Vibration of Complex, Branched shells of Revolution", in STRUCTURAL ANALYSIS SYSTEMS, A. Niku-Lari, editor, Vol. 2, pp. 25-54, Pergamon Press, 1986

[23] Bushnell, D., Supplemental reports written in September, 2010, as follows:
/home/progs/genopt/case/trusscomp/trusscomp.sup.docx
/home/progs/genopt/case/trusscomp/nasatruss2.sup.docx
/home/progs/genopt/case/trusscomp/nasatruss3.sup.docx
/home/progs/genopt/case/trusscomp/isotruss.sup.docx
/home/progs/genopt/case/trusscomp/isotruss2.sup.docx

Table 1 Glossary of variables used in the generic case, "trusscomp". The variable names and one-line definitions are created by the GENOPT user. This list is produced automatically by GENOPT as part of the trusscomp.DEF file.

```
=================================================================================
ARRAY  NUMBER OF            PROMPT
  ?   (ROWS,COLS)  ROLE   NUMBER  NAME        DEFINITION OF VARIABLE
                          (trusscomp.PRO)
=================================================================================

  n  (   0,   0)     2       10   LENGTH = length of the cylindrical shell
  n  (   0,   0)     2       20   FACLEN = fraction of LENGTH for local buckling
  n  (   0,   0)     2       25   RADIUS = inner radius of the cylindrical shell
  n  (   0,   0)     1       30   PITCH  = circumferential width of a single module
  n  (   0,   0)     1       35   BCROWN = circumferential width of the trapezoid crown
  n  (   0,   0)     1       40   HEIGHT = height of the truss-core sandwich
  n  (   0,   0)     2       50   IWRAP  = Fabrication method,  0  or  1
  n  (   0,   0)     1       55   RACUTE = local radius from base to side of trapezoidal tool
  n  (   0,   0)     1       60   ROBTUS = local radius from side to crown of trapezoidal tool
  n  (   0,   0)     2       65   ENOODL = axial modulus of a corner "noodle"
  n  (   0,   0)     2       70   GNOODL = shear modulus of noodle
  n  (   0,   0)     2       75   DNOODL = weight density of the "noodle" material
  n  (   0,   0)     2       80   EFOUND = elastic foam "Winkler" foundation stiffness
  n  (   0,   0)     2       85   EFNOOD = elastic "noodle" Winkler foundation modulus
  n  (   0,   0)     2       90   IEMOD1 = material type in EMOD1(IEMOD1)
  y  (  10,   0)     2       95   EMOD1  = elastic modulus in the fiber direction
  y  (  10,   0)     2      100   EMOD2  = elastic modulus transverse to fibers
  y  (  10,   0)     2      105   G12    = in-plane shear modulus
  y  (  10,   0)     2      110   G13    = out-of-plane x-z shear modulus
  y  (  10,   0)     2      115   G23    = out-of-plain y-z shear modulus
  y  (  10,   0)     2      120   NU     = minor (small) Poisson ratio
  y  (  10,   0)     2      125   ALPHA1 = coef. of thermal expansion along the fibers
  y  (  10,   0)     2      130   ALPHA2 = coef. of thermal expansion transverse to fibers
  y  (  10,   0)     2      135   TEMCUR = curing temperature difference
  y  (  10,   0)     2      140   DENSTY = weight density of material
  n  (   0,   0)     2      145   ITHICK = layer type (thickness,layup angle,material type)
  y  (  30,   0)     1      150   THICK  = layer type thickness
  y  (  30,   0)     2      155   ANGLE  = layer type layup angle
  y  (  30,   0)     2      160   MATTYP = layer type material type
  n  (   0,   0)     2      165   JLAYTYP= shell segment number in LAYTYP(ILAYTYP,JLAYTYP)
  n  (   0,   0)     2      170   ILAYTYP= layer number in LAYTYP(ILAYTYP,JLAYTYP)
  y  (  90,  50)     2      175   LAYTYP = layer type
  n  (   0,   0)     2      180   NLAYRF = number of layers in each face sheet
  n  (   0,   0)     2      185   NLAYRC = number of layers around trapezoidal tool
  n  (   0,   0)     2      190   INTEXT = 0=pressure on top face sheet; 1=bottom face sheet
  n  (   0,   0)     2      200   ILINKS = type of BIGBOSOR4 model for local buckling
  n  (   0,   0)     2      210   ICLAMP = Choose 0 (free) or 1 (clamped); LOCAL buckling model
  n  (   0,   0)     2      220   IELMNT = type of STAGS finite element
  n  (   0,   0)     2      230   NROWSL = number of rows: STAGS local buckling model
  n  (   0,   0)     2      235   NROWSG = number of rows: STAGS general buckling model
```

```
n  (   0,   0)   2    240   NCOLSG = number of columns/segment: STAGS general buckling
n  (   0,   0)   2    250   NMODULL= number of modules for local buckling
n  (   0,   0)   2    255   MLOWG  = low end of the M-range for general buckling
n  (   0,   0)   2    260   MHIGHG = high end of the M-range for general buckling
n  (   0,   0)   2    265   MLOWL  = low end of the range of local buckling waves
n  (   0,   0)   2    270   MHIGHL = high end of the M-range for local buckling
n  (   0,   0)   2    275   NCASES = Number of load cases (number of environments)
y  (  20,   0)   3    280   PX     = total axial load (2 x pi x r x resultant)
y  (  20,   0)   3    285   PRESS  = pressure (negative for external pressure)
y  (  20,   0)   3    290   PX0    = total "Load Set B" load
y  (  20,   0)   3    295   PRESS0 = "Load Set B" pressure (external=negative)
y  (  20,   0)   4    300   LOCBUK = local buckling load factor
y  (  20,   0)   5    305   LOCBUKA= allowable for local buckling load factor
y  (  20,   0)   6    310   LOCBUKF= factor of safety for local buckling
y  (  20,   0)   4    315   GENBUK = general buckling load factor
y  (  20,   0)   5    320   GENBUKA= allowable for general buckling load factor
y  (  20,   0)   6    325   GENBUKF= general buckling factor of safety
n  (   0,   0)   2    330   JSTRM1 = number of stress constraints in STRM1(NCASES,JSTRM1)
y  (  20,   6)   4    335   STRM1  = stress component in material 1
y  (  20,   6)   5    340   STRM1A = allowable stress in material 1
y  (  20,   6)   6    345   STRM1F = factor of safety for stress in material 1
y  (  20,   6)   4    350   STRM2  = stress component in material 2
y  (  20,   6)   5    355   STRM2A = allowable for stress in material 2
y  (  20,   6)   6    360   STRM2F = factor of safety for stress in material 2
n  (   0,   0)   7    365   WEIGHT = weight/area of the truss-core sandwich wall
=============================================================================
```

Table 2 The entire file, trusscomp.PRO, generated automatically by GENOPT during the GENTEXT interactive session. The variable names, one-line definitions, and "help" paragraphs are created by the GENOPT user. The prompting numbers and overall format of the *.PRO file are created by GENOPT.

```
=========================================================================
    5.0
        Please read the paper and the report:

        REFERENCE [1]:
        "Use of GENOPT and BIGBOSOR4 to obtain optimum designs
        of an axially compressed cylindrical shell with a
        composite truss-core sandwich wall", David Bushnell
        and Charles Rankin, AIAA Paper 2010-xxxx, 52nd AIAA
        structures meeting, Denver, CO, April 2011.
        NOTE: The references to figure numbers are from that
        paper. This is Reference [1] referred to below.

        REFERENCE [3] cited in Reference [1]:
        "Use of GENOPT and BIGBOSOR4 to obtain optimum designs
        of a cylindrical shell with a composite truss-core
        sandwich wall", David Bushnell, June 20, 2009

        This GENOPT case is for a cylindrical shell the wall of
        which is a truss-core sandwich. Each segment of a truss-
        core sandwich module may be a composite laminate. Hence,
        the name, "trusscomp". The truss-core module used for local
        buckling consists of 22 shell segments of the type used
        in BIGBOSOR4. Figure 4 shows the segment numbering and
        direction of travel along each segment. Up to nine 22-segment
        modules may be chained together to form the model used for
        local buckling (Figs.23,24). The truss-core sandwich module
        used for general buckling consists of 6 shell segments. Fig.
        6 (top) shows the segment numbering and direction of travel
        along each segment. Many 6-segment modules are chained together
        (46 modules) to form the model used for general buckling (Fig.1b).
        General and local buckling load factors are determined
        from BIGBOSOR4. The shell is modeled as a part of a "huge
        torus" (Fig.1a). A membrane prebuckled state is assumed to exist.
        The axial resultant in each module segment is assumed to
        be proportional to the axial stiffness of that segment (Fig.1g).
```

Local buckling can be determined from a single module (Fig.1c,
1e,1f) or from a multiple-module model (Figs 1d,3a,3b,23,24).
General buckling is determined from a number of analogous
simpler modules (Fig.6) strung together. The stress constraints
are computed from a much simplified version of the code
in SUBROUTINE STRTHX of BIGBOSOR4, simplified because
the prebuckled state is a membrane state. The stresses
are computed in each layer in each truss-core sandwich
segment.

Occasionally an optimization run with SUPEROPT may
abort early. If this happens, inspect the end of the
xxx.OUT file to see if there are any error messages. You
may have to modify your inequality constraints in the
xxx*DEC file (input to "DECIDE") in order to avoid
an early and unexpected termination of the SUPEROPT run.
Most of the early terminations of the SUPEROPT run can
be avoided by increasing the lower bound of the thickness
of the truss-core, that is, increasing the lower bound
of the variable called "HEIGHT".

10.1 length of the cylindrical shell: LENGTH
10.2
      NOTE: the cylindrical shell is assumed to be simply
      supported along its two curved ends. See Section 2 of
      Reference [1] for a discussion concerning these boundary
      conditions.

15.0
      Next you will be asked to provide the fraction
      of the shell axial length to be used in the
      local buckling analysis. If the shell is
      subjected to uniform end shortening (axial
      compression), then this fraction of the total
      shell length can be estimated by assuming that
      the critical buckling mode will have approximately
      square buckles. The portion of the truss-core
      sandwich most likely to buckle will probably have the
      longest unsupported width. Suppose the total
      length of the cylindrical shell is 100 inches.
      Suppose the width of the segment of the truss-core
      sandwich most likely to buckle locally is 2 inches.
      Then, for square buckles, the critical local buckling
      mode will have approximately 50 half-waves along
      the total axial length of the cylindrical shell.
      In order to save computer time you don't want to
      have to search over a large range of axial half-waves.

American Institute of Aeronautics and Astronautics

Therefore, in this example, choose a fraction, FACLEN,
of axial length equal to about 1/10th (FACLEN=0.1). Then
the critical local buckling mode will have about 5 axial
half-waves over the length, 0.1 x LENGTH = 10 inches,
and you can establish the range of axial half-waves
to be covered to be from 1 to 10 axial halfwaves.
(MLOWL = 1, MHIGHL = 10). The critical local buckling mode
will probably be somewhere near the middle of this range.

20.1 fraction of LENGTH for local buckling: FACLEN
20.2

If the cylindrical shell is subjected to axial compression
set FACLEN such that if the local buckles are square the
critical local buckling mode will fall in the middle of
the range of axial wave numbers, MLOWL to MHIGHL, that
you will later establish during this interactive session.

25.1 inner radius of the cylindrical shell: RADIUS
25.2

This is the radius to the middle surface of the INNER
face sheet of the truss-core sandwich wall.

30.1 circumferential width of a single module: PITCH
30.2

A single module consists essentially of one "upside-
down" trapezoid and its adjacent "rignt-side-up"
neighbor. There are 22 shell segments in the single
truss-core sandwich module used for local buckling.
(See Fig. 4.) PITCH is called "b" in Fig. 4.

35.1 circumferential width of the trapezoid crown: BCROWN
35.2

BCROWN is the width of the narrow horizontal face of
the trapezoid. BCROWN is called "b2" in Fig. 4.

40.1 height of the truss-core sandwich: HEIGHT
40.2

HEIGHT is measured from the middle surface of the
bottom face sheet to the middle surface of the top
face sheet. HEIGHT is called "h" in Fig. 4.

45.0

Next, you will be asked to provide the index, IWRAP.
IWRAP can be 0 or 1 .
IWRAP = 0 means that the truss-core sandwich wall is
fabricated by forming and curing three parts separately:
PART 1: The corrugated core

```
       PART 2: The lower face sheet
       PART 3: The upper face sheet
       After the forming and curing of these three parts the lower
       and upper face sheets are cold-bonded to the corrugated core.

       IWRAP = 1 means that the entire truss-core sandwich wall is
       formed and cured at the same time. The core is formed by
       wrapping right-side-up and upside-down trapezoidal mandrels
       with NLAYRC layers of composite material, then laying the
       bottom and top face sheets that each have NLAYRF layers.
       Then the entire truss-core assembly is cured together.

50.1 Fabrication method,  0  or  1: IWRAP
50.2
       Use IWRAP = 0 if the core is formed by stamping and
       then cold-bonding the corrugated core to the face sheets.
       Use IWRAP = 1 if the core is formed by wrapping
       trapezoidal mandrels and curing everything together.
       NOTE: If IWRAP = 0 the two radii, RACUTE and ROBTUS,
       will always be reset to zero no matter what you
       provide as input values. It is ordinarily best to use
       IWRAP = 0 if the truss-core sandwich is made of metal.


55.1 local radius from base to side of trapezoidal tool: RACUTE
55.2
       RACUTE is the transition radius by means of which
       the base surface of the trapezoidal tool is smoothly
       faired into the sloping side walls of the trapezoidal
       tool. The trapezoidal tool is the object around which
       the layers of the core laminate are laid up. RACUTE
       is the radius that spans the acute angle from trapezoid
       base to trapezoid sloping sides. RACUTE is similar
       to the dimension called "R1" in Fig. 4.
       (R1 = RACUTE + total thickness of shell segment 5 in Fig.4).


60.1 local radius from side to crown of trapezoidal tool: ROBTUS
60.2
       ROBTUS is the radius that fairs each side wall of the
       trapezoidal tool into the crown of the trapezoidal
       tool. The trapezoidal tool is the object around which
       the core laminate is laid up. ROBTUS is the radius
       that spans the obtuse angle from trapezoid crown to
       trapezoid sloping sides. ROBTUS is similar
       to the dimension called "R2" in Fig. 4.
       (R2 = ROBTUS + total thickness of shell segment 2 in Fig.4).


65.1 axial modulus of a corner "noodle": ENOODL
65.2
```

American Institute of Aeronautics and Astronautics

ENOODL is the axial modulus of the "noodle"
material. A "noodle" is the material that is
fills a "corner" (gap) between adjacent trapezoidal
core segments. Each truss-core sandwich module has
four "noodles", two at the bottom and two at the top
of the single module in Fig.4. The "noodles" fit into
the triangular-like gaps adjacent to the slanted
core walls and the bottom and top face sheets. For
example, one of the "triangular" gaps shown in Fig. 4
is the small region enclosed by shell segments 2, 3,
4, and 5. ENOODL is the axial modulus of the
material that fills each of the four "triangular"
prismatic cavities in the single truss-core sandwich
module. Each "noodle" is treated in the BIGBOSOR4
model as one discrete beam (general buckling model)
or as two discrete beams (local buckling model)
attached to one or two of the curved shell segments
that enclose the "noodle".

70.1 shear modulus of noodle: GNOODL
70.2
   See the "help" paragraph for ENOODL in the xxx.PRO file.

75.1 weight density of the "noodle" material: DNOODL
75.2
   DNOODL is the density analogous to that of
   aluminum's weight density of 0.1 lb/in^3. Usually,
   the "noodle" will be made from the same material
   as one of the layers in the truss-core. If so,
   just use the same value for DNOODL as you will
   use later for the material density of one
   of the layers in the truss-core laminate.

80.1 elastic foam "Winkler" foundation stiffness: EFOUND
80.2
   EFOUND is used only for the LOCAL buckling analysis.
   The volume inside the truss-core sandwich may
   be filled with an elastic foam that is bonded
   to the face sheets and sloping side walls of
   the core. A Winkler foundation is assumed. A Winkler
   foundation reacts only normal to the shell surface;
   it is like an array of closely spaced springs
   oriented normal to the shell surface. Units of the
   foundation stiffness, K, are force per length
   cubed (lb/in**3, for example). IMPORTANT NOTE:
   The elastic foundation is assumed to be connected
   to GROUND. Therefore, the elastic foam inside each
   truss core module CANNOT TRANSLATE AND ROTATE AS

34
American Institute of Aeronautics and Astronautics

A RIGID BODY. Hence, the elastic foam is assumed
to be present ONLY IN THE LOCAL BUCKLING ANALYSIS.
Still, it is probably somewhat unconservative to
include a non-zero EFOUND in your model unless
you use a significantly conservative value for
EFOUND, that is, an underestimate of what you think
EFOUND might actually be. It is probably best first
to optimize with EFOUND = 0.0, then possibly re-
optimize with some small non-zero value of EFOUND later.

85.1 elastic "noodle" Winkler foundation modulus: EFNOOD
85.2

EFNOOD is used only for the LOCAL buckling analysis.
EFNOOD is the effective elastic foundation stiffness
that supports the segments of the single module
that form triangular-shaped gaps (Fig. 1c) adjacent
to the slanted webs of the truss-core and the
bottom and top face sheets. EFNOOD is a "noodle"
property. A Winkler foundation is assumed. A Winkler
foundation reacts only normal to the shell surface;
it is like an array of closely spaced springs
oriented normal to the shell surface. Units of the
foundation stiffness, K, are force per length
cubed (lb/in**3, for example). Note that the same
comment applies to EFNOOD that occurs in the "help"
paragraph associated with the variable, EFOUND.
In Reference [1] there is a study of the effect of
the noodle elastic foundation stiffness, EFNOOD,
on the local buckling load factor and mode shape (Fig.22).
Also in Reference [1] there are results from "LINKS=1"
and from "ILINKS=2" models. In the "LINKS=1" model
the effect of the support provided by each noodle
to the little shell segments that enclose it is
simulated by rigid links between shell segments that
have gaps between them. See Fig. 24 and the discussion
associated with Fig. 24 in Reference [1]. In the
"ILINKS=2" model the bending stiffnesses in the plane
of the truss-core sandwich cross section of the
little shell segments that enclose each noodle
are greatly increased by adding thick inner and outer
layers with very high modulus in the meridional
direction, with essentially zero in-plane shear
modulus and with essentially zero modulus in the
axial direction.

90.1 Number IEMOD1 of rows in the array EMOD1: IEMOD1
95.1 elastic modulus in the fiber direction: EMOD1
100.1 elastic modulus transverse to fibers: EMOD2

105.1 in-plane shear modulus: G12
110.1 out-of-plane x-z shear modulus: G13
115.1 out-of-plain y-z shear modulus: G23
120.1 minor (small) Poisson ratio: NU
120.2

      NU is the "NU21" Poisson ratio, governed by the
      equation, E1*NU21 = E2*NU12. (Same input as for
      BOSOR4 and PANDA2).

125.1 coef. of thermal expansion along the fibers: ALPHA1
130.1 coef. of thermal expansion transverse to fibers: ALPHA2
135.1 curing temperature difference: TEMCUR
135.2

      TEMCUR is the difference between the temperature
      at which the material "sets" during curing and the
      service ("room") temperature. Use a POSITIVE number.

140.1 weight density of material: DENSTY
140.2

      For example, Aluminum = 0.1 lb/in^3

145.1 Number ITHICK of rows in the array THICK: ITHICK
150.1 layer type thickness: THICK
155.1 layer type layup angle: ANGLE
160.1 layer type material type: MATTYP
165.1 Number JLAYTYP of columns in the array, LAYTYP: JLAYTYP
170.1 Number ILAYTYP of rows in this column of LAYTYP: ILAYTYP
175.1 layer type: LAYTYP
175.2

      LAYTYP(layer no., segment no.) identifies the type of
      that particular layer in "segment no." of the single
      module model (Fig.4). LAYTYP(layer no., segment no.)
      points to the layer with a certain thickness, THICK,
      layup angle, ANGLE, and material type, MATTYP.

180.1 number of layers in each face sheet: NLAYRF
180.2

      This is the number of layers, such that when
      added to the number of layers wrapped around the
      trapezoidal tool (NLAYRC, the next role 2 variable),
      gives the total number of layers in the laminate
      that forms the wall of the horizontal shell
      segments that run along the base and crown of
      each trapezoidal segment of the truss-core
      sandwich structure. See Figs. 4 and 8 of Ref.[1].

185.1 number of layers around trapezoidal tool: NLAYRC
185.2

NLAYRC is the number of layers wrapped around the trapezoidal
tool, that is, the number of layers in the truss core.
For the upper and lower face sheets NLAYRC is added to
the number of layers, NLAYRF, to form the total number
of layers in the horizontal shell segment walls.
The number of layers in the truss-core webs will be
2 x NLAYRC. See Fig. 8.

190.1 0=pressure on top face sheet; 1=bottom face sheet: INTEXT
190.2
       INTEXT = 0 means pressure acts on the top face sheet.
       INTEXT = 1 means pressure acts on the bottom face sheet.
       In the model used here the circumferential resultant
       in each face sheet is assumed to be (PRESS x RADIUS)/2.
       in which PRESS is the applied pressure (negative for
       external pressure), and RADIUS is the radius of the
       cylindrical shell. (Not checked as of October, 2010).

195.0
       You will next be asked to provide an index, ILINKS, for
       the type of BIGBOSOR4 model. ILINKS is a "noodle support"
       index that affects only LOCAL buckling. ILINKS means:

       ILINKS = 0 means an "ordinary" BIGBOSOR4 local buckling
       model such as those displayed in Figs. 2, 3, and 9 of Ref.[1].
       The noodle does not support the little shell segments
       that enclose it. This is a conservative assumption, and
       ILINKS = 0 is the recommended option.

       ILINKS = 1 means a "rigid links" BIGBOSOR4 local buckling
       model such as those shown in Figs 1d, 1e and 24: BIGBOSOR4
       models with discontinuities (gaps) between segments that
       represent the noodle gaps. The ILINKS = 1 model is based
       on the assumption that the noodle material supports the
       little shell segments (Fig. 4) that enclose each noodle
       and that this support is "rigid", that is, the cross
       section of the noodle cannot deform but can translate
       and rotate in the buckling mode shape. ILINKS = 1 leads
       to a BIGBOSOR4 model for local buckling that is sometimes
       unconservative. However, you can, with ILINKS = 1,
       optain an approximate idea how much the noodle support
       increases the local buckling load factor. Compare Fig. 24b
       with Fig. 9 to see how the "noodle support" index, ILINKS=1,
       affects local buckling. NOTE: Gaps between shell
       segments are never used in the general buckling models.

       ILINKS = 2 means a BIGBOSOR4 local buckling model analogous

to the elaborate 22-segment module depicted in Fig. 4
except that two additional thick layers are added to the
little shell segments that surround each noodle gap: an
inner thick layer and an outer thick layer. These extra
layers act to prevent meridional bending in the huge
torus model (hoop bending in the prismatic model). Hence,
the little shell segments that surround each noodle gap
essentially translate and rotate as "rigid" bodies,
simulating strong support by the noodle within the noodle
gap. ILINKS=2 is probably better than ILINKS = 1 because
BIGBOSOR4 sometimes yields unconservative buckling
load factors in models with gaps between shell segments.
(See page 52 of Ref.[22] that is cited in Ref.[1].)
NOTE: There are no gaps between shell
segments in the ILINKS = 2 model for local buckling.
It is recommended that you first optimize with ILINKS = 0
and then, for the optimized design, see what results you
obtain with ILINKS = 2 , then see what results you obtain
with ILINKS = 1 for the optimized design. See Figs. 26 and
27 of Ref.[1] for optimizations with ILINKS = 2 and
with ILINKS = 1, respectively.

200.1 type of BIGBOSOR4 model for local buckling: ILINKS
200.2

ILINKS = 0 means an "ordinary" BIGBOSOR4 model of the
truss-core sandwich cross section (no gaps between shell
segments). Noodles do NOT support the enclosing segments.

ILINKS = 1 means that the noodle gaps are replaced by
rigid links between shell segments (Fig. 24). Also see
Fig. A1 on p. 52 of Ref.[22] cited in Ref.[1].

ILINKS = 2 means that the little shell segments that
surround each noodle are given extra thick layers that
greatly raise their bending stiffness in the plane of
the cross section of the truss-core sandwich wall (Fig.23).
It is recommended that you use ILINKS = 0 for initial
optimization, then check the behavior of the optimized
design with the use of ILINKS = 2 in order to get an
approximate idea of how much the support of each noodle
on the little shell segments that enclose the noodle
(Fig. 4) affects the local buckling load factor and
mode shape. See Figs. 26 and 27 of Ref.[1] for
optimizations with ILINKS=2 and ILINKS=1, respectively.

205.0
You will next be asked to provide an index, ICLAMP, that

governs the boundary condition to be applied to the two
axially oriented edges (generators) of the LOCAL buckling
model. (Those edges are always simply supported in the
GENERAL buckling model.) ICLAMP = 0 means that the two
straight edges are unrestrained. ICLAMP = 1 means that the
two straight edges in the LOCAL buckling model are clamped.
If you plan to use three modules or more in the LOCAL
buckling analysis, then ICLAMP = 1 is the best choice.
However, the use of more than three modules in the LOCAL
buckling analysis leads to long computer times for
optimization. If you plan to use one module for LOCAL
buckling (Fig. 2 in Reference [1]), then the best choice
for ICLAMP depends on the case. If the truss-core sandwich
is to be made of isotropic material, then ICLAMP = 1 seems
to be the best choice. If laminated composite material is
to be used then ICLAMP = 0 seems to be the best choice.
If you don't have a preference, ICLAMP = 0 is the more
conservative choice. You can optimize with the use of a
one-module LOCAL buckling model, then check the optimized
design with a multi-module LOCAL buckling model (Fig. 3 in
Reference [1]) with both ICLAMP = 1 and ICLAMP = 0. If it
turns out that there is a significant difference in the two
predictions, you can do more optimization, this time with
a multi-module LOCAL buckling model with at least three
modules and with ICLAMP = 1. Recommended: 3 modules, ICLAMP=1
NOTE: ICLAMP does not affect STAGS models.

210.1 Choose 0 (free) or 1 (clamped) for LOCAL buckling model: ICLAMP
210.2
     If you plan to use a multi-module model (Fig.3) for LOCAL
     buckling (at least three modules) use ICLAMP = 1. If you plan
     to use a one-module LOCAL buckling model choose ICLAMP = 0
     (the more conservative choice) for initial optimization,
     then check the optimized design with the use of a multi-
     module model (at least three modules) with ICLAMP = 1 .
     Recommended: use 3 modules and use ICLAMP=1

215.0
     You will next be asked to identify which STAGS
     finite element (410, 480, or 940) to use in STAGS
     models of the optimized design.

220.1 type of STAGS finite element: IELMNT
220.2
     It is recommended that you choose either 480 or 940
     because these STAGS finite elements include the effect
     of transverse shear deformation, which is especially

significant in the local buckling of laminated composite
truss-core sandwich shell walls. Also, use of the STAGS
410 finite element often leads to spurious modes for
general buckling.

225.0

Next, you will be asked to provide the mesh density
to be used in the various STAGS models. You will be asked
for the following:
1. NROWSL = number of rows in the STAGS local buckling model
2. NROWSG = number of rows in the STAGS general buckling model
3. NCOLSG = number of columns in each segment of the STAGS
general buckling model.

A suggestion: NROWSL = 51, NROWSG = 101, NCOLSG = 5 (Fig.20).
If, after you have executed STAGS with the use of both the
local buckling and general buckling models, you can always
restart the specific case with more appropriate values used
for NROWSL, NROWSG, and NCOLSG.

Keep in mind that local buckles tend to be square, and
that the axial length of the STAGS model for local buckling
is equal to FACLEN x LENGTH. You can compute what will
probably be close to the axial half-wavelength of the
critical local buckling mode shape, using the assumptions
that the local buckles are squarish and the axial length
of the STAGS local buckling model is FACLEN x LENGTH.
NOTE: The number of columns to be used in each segment of
the STAGS LOCAL buckling model is assigned internally.

230.1 number of rows: STAGS local buckling model: NROWSL
230.2

NROWSL must be odd. NROWSL = number of nodes in the
axial diection in a STAGS LOCAL buckling model.
Try 51, and if that turns out to be a poor choice
increase it or decrease it after you have run a STAGS
local buckling model. An appropriate value for NROWSL
depends on the values you provided for LENGTH and FACLEN.
Keep in mind that local buckles tend to be square, and
that the axial length of the STAGS model for local buckling
is equal to FACLEN x LENGTH. You can compute what will
probably be close to the axial half-wavelength of the
critical local buckling mode shape, using the assumptions
that the local buckles are squarish and the axial length
of the STAGS local buckling model is FACLEN x LENGTH.

235.1 number of rows: STAGS general buckling model: NROWSG

American Institute of Aeronautics and Astronautics

235.2
    NROWSG must be odd. Try NROWSG = 101, then change it later
    if that choice turns out to be inappropriate from your
    experience with a STAGS general buckling execution.
    NROWSG = number of nodes in the axial direction in the
    STAGS GENERAL buckling model.

240.1 number of columns/segment: STAGS general buckling: NCOLSG
240.2
    NCOLSG must be odd. Try NCOLSG = 3, then increase it later
    if a STAGS general buckling analysis reveals that NCOLSG = 3
    may be too small. If NCOLSG=3 is too small, try NCOLSG=5 next.
    If NCOLSG = 5 is too small, try NCOLSG = 7 next. NOTE: the
    size of the eigenvalue problem increases dramatically with
    each increase in NCOLSG. You may find that you need more
    memory in order to obtain a converged solution for general
    buckling. Fig. 20b in Ref.[1] shows part of a STAGS
    general buckling model in which NCOLSG = 5 .

245.0
    You will next be asked to provide the number of modules
    to be used in the model for LOCAL buckling (NMODULL)
    you should use NMODULL = 3 until you have a preliminary
    optimum design. Then, to refine the design, possibly
    optimize again with NMODULL > 3 . Figures 23 and 24 of
    Ref.[1] show convergence of the local buckling load
    factor versus the number, NMODULL, of local buckling
    modules.
    NOTE: The computer time increases significantly the
    higher the value of NMODULL. Recommended: Use NMODULL = 3

250.1 number of modules for local buckling: NMODULL
250.2
    NMODULL is the number of modules, each of which
    contains 22 shell segments (Fig.4). In this application
    the best answer is usually 3 (that is, three modules).
    That is because the buckling (or stress) model
    that consists of 22 shell segments is used
    for obtaining LOCAL behavior, such as local
    buckling. Only three modules of 22 shell segments each
    is needed for the determination of LOCAL behavior
    with fair accuracy. However, there is some dependence
    of the local buckling load on the number of modules,
    as displayed in Figs 3, 23, and 24.
    After you have optimized with the use of NMODULL = 3
    you may want to check the optimum design with use of
    NMODULL = 5 or 7 or something like that. See Figs.

2, 3, 23, and 24 in Reference [1] for examples.

255.1 low end of the M-range for general buckling: MLOWG
255.2
        MLOWG should be 1 (an integer).

260.1 high end of the M-range for general buckling: MHIGHG
260.2
        Perhaps one should give a value 10 (or something
        like that). It depends on how many axial halfwaves
        you think will correspond to the critical general
        buckling mode. That number depends on the axial
        bending stiffness of the cylindrical shell wall,
        the length of the cylindrical shell, and the
        radius of the cylindrical shell. Use at least
        double the value of what you think is the critical
        value, that is, the value that corresponds to the
        lowest general buckling load. You may have to
        adjust the value of MHIGHG as your project proceeds.

265.1 low end of the range of local buckling waves: MLOWL
265.2
        You should use MLOWL = 1 because the axial length of
        the portion of the cylindrical shell to be used in the
        LOCAL buckling analysis is equal to LENGTH x FACLEN,
        in which LENGTH is the actual axial length of the
        cylindrical shell, and FACLEN is the fraction of
        LENGTH to be included in the local buckling model.

270.1 high end of the M-range for local buckling: MHIGHL
270.2
        We're referring here to the range of axial halfwaves
        to be used in the search for the critical LOCAL
        buckling load factor of the truss-core sandwich
        model. Use a number such as 10 and adjust it later
        if necessary. MHIGHL depends on what you used for
        the axial length fraction, FACLEN.

275.1 Number NCASES of load cases (environments): NCASES
280.1 total axial load (2 x pi x r x resultant): PX
280.2
        PX = 2 x pi x r x axial resultant. Units = lb,
        for example. PX is negative for axial compression.
        The axial resultant in each shell segment is computed
        as if the shell were subject to uniform end shortening
        and the prebuckled state is a membrane state (no
        imperfections, no bending, no end "boundary layers").
        See Fig. 1g for an example of a typical pre-buckled

state of the axially compressed cylindrical shell.

285.1 pressure (negative for external pressure): PRESS
290.1 total "Load Set B" load: PX0
290.2

     PX0 = 2 x pi x r x Nx0, in which Nx0 is an
     axial stress resultant. PX0 = positive for axial
     tension. Load Set B is the load set that is NOT to be
     multiplied by the buckling eigenvalue. NOT CHECKED.

295.1 "Load Set B" pressure (external=negative): PRESS0
295.2

     PRESS0 is positive for internal pressure. Load Set B
     is the load set that is NOT to be multiplied by
     the buckling eigenvalue. NOT CHECKED.

300.0 local buckling load factor: LOCBUK
305.1 allowable for local buckling load factor: LOCBUKA
305.2

     Usually, you supply 1.0 for LOCBUKA because LOCBUK is
     a buckling load FACTOR, that is, a quantity that is
     to be multiplied by the design loads, PX and PRESS,
     in order to obtain the buckling load.

310.1 factor of safety for local buckling: LOCBUKF
310.2

     In this "huge torus" model of the shell there cannot
     exist any specified initial imperfection. Therefore,
     you should probably use a factor of safety of 1.5
     or something like that. Also, the factor of safety
     for local buckling should be greater than unity
     especially in cases that involve laminated composite
     material in order to compensate for the fact that
     BIGBOSOR4 cannot handle the effects of transverse
     shear deformation (t.s.d.) or local shell wall
     anisotropy.

315.0 general buckling load factor: GENBUK
320.1 allowable for general buckling load factor: GENBUKA
320.2

     Usually, you supply 1.0 for GENBUKA because GENBUK is
     a buckling load FACTOR, that is, a quantity that is
     to be multiplied by the design loads, PX and PRESS,
     in order to obtain the buckling load.

325.1 general buckling factor of safety: GENBUKF
325.2

     In this "huge torus" model of the shell there cannot

exist any specified initial imperfection. Therefore,
you should probably use a factor of safety of 2.0
or something like that.

330.1 Number JSTRM1 of columns in the array, STRM1: JSTRM1
335.0 stress component in material 1: STRM1
335.2

For a composite laminate there are 6 stress components
for which stress constraints are generated:
1. maximum tensile stess in the fiber direction
2. maximum compressive stress in the fiber direction
3. maximum tensile stress transverse to the fibers
4. maximum compressive stress transverse to the fibers
5. maximum in-plane shear stress
6. maximum effective (VonMises) stress for an
isotropic layer.

340.1 allowable stress in material 1: STRM1A
340.2

For a composite laminate there are 6 stress components
for which stress constraints are generated:
1. maximum tensile stess in the fiber direction:
STRM1A(i,1), in which "i" is the load set number
2. maximum compressive stress in the fiber direction:
STRM1A(i,2), in which "i" is the load set number
3. maximum tensile stress transverse to the fibers:
STRM1A(i,3), in which "i" is the load set number
4. maximum compressive stress transverse to the fibers:
STRM1A(i,4), in which "i" is the load set number
5. maximum in-plane shear stress:
STRM1A(i,5), in which "i" is the load set number
6. maximum effective (VonMises) stress for an
isotropic layer:
STRM1A(i,6), in which "i" is the load set number

345.1 factor of safety for stress in material 1: STRM1F
345.2

In this "huge torus" model of the shell there cannot
exist any specified initial imperfection. Therefore,
you should probably use a factor of safety of 1.5
or something like that.

350.0 stress component in material 2: STRM2
355.1 allowable for stress in material 2: STRM2A
360.1 factor of safety for stress in material 2: STRM2F
365.0 weight/area of the truss-core sandwich wall: WEIGHT
365.2

WEIGHT = weight per surface area of the truss-core

sandwich shell wall.

999.0 DUMMY ENTRY TO MARK END OF FILE
==

Table 3 Edited version of the file, nasatruss2.OPM, corresponding to the starting design of "nasatruss2"

```
=================================================================
  STRUCTURAL ANALYSIS WITH UNPERTURBED DECISION VARIABLES
 VAR. DEC. ESCAPE LINK. LINKED  LINKING    LOWER    CURRENT   UPPER      DEFINITION
 NO. VAR.  VAR.   VAR.   TO     CONSTANT   BOUND     VALUE    BOUND
  1   Y     N      N     0      0.00E+00  5.00E-01 1.8400E+00 4.50E+00  circumferential width of a single module: PITCH
  2   Y     N      N     0      0.00E+00  1.00E-01 5.4000E-01 2.00E+00  circumfer. width of the trapezoid crown: BCROWN
  3   Y     N      N     0      0.00E+00  2.00E-01 6.9560E-01 2.00E+00  height of the truss-core sandwich: HEIGHT
  4   Y     N      N     0      0.00E+00  5.00E-02 1.0700E-01 2.00E-01  local radius from base to side of trapezoidal
tool: RACUTE
  5   Y     N      N     0      0.00E+00  5.00E-02 1.0700E-01 2.00E-01  local radius from side to crown of trapezoidal
tool: ROBTUS
  6   Y     Y      N     0      0.00E+00  5.70E-03 5.7000E-03 1.71E-01  layer type thickness: THICK(1 ) ←+45 degrees
  7   N     N      Y     6      1.00E+00  0.00E+00 5.7000E-03 0.00E+00  layer type thickness: THICK(2 ) ←-45 degrees
  8   N     N      Y     6      1.00E+00  0.00E+00 5.7000E-03 0.00E+00  layer type thickness: THICK(3 ) ←  0 degrees
  9   N     N      Y     6      1.00E+00  0.00E+00 5.7000E-03 0.00E+00  layer type thickness: THICK(4 ) ← 90 degrees
-----------------------------------------------------------


 LOCAL BUCKLING LOAD FACTORS AND MODES (BEHX1)
         4.2199E+00(      1)
         2.5173E+00(      2)
         1.8240E+00(      3)
         1.6251E+00(      4)
         1.6075E+00(      5) ←critical local buckling mode (See Fig. 9)
         1.6750E+00(      6)
         1.7983E+00(      7)
         1.9580E+00(      8)
         2.1399E+00(      9)
 Critical buckling load factor, LOCBUK=  1.6075E+00
 Critical number of axial half-waves, NWVCRT=     5


-----------------------------------------------------------


 GENERAL BUCKLING LOAD FACTORS AND MODES (BEHX2)
         1.0815E+00(      1)
         9.0304E-01(      2)
         8.8751E-01(      3) ←critical general buckling mode (See Fig. 13)
         9.3325E-01(      4)
         1.0347E+00(      5)
 Critical buckling load factor, GENBUK=  8.8751E-01
 Critical number of axial half-waves, NWVCRT=     3


-----------------------------------------------------------


 Maximum stress components from BEHX3 (Material type 1):
 Stress component no. 1:  0 deg. tension  2.659150E+04
 Stress component no. 2:  0 deg. comp.    8.909657E+04
 Stress component no. 3: 90 deg. tension  4.475377E+01
```

```
 Stress component no. 4: 90 deg. comp.      6.305358E+03
 Stress component no. 5: in-plane shear    5.114378E+03
 ----------------------------------------------------------------


 ***** RESULTS FOR LOAD SET NO.  1  ******
 PARAMETERS WHICH DESCRIBE BEHAVIOR (e.g. stress, buckling load)
 BEH.    CURRENT
 NO.     VALUE            DEFINITION
  1    1.607E+00    local buckling load factor: LOCBUK(1 )
  2    8.875E-01    general buckling load factor: GENBUK(1 )
  3    2.659E+04    stress component in material 1: STRM1(1 ,1 )
  4    8.910E+04    stress component in material 1: STRM1(1 ,2 )
  5    4.475E+01    stress component in material 1: STRM1(1 ,3 )
  6    6.305E+03    stress component in material 1: STRM1(1 ,4 )
  7    5.114E+03    stress component in material 1: STRM1(1 ,5 )
 ----------------------------------------------------------------


 MARGINS CORRESPONDING TO CURRENT DESIGN (F.S.= FACTOR OF SAFETY)
 MARGIN CURRENT
 NO.     VALUE            DEFINITION
  1    2.880E-01   1+0.45*V(1)-1.00*V(2) -1.
  2    2.365E-01   (LOCBUK(1 )/LOCBUKA(1 )) / LOCBUKF(1 )-1; F.S.=  1.30
  3   -1.125E-01   (GENBUK(1 )/GENBUKA(1 )) / GENBUKF(1 )-1; F.S.=  1.00
  4    4.286E+00   (STRM1A(1 ,1 )/STRM1(1 ,1 )) / STRM1F(1 ,1 )-1; F.S.=  1.00
  5    1.753E-01   (STRM1A(1 ,2 )/STRM1(1 ,2 )) / STRM1F(1 ,2 )-1; F.S.=  1.00
  6    2.349E+02   (STRM1A(1 ,3 )/STRM1(1 ,3 )) / STRM1F(1 ,3 )-1; F.S.=  1.00
  7    1.304E+00   (STRM1A(1 ,4 )/STRM1(1 ,4 )) / STRM1F(1 ,4 )-1; F.S.=  1.00
  8    2.299E-01   (STRM1A(1 ,5 )/STRM1(1 ,5 )) / STRM1F(1 ,5 )-1; F.S.=  1.00
Critical margins are in boldface
```

NOTE: See Margin No. 6 in Table 6 for the significant effect of thermal curing.

```
 ----------------------------------------------------------------

     CURRENT VALUE OF THE OBJECTIVE FUNCTION:
 VAR. CURRENT
 NO.   VALUE           DEFINITION
```

  1 7.314E-03 weight/area of the truss-core sandwich wall:WEIGHT

```
 ----------------------------------------------------------------


 PARAMETERS WHICH ARE ALWAYS FIXED.  NONE CAN BE DECISION VARIAB.
 VAR.   CURRENT
 NO.     VALUE           DEFINITION
  1    1.090E+02  length of the cylindrical shell: LENGTH
  2    5.000E-02  fraction of LENGTH for local buckling: FACLEN
  3    7.815E+01  inner radius of the cylindrical shell: RADIUS
  4    2.120E+07  axial modulus of a corner "noodle": ENOODL
  5    3.340E+05  shear modulus of noodle: GNOODL
  6    5.700E-02  weight density of the "noodle" material: DNOODL
  7    0.000E+00  elastic foam "Winkler" foundation stiffness: EFOUND
```

```
 8    0.000E+00  elastic "noodle" Winkler foundation modulus: EFNOOD
 9    2.120E+07  elastic modulus in the fiber direction: EMOD1(1 )
10    1.600E+06  elastic modulus transverse to fibers: EMOD2(1 )
11    6.790E+05  in-plane shear modulus: G12(1 )
12    6.270E+05  out-of-plane x-z shear modulus: G13(1 )
13    3.340E+05  out-of-plain y-z shear modulus: G23(1 )
14    2.370E-02  minor (small) Poisson ratio: NU(1 )
15    1.000E-05  coef. of thermal expansion along the fibers: ALPHA1(1 )
16    1.000E-04  coef. of thermal expansion transverse to fibers: ALPHA2(1 )
17    0.000E+00  curing temperature difference: TEMCUR(1 )
18    5.700E-02  weight density of material: DENSTY(1 )
19    4.500E+01  layer type layup angle: ANGLE(1 )
20   -4.500E+01  layer type layup angle: ANGLE(2 )
21    0.000E+00  layer type layup angle: ANGLE(3 )
22    9.000E+01  layer type layup angle: ANGLE(4 )
--------------------------------------------------------------------


 PARAMETERS WHICH ARE ENVIRONMENTAL FACTORS (e.g. loads, temps.)
 VAR.    CURRENT
 NO.      VALUE            DEFINITION
  1   -2.535E+06  total axial load (2 x pi x r x resultant):PX(1)
  2    0.000E+00  pressure (negative for external pressure):PRESS(1)
  3    0.000E+00  total "Load Set B" load: PX0(1 )
  4    0.000E+00  "Load Set B" pressure (external=negative):PRESS0(1)
--------------------------------------------------------------------


 PARAMETERS WHICH ARE CLASSIFIED AS ALLOWABLES (e.g. max. stress)
 VAR.    CURRENT
 NO.      VALUE            DEFINITION
  1    1.000E+00  allowable for local buckling load factor: LOCBUKA(1 )
  2    1.000E+00  allowable for general buckling load factor: GENBUKA(1 )
  3    1.406E+05  allowable stress in material 1: STRM1A(1 ,1 )
  4    1.047E+05  allowable stress in material 1: STRM1A(1 ,2 )
  5    1.056E+04  allowable stress in material 1: STRM1A(1 ,3 )
  6    1.453E+04  allowable stress in material 1: STRM1A(1 ,4 )
  7    6.290E+03  allowable stress in material 1: STRM1A(1 ,5 )
```

NOTE: These maximum allowable stresses are very different from those on which Ref.[3] is based.

```
--------------------------------------------------------------------


 PARAMETERS WHICH ARE FACTORS OF SAFETY
 VAR.    CURRENT
 NO.      VALUE            DEFINITION
  1    1.300E+00  factor of safety for local buckling: LOCBUKF(1 )
  2    1.000E+00  general buckling factor of safety: GENBUKF(1 )
  3    1.000E+00  factor of safety for stress in material 1: STRM1F(1 ,1 )
  4    1.000E+00  factor of safety for stress in material 1: STRM1F(1 ,2 )
```

```
 5     1.000E+00   factor of safety for stress in material 1: STRM1F(1 ,3 )
 6     1.000E+00   factor of safety for stress in material 1: STRM1F(1 ,4 )
 7     1.000E+00   factor of safety for stress in material 1: STRM1F(1 ,5 )
 8     1.000E+00   factor of safety for stress in material 2: STRM2F(1 ,1 )
 9     1.000E+00   factor of safety for stress in material 2: STRM2F(1 ,2 )
10     1.000E+00   factor of safety for stress in material 2: STRM2F(1 ,3 )
11     1.000E+00   factor of safety for stress in material 2: STRM2F(1 ,4 )
12     1.000E+00   factor of safety for stress in material 2: STRM2F(1 ,5 )
```

NOTE: The factor of safety for local buckling (1.3) is greater than unity in order to compensate for the fact that BIGBOSOR4 cannot handle transverse shear deformation nor anisotropy.

```
   1 INEQUALITY CONSTRAINTS WHICH MUST BE SATISFIED
```

```
 1 <1+0.45*V(1)-1.00*V(2)
```
(This inequality constraint forces the crown of the trapezoidal core to be narrower than its base. The variable, V(1)=PITCH, and the variable, V(2)=BCROWN. BCROWN < 0.45 x PITCH).

American Institute of Aeronautics and Astronautics

Table 4 Edited version of the file, nasatruss2.OPM, corresponding to the optimized design of "nasatruss2"

```
================================================================================
STRUCTURAL ANALYSIS FOR DESIGN ITERATION NO.   0:
STRUCTURAL ANALYSIS WITH UNPERTURBED DECISION VARIABLES
 VAR. CURRENT         DEFINITION
  NO.  VALUE
   1 1.6240E+00  circumferential width of a single module: PITCH
   2 3.3690E-01  circumferential width of the trapezoid crown: BCROWN
   3 5.7230E-01  height of the truss-core sandwich: HEIGHT
   4 5.9740E-02  local radius from base to side of trapezoidal tool: RACUTE
   5 5.0000E-02  local radius from side to crown of trapezoidal tool: ROBTUS
   6 5.7000E-03  layer type thickness: THICK(1 ) ←+45 degrees
   7 5.7000E-03  layer type thickness: THICK(2 ) ←-45 degrees
   8 5.7000E-03  layer type thickness: THICK(3 ) ←  0 degrees
   9 5.7000E-03  layer type thickness: THICK(4 ) ← 90 degrees
----------------------------------------------------------


 LOCAL BUCKLING LOAD FACTORS AND MODES (BEHX1)
        3.2983E+00(      1)
        2.0956E+00(      2)
        1.5171E+00(      3)
        1.3374E+00(      4)
        1.3102E+00(      5) ←critical local buckling mode (see Fig. 2b)
        1.3617E+00(      6)
        1.4675E+00(      7)
        1.6173E+00(      8)
        1.8016E+00(      9)
 Critical buckling load factor, LOCBUK=  1.3102E+00
 Critical number of axial half-waves, NWVCRT=     5


----------------------------------------------------------


 GENERAL BUCKLING LOAD FACTORS AND MODES (BEHX2)
        1.0903E+00(      1)
        1.1337E+00(      2)
        9.9523E-01(      3)
        9.9149E-01(      4) ←critical general buckling mode (see Fig. 5)
        1.0197E+00(      5)
 Critical buckling load factor, GENBUK=  9.9149E-01
 Critical number of axial half-waves, NWVCRT=     4


----------------------------------------------------------
```

American Institute of Aeronautics and Astronautics

```
Maximum stress components from BEHX3 (Material type 1):
Stress component no. 1:  0 deg. tension  3.123998E+04
Stress component no. 2:  0 deg. comp.    1.046716E+05
Stress component no. 3: 90 deg. tension  5.257718E+01
Stress component no. 4: 90 deg. comp.    7.407604E+03
Stress component no. 5: in-plane shear   6.008428E+03
---------------------------------------------------------------------


***** RESULTS FOR LOAD SET NO.  1  ******
PARAMETERS WHICH DESCRIBE BEHAVIOR (e.g. stress, buckling load)
BEH.    CURRENT
NO.      VALUE              DEFINITION
 1    1.310E+00     local buckling load factor: LOCBUK(1 )
 2    9.915E-01     general buckling load factor: GENBUK(1 )
 3    3.124E+04     stress component in material 1: STRM1(1 ,1 )
 4    1.047E+05     stress component in material 1: STRM1(1 ,2 )
 5    5.258E+01     stress component in material 1: STRM1(1 ,3 )
 6    7.408E+03     stress component in material 1: STRM1(1 ,4 )
 7    6.008E+03     stress component in material 1: STRM1(1 ,5 )
---------------------------------------------------------------------


MARGINS CORRESPONDING TO CURRENT DESIGN (F.S.= FACTOR OF SAFETY)
MARGIN CURRENT
NO.      VALUE              DEFINITION
 1    3.939E-01   1+0.45*V(1)-1.00*V(2) -1.
 2    7.858E-03   (LOCBUK(1 )/LOCBUKA(1 )) / LOCBUKF(1 )-1; F.S.=  1.30
 3   -8.510E-03   (GENBUK(1 )/GENBUKA(1 )) / GENBUKF(1 )-1; F.S.=  1.00
 4    3.500E+00   (STRM1A(1 ,1 )/STRM1(1 ,1 )) / STRM1F(1 ,1 )-1; F.S.=  1.00
 5    4.047E-04   (STRM1A(1 ,2 )/STRM1(1 ,2 )) / STRM1F(1 ,2 )-1; F.S.=  1.00
 6    1.998E+02   (STRM1A(1 ,3 )/STRM1(1 ,3 )) / STRM1F(1 ,3 )-1; F.S.=  1.00
 7    9.614E-01   (STRM1A(1 ,4 )/STRM1(1 ,4 )) / STRM1F(1 ,4 )-1; F.S.=  1.00
 8    4.686E-02   (STRM1A(1 ,5 )/STRM1(1 ,5 )) / STRM1F(1 ,5 )-1; F.S.=  1.00
Critical margins are in boldface
-----------------------------------------------------------------


    CURRENT VALUE OF THE OBJECTIVE FUNCTION:
 VAR. CURRENT
NO.    VALUE              DEFINITION
 1  6.883E-03  weight/area of the truss-core sandwich wall: WEIGHT
=====================================================================
```

Table 5 Optimized design for the specific case, nasatruss3, in which the lower bound of THICK(4), the 90-degree layer, is set to 0.00285 inches, which is half the thickness of a single ply. Therefore, only one 90-degree ply of thickness 0.0057 inches is required in each face sheet of the optimized truss-core sandwich wall. "noodle support" index, ILINKS = 0

```
================================================================
  VALUES OF DESIGN VARIABLES CORRESPONDING TO BEST FEASIBLE DESIGN
 VAR.    CURRENT
 NO.      VALUE            DEFINITION
  1     1.4249E+00  circumferential width of a single module: PITCH
  2     2.8256E-01  circumferential width of the trapezoid crown: BCROWN
  3     5.8772E-01  height of the truss-core sandwich: HEIGHT
  4     6.4605E-02  local radius from base to side of trapezoidal tool: RACUTE
  5     5.0000E-02  local radius from side to crown of trapezoidal tool: ROBTUS
  6     5.7000E-03  layer type thickness: THICK(1 ) ←the +45-degree layers
  7     5.7000E-03  layer type thickness: THICK(2 ) ←the -45-degree layers
  8     5.7000E-03  layer type thickness: THICK(3 ) ←the   0-degree layers
  9     2.8500E-03  layer type thickness: THICK(4 ) ←the  90-degree layers
```

NOTE: The face sheet laminates in Segments 1, 6, 15, and 18 in Fig. 4 have the stacking sequence: [+45, -45, 0, 90, 90, 0 -45, +45]total. Since the two adjacent 90-degree plies each have thickness equal to 0.00285 inches, the truss-core sandwich wall can be fabricated with only a single 90-degree ply of thickness 0.0057 inches.

```
--------------------------------------------------------------------

 LOCAL BUCKLING LOAD FACTORS AND MODES (BEHX1)
         3.7338E+00(      1)
         2.3458E+00(      2)
         1.6341E+00(      3)
         1.3795E+00(      4)
         1.2965E+00(      5) <--critical local buckling mode
         1.2970E+00(      6) <--critical local buckling mode
         1.3493E+00(      7)
         1.4387E+00(      8)
         1.5547E+00(      9)
 Critical buckling load factor, LOCBUK=  1.2965E+00
 Critical number of axial half-waves, NWVCRT=     5


 ---------------------------------------------------------------

 GENERAL BUCKLING LOAD FACTORS AND MODES (BEHX2)
```

American Institute of Aeronautics and Astronautics

```
       1.1426E+00(        1)
       1.0007E+00(        2) <--critical general buckling mode
       1.0335E+00(        3)
       1.0115E+00(        4)
       1.0100E+00(        5) <--almost critical general buckling mode
 Critical buckling load factor, GENBUK=  1.0007E+00
 Critical number of axial half-waves, NWVCRT=     2


-----------------------------------------------------------

 Maximum stress components from BEHX3 (Material type 1):
 Stress component no. 1:  0 deg. tension  4.437302E+04
 Stress component no. 2:  0 deg. comp.    1.046922E+05
 Stress component no. 3: 90 deg. tension  1.037412E+03
 Stress component no. 4: 90 deg. comp.    7.160777E+03
 Stress component no. 5: in-plane shear   6.024948E+03

Behavior  Stress         Definition of behavior
 Number    (psi)
   3     4.437E+04     stress component in material 1: STRM1(1 ,1 )
   4     1.047E+05     stress component in material 1: STRM1(1 ,2 )
   5     1.037E+03     stress component in material 1: STRM1(1 ,3 )
   6     7.161E+03     stress component in material 1: STRM1(1 ,4 )
   7     6.025E+03     stress component in material 1: STRM1(1 ,5 )
------------------------------------------------------------------

 PARAMETERS WHICH DESCRIBE BEHAVIOR (e.g. stress, buckling load)
 BEH.    CURRENT
 NO.      VALUE            DEFINITION
  1    1.297E+00    local buckling load factor: LOCBUK(1 )
  2    1.001E+00    general buckling load factor: GENBUK(1 )
  3    4.437E+04    stress component in material 1: STRM1(1 ,1 )
  4    1.047E+05    stress component in material 1: STRM1(1 ,2 )
  5    1.037E+03    stress component in material 1: STRM1(1 ,3 )
  6    7.161E+03    stress component in material 1: STRM1(1 ,4 )
  7    6.025E+03    stress component in material 1: STRM1(1 ,5 )
------------------------------------------------------------------

 MARGINS CORRESPONDING TO CURRENT DESIGN (F.S.= FACTOR OF SAFETY)
 MAR.    CURRENT
 NO.      VALUE            DEFINITION
  1    3.586E-01   1+0.45*V(1)-1.00*V(2) -1.
  2   -2.692E-03   (LOCBUK(1 )/LOCBUKA(1 )) / LOCBUKF(1 )-1; F.S.=  1.30
  3    6.945E-04   (GENBUK(1 )/GENBUKA(1 )) / GENBUKF(1 )-1; F.S.=  1.00
  4    2.168E+00   (STRM1A(1 ,1 )/STRM1(1 ,1 )) / STRM1F(1 ,1 )-1; F.S.=  1.00
  5    2.079E-04   (STRM1A(1 ,2 )/STRM1(1 ,2 )) / STRM1F(1 ,2 )-1; F.S.=  1.00
  6    9.176E+00   (STRM1A(1 ,3 )/STRM1(1 ,3 )) / STRM1F(1 ,3 )-1; F.S.=  1.00
  7    1.029E+00   (STRM1A(1 ,4 )/STRM1(1 ,4 )) / STRM1F(1 ,4 )-1; F.S.=  1.00
```

American Institute of Aeronautics and Astronautics

```
   8     4.399E-02  (STRM1A(1 ,5 )/STRM1(1 ,5 )) / STRM1F(1 ,5 )-1; F.S.=  1.00
Critical margins are in boldface.
-----------------------------------------------------------------

    CURRENT VALUE OF THE OBJECTIVE FUNCTION:
 VAR.   CURRENT
 NO.    VALUE              DEFINITION
  1     6.456E-03  weight/area of the truss-core sandwich wall: WEIGHT
=================================================================
```

Table 6 Mechanical and thermal quantities corresponding to the starting design listed in Table 3. The thermal (curing) results were obtained with the use of coefficients of thermal expansion, alpha1 (in fiber direction)=0.00001 and alpha2 (normal to fibers) = 0.0001 and curing temperature, TEMCUR=200 degrees.

```
========================================================================
PRE-BUCKLING MECHANICAL AND THERMAL CURING RESULTANTS IN EACH SEGMENT
OF THE 22-SEGMENT SINGLE MODULE MODEL DISPLAYED IN FIG. 4:

Some definitions:
 FN10 = torus meridional resultant from applied load
 FN20 = torus circumfer. resultant from applied load
 FN20T= torus circumfer. resultant from thermal curing load
 FN20 is the AXIAL applied resultant in the cylindrical shell
 FN20T is the AXIAL thermal resultant in the cylindrical shell
 ISEG = shell segment number (See Fig. 4)

Data:
 ISEG,FN10(ISEG),FN20(ISEG),FN20T(ISEG)=   1  0.0000E+00 -1.5575E+03  2.2041E+02
 ISEG,FN10(ISEG),FN20(ISEG),FN20T(ISEG)=   2  0.0000E+00 -1.1661E+02  1.6502E+01
 ISEG,FN10(ISEG),FN20(ISEG),FN20T(ISEG)=   3  0.0000E+00 -1.3524E+03  1.9138E+02
 ISEG,FN10(ISEG),FN20(ISEG),FN20T(ISEG)=   4  0.0000E+00 -1.1661E+02  1.6502E+01
 ISEG,FN10(ISEG),FN20(ISEG),FN20T(ISEG)=   5  0.0000E+00 -1.1661E+02  1.6502E+01
 ISEG,FN10(ISEG),FN20(ISEG),FN20T(ISEG)=   6  0.0000E+00 -1.5575E+03  2.2041E+02
 ISEG,FN10(ISEG),FN20(ISEG),FN20T(ISEG)=   7  0.0000E+00 -2.3322E+02  3.3005E+01
 ISEG,FN10(ISEG),FN20(ISEG),FN20T(ISEG)=   8  0.0000E+00 -1.3524E+03  1.9138E+02
 ISEG,FN10(ISEG),FN20(ISEG),FN20T(ISEG)=   9  0.0000E+00 -1.1661E+02  1.6502E+01
 ISEG,FN10(ISEG),FN20(ISEG),FN20T(ISEG)=  10  0.0000E+00 -1.1661E+02  1.6502E+01
 ISEG,FN10(ISEG),FN20(ISEG),FN20T(ISEG)=  11  0.0000E+00 -1.1661E+02  1.6502E+01
 ISEG,FN10(ISEG),FN20(ISEG),FN20T(ISEG)=  12  0.0000E+00 -2.3322E+02  3.3005E+01
 ISEG,FN10(ISEG),FN20(ISEG),FN20T(ISEG)=  13  0.0000E+00 -1.1661E+02  1.6502E+01
 ISEG,FN10(ISEG),FN20(ISEG),FN20T(ISEG)=  14  0.0000E+00 -1.1661E+02  1.6502E+01
 ISEG,FN10(ISEG),FN20(ISEG),FN20T(ISEG)=  15  0.0000E+00 -1.5575E+03  2.2041E+02
 ISEG,FN10(ISEG),FN20(ISEG),FN20T(ISEG)=  16  0.0000E+00 -1.1661E+02  1.6502E+01
 ISEG,FN10(ISEG),FN20(ISEG),FN20T(ISEG)=  17  0.0000E+00 -1.3524E+03  1.9138E+02
 ISEG,FN10(ISEG),FN20(ISEG),FN20T(ISEG)=  18  0.0000E+00 -1.5575E+03  2.2041E+02
 ISEG,FN10(ISEG),FN20(ISEG),FN20T(ISEG)=  19  0.0000E+00 -1.1661E+02  1.6502E+01
 ISEG,FN10(ISEG),FN20(ISEG),FN20T(ISEG)=  20  0.0000E+00 -1.1661E+02  1.6502E+01
 ISEG,FN10(ISEG),FN20(ISEG),FN20T(ISEG)=  21  0.0000E+00 -1.1661E+02  1.6502E+01
 ISEG,FN10(ISEG),FN20(ISEG),FN20T(ISEG)=  22  0.0000E+00 -1.3524E+03  1.9138E+02

PRE-BUCKLING MECHANICAL AND THERMAL FORCES IN "NOODLES":

Some definitions:
 FNOOD1 = force from applied load in noodle of area, AREA1
 FNOOD2 = force from applied load in noodle of area, AREA2
```

```
FNOODL = force from applied load in noodle of area, AREA
FNOOD1T= force from thermal load in noodle of area, AREA1
FNOOD2T= force from thermal load in noodle of area, AREA2
FNOODLT= force from thermal load in noodle of area, AREA
```

Data:
```
 FNOOD1,FNOOD2,FNOODL   = -8.1039E+02 -7.2013E+01  0.0000E+00
 FNOOD1T,FNOOD2T,FNOODLT= -1.9260E+02 -1.7115E+01  0.0000E+00
```

IN-PLANE THERMAL STRAINS IN THREE SAMPLE SEGMENTS (1, 3, AND 5)
OF THE 22-SEGMENT SINGLE MODULE MODEL SHOWN IN FIG. 4:
 The in-plane thermal meridional and circumferential strains,
 e1 and e2, are computed for the huge torus as follows:
 N1 = e1*C11 + e2*C12; N2 = e1*C12 + e2*C22   (1)
 in which N1,N2 are the meridional, circumferential thermal
 resultants, and C11,C12,C22 are the in-plane membrane wall
 stiffnesses. Since N1 and N2 are known from BIGBOSOR4,
 the in-plane thermal strain components, e1 and e2, in each
 shell segment can be computed from the following equations:
         e1 = (N1*C22 - N2*C12)/(C11*C22 - C12*C12)   (2)
         e2 = (N2*C11 - N1*C12)/(C11*C22 - C12*C12)   (3)
 e1 for the huge torus is the same as ETHERM(2,i) for the
 cylindrical shell, and e2 for the huge torus is the same as
 ETHERM(1,i) for the cylindrical shell in the following list:

Some definitions:
 e2(1)=ETHERM(1,1)=axial thermal strain in Segment 1 of the 22-segment model
 e2(3)=ETHERM(1,3)=axial thermal strain in Segment 3 of the 22-segment model
 e2(5)=ETHERM(1,5)=axial thermal strain in Segment 5 of the 22-segment model
 e1(1)=ETHERM(2,1)="hoop" thermal strain in Segment 1 of the 22-segment model
 e1(3)=ETHERM(2,3)="hoop" thermal strain in Segment 3 of the 22-segment model
 e1(5)=ETHERM(2,5)="hoop" thermal strain in Segment 5 of the 22-segment model

Data:
 ETHERM(1,1),ETHERM(1,3),ETHERM(1,5)= -3.5898E-03 -3.5898E-03 -3.5898E-03
 ETHERM(2,1),ETHERM(2,3),ETHERM(2,5)= -3.5898E-03 -3.5898E-03 -3.5898E-03

COMPUTATION OF THE WEIGHTED AVERAGE AXIAL THERMAL STRAIN
OF THE CURED TRUSS-CORE SANDWICH CYLINDRICAL SHELL:
 In order to compute the residual thermal stress resultants
 and to compute the contribution of thermal curing to the
 stresses in each ply of the truss-core sandwich wall, we
 need to obtain the weighted average axial thermal strain,
 EPSAVE. We obtain EPSAVE from the following equation:
 EPSAVE = SUM-OVER-SEGMENTS[Li*C11iMD*ETHERM(1,i)]/   (4)
          SUM-OVER-SEGMENTS[Li*C11iMD]

 in which Li is the arc length of the ith shell segment, and
 C11iMD is the effective axial stiffness/length of the ith
 shell segment, given by:
       C11iMD = C22i - C12i/C11i   (5)
 where C22i, C12i, C11i, are the membrane stiffnesses/length

American Institute of Aeronautics and Astronautics

of the ith shell segment in the huge torus notation. The
C22i, C12i, C11i are known from computations in BIGBOSOR4.

Definition:
 EPSAVE=Weighted average axial thermal strain of assembled truss-core sandwich

Datum:
 EPSAVE= -2.9964E-03

NET AXIAL THERMAL STRAINS IN THREE SAMPLE SEGMENTS (1, 3, AND 5)
OF THE 22-SEGMENT SINGLE MODULE MODEL OF THE TRUSS-CORE SANDWICH WALL:

Some definitions:
 EPSNET(1)=net axial thermal strain in Segment 1; 22-seg.model
 EPSNET(3)=net axial thermal strain in Segment 3; 22-seg.model
 EPSNET(5)=net axial thermal strain in Segment 5; 22-seg.model
 EPSNET(i)=EPSAVE-ETHERM(1,i); produces the residual thermal
       resultant, given by FNXRES(i) = EPSNET(i)*C11iMD, in
       which C11iMD is the effective axial stiffness/arc length
       of the ith segment in the 22-segment single module model.

Data:
 EPSNET(1),EPSNET(3),EPSNET(5)= 5.9333E-04 5.9333E-04 5.9333E-04

RESIDUAL THERMAL RESULTANTS IN THREE SAMPLE SEGMENTS (1, 3, AND 5)
OF THE 22-SEGMENT SINGLE MODULE MODEL OF THE TRUSS-CORE SANDWICH WALL:

Some definitions:
 FNXRES(1)=residual axial thermal resultant in Segment 1 of the 22-segment model
 FNXRES(3)=residual axial thermal resultant in Segment 3 of the 22-segment model
 FNXRES(5)=residual axial thermal resultant in Segment 5 of the 22-segment model.
 FNXRES(5)=half of the residual axial thermal resultant,
           FN20T, of the truss-core sandwich webs.

Data:
 FNXRES(1),FNXRES(3),FNXRES(5)= 2.2041E+02 1.9138E+02 1.6502E+01

TOTAL AXIAL RESIDUAL THERMAL FORCE IN THE TRUSS-CORE SANDWICH WALL:

Definition:
 FCESHL=Axial residual thermal force of assembled truss-core sandwich wall
         (FCESHL should be close to zero because the residual
          thermal forces in the individual segments plus the thermal
          forces in the "noodles" must add to zero.)

Datum:
 FCESHL= -1.8511E-04

COMPUTATION OF FOUR STRAIN COMPONENTS NEEDED FOR CALCULATION
OF THE STRESSES IN EACH PLY OF EACH SEGMENT OF THE TRUSS-CORE
SANDWICH WALL:

Some definitions:
 In order to obtain the correct stresses in each ply of each
 segment of the truss-core sandwich wall, we need correct
 values for the four in-plane strain components:

 EPSX, EPSY1, EPSY3, EPSY5, in which:
 EPSX = axial strain (assumed to be the same in all shell
         segments and in the noodles)
 EPSY1 = "hoop" strain in "segment 1 type" shell segments.
 EPSY3 = "hoop" strain in "segment 3 type" shell segments.
 EPSY5 = "hoop" strain in "segment 5 type" shell segments.

 "segment i type" shell segments means "shell segments in the
 elaborate 22-segment single module model (Fig.4) that all
 have the same properties".

 The axial strain component, EPSX, is divided into two parts,

 Part 1: the axial strain created by mechanical and residual
         thermal loading, called "EPSLOD", given by:
         EPSLOD = (FNX1+FNXRES(1))/C111MD, in which
         FNX1=axial resultant in shell segment 1 (Fig.4)
             generated by the applied loading, and
         FNXRES(1)=residual thermal axial resultant in shell
                 segment 1, and
         C111MD=effective axial stiffness/length of shell
                 segment 1.

 Part 2: The weighted average axial thermal strain, EPSAVE.

 Hence, EPSX = EPSLOD + EPSAVE.

 The three "hoop" strain components, EPSY1, EPSY3, EPSY5,
 are given by the following:

 EPSY1 = (FN10(1) - EPSLOD*CSKIN1(1,2,1))/CSKIN1(1,1,1) + ETHERM(2,1)
 EPSY3 = (FN10(3) - EPSLOD*CSKIN1(1,2,3))/CSKIN1(1,1,3) + ETHERM(2,3)
 EPSY3 = (FN10(5) - EPSLOD*CSKIN1(1,2,5))/CSKIN1(1,1,5) + ETHERM(2,5)

 in which FN10(i) is the meridional resultant in the ith
 shell segment (torus notation), and CSKIN1(j,k,i) are the
 membrane stiffnesses/arc length (torus notation) computed
 by BIGBOSOR4. The quantities, ETHERM(j,i), are defined above.

Data:
 EPSX,EPSY1,EPSY3,EPSY5= -6.5957E-03 -2.4357E-03 -2.8213E-03 -7.2275E-04

AXIAL AND "HOOP" STRAINS IN EACH SEGMENT OF THE 22-SEGMENT
SINGLE MODULE MODEL SHOWN IN FIG. 4:

Some definitions:
 In the following list EPSX is the strain in the

axial direction. EPSY is the in-plane strain at
90 degrees from EPSX.

The axial strain, EPSX, is uniform over the entire
cross-section of the truss-core sandwich wall.

The prestress state is a uniform membrane state.

Data:
```
Entering Sub.BEHX3: Axial strain, EPSX = -6.5957E-03
 ISEG=   1: Widthwise strain, EPSY(i)= -2.4357E-03
 ISEG=   2: Widthwise strain, EPSY(i)= -7.2275E-04
 ISEG=   3: Widthwise strain, EPSY(i)= -2.8213E-03
 ISEG=   4: Widthwise strain, EPSY(i)= -7.2275E-04
 ISEG=   5: Widthwise strain, EPSY(i)= -7.2275E-04
 ISEG=   6: Widthwise strain, EPSY(i)= -2.4357E-03
 ISEG=   7: Widthwise strain, EPSY(i)= -7.2275E-04
 ISEG=   8: Widthwise strain, EPSY(i)= -2.8213E-03
 ISEG=   9: Widthwise strain, EPSY(i)= -7.2275E-04
 ISEG=  10: Widthwise strain, EPSY(i)= -7.2275E-04
 ISEG=  11: Widthwise strain, EPSY(i)= -7.2275E-04
 ISEG=  12: Widthwise strain, EPSY(i)= -7.2275E-04
 ISEG=  13: Widthwise strain, EPSY(i)= -7.2275E-04
 ISEG=  14: Widthwise strain, EPSY(i)= -7.2275E-04
 ISEG=  15: Widthwise strain, EPSY(i)= -2.4357E-03
 ISEG=  16: Widthwise strain, EPSY(i)= -7.2275E-04
 ISEG=  17: Widthwise strain, EPSY(i)= -2.8213E-03
 ISEG=  18: Widthwise strain, EPSY(i)= -2.4357E-03
 ISEG=  19: Widthwise strain, EPSY(i)= -7.2275E-04
 ISEG=  20: Widthwise strain, EPSY(i)= -7.2275E-04
 ISEG=  21: Widthwise strain, EPSY(i)= -7.2275E-04
 ISEG=  22: Widthwise strain, EPSY(i)= -2.8213E-03
```

**IN-PLANE STRESSES IN EACH PLY OF EACH SEGMENT OF THE 22-SEGMENT
SINGLE MODULE MODEL SHOWN IN FIG. 4:**

Some definitions:
In the following list:
SIG1 is the stress along the fibers.
SIG2 is the stress normal to the fibers.
SIG12 is the in-plane shear stress.
Layer numbering is from left to right as we face in the
direction of increasing arc length along each of the shell
segments in the elaborate 22-segment single module model
shown in Fig. 4.

Data: **LAYUP ANGLE**
```
 Seg. 1, LAYER  1 SIG1,SIG2,SIG12= -4.5894E+04  2.3687E+04  2.8247E+03  4.5000E+01
 Seg. 1, LAYER  2 SIG1,SIG2,SIG12= -4.5894E+04  2.3687E+04 -2.8247E+03 -4.5000E+01
 Seg. 1, LAYER  3 SIG1,SIG2,SIG12= -8.9268E+04  2.5987E+04  0.0000E+00  0.0000E+00
 Seg. 1, LAYER  4 SIG1,SIG2,SIG12= -2.5198E+03  2.1387E+04  6.8741E-05  9.0000E+01
 Seg. 1, LAYER  5 SIG1,SIG2,SIG12= -2.5198E+03  2.1387E+04  6.8741E-05  9.0000E+01
```

```
Seg. 1, LAYER  6 SIG1,SIG2,SIG12= -8.9268E+04   2.5987E+04   0.0000E+00   0.0000E+00
Seg. 1, LAYER  7 SIG1,SIG2,SIG12= -4.5894E+04   2.3687E+04  -2.8247E+03  -4.5000E+01
Seg. 1, LAYER  8 SIG1,SIG2,SIG12= -4.5894E+04   2.3687E+04   2.8247E+03   4.5000E+01

Seg. 2, LAYER  1 SIG1,SIG2,SIG12= -2.7167E+04   2.5501E+04   3.9877E+03   4.5000E+01
Seg. 2, LAYER  2 SIG1,SIG2,SIG12= -2.7167E+04   2.5501E+04  -3.9877E+03  -4.5000E+01

Seg. 3, LAYER  1 SIG1,SIG2,SIG12= -8.9463E+04   2.5366E+04   0.0000E+00   0.0000E+00
Seg. 3, LAYER  2 SIG1,SIG2,SIG12= -1.0757E+04   2.1192E+04   6.2368E-05   9.0000E+01
Seg. 3, LAYER  3 SIG1,SIG2,SIG12= -1.0757E+04   2.1192E+04   6.2368E-05   9.0000E+01
Seg. 3, LAYER  4 SIG1,SIG2,SIG12= -8.9463E+04   2.5366E+04   0.0000E+00   0.0000E+00
Seg. 3, LAYER  5 SIG1,SIG2,SIG12= -5.0110E+04   2.3279E+04  -2.5628E+03  -4.5000E+01
Seg. 3, LAYER  6 SIG1,SIG2,SIG12= -5.0110E+04   2.3279E+04   2.5628E+03   4.5000E+01

Seg. 4, LAYER  1 SIG1,SIG2,SIG12= -2.7167E+04   2.5501E+04   3.9877E+03   4.5000E+01
Seg. 4, LAYER  2 SIG1,SIG2,SIG12= -2.7167E+04   2.5501E+04  -3.9877E+03  -4.5000E+01

Seg. 5, LAYER  1 SIG1,SIG2,SIG12= -2.7167E+04   2.5501E+04   3.9877E+03   4.5000E+01
Seg. 5, LAYER  2 SIG1,SIG2,SIG12= -2.7167E+04   2.5501E+04  -3.9877E+03  -4.5000E+01

Seg. 6, LAYER  1 SIG1,SIG2,SIG12= -4.5894E+04   2.3687E+04   2.8247E+03   4.5000E+01
Seg. 6, LAYER  2 SIG1,SIG2,SIG12= -4.5894E+04   2.3687E+04  -2.8247E+03  -4.5000E+01
Seg. 6, LAYER  3 SIG1,SIG2,SIG12= -8.9268E+04   2.5987E+04   0.0000E+00   0.0000E+00
Seg. 6, LAYER  4 SIG1,SIG2,SIG12= -2.5198E+03   2.1387E+04   6.8741E-05   9.0000E+01
Seg. 6, LAYER  5 SIG1,SIG2,SIG12= -2.5198E+03   2.1387E+04   6.8741E-05   9.0000E+01
Seg. 6, LAYER  6 SIG1,SIG2,SIG12= -8.9268E+04   2.5987E+04   0.0000E+00   0.0000E+00
Seg. 6, LAYER  7 SIG1,SIG2,SIG12= -4.5894E+04   2.3687E+04  -2.8247E+03  -4.5000E+01
Seg. 6, LAYER  8 SIG1,SIG2,SIG12= -4.5894E+04   2.3687E+04   2.8247E+03   4.5000E+01

Seg. 7, LAYER  1 SIG1,SIG2,SIG12= -2.7167E+04   2.5501E+04   3.9877E+03   4.5000E+01
Seg. 7, LAYER  2 SIG1,SIG2,SIG12= -2.7167E+04   2.5501E+04  -3.9877E+03  -4.5000E+01
Seg. 7, LAYER  3 SIG1,SIG2,SIG12= -2.7167E+04   2.5501E+04   3.9877E+03   4.5000E+01
Seg. 7, LAYER  4 SIG1,SIG2,SIG12= -2.7167E+04   2.5501E+04  -3.9877E+03  -4.5000E+01

Seg. 8, LAYER  1 SIG1,SIG2,SIG12= -8.9463E+04   2.5366E+04   0.0000E+00   0.0000E+00
Seg. 8, LAYER  2 SIG1,SIG2,SIG12= -1.0757E+04   2.1192E+04   6.2368E-05   9.0000E+01
Seg. 8, LAYER  3 SIG1,SIG2,SIG12= -1.0757E+04   2.1192E+04   6.2368E-05   9.0000E+01
Seg. 8, LAYER  4 SIG1,SIG2,SIG12= -8.9463E+04   2.5366E+04   0.0000E+00   0.0000E+00
Seg. 8, LAYER  5 SIG1,SIG2,SIG12= -5.0110E+04   2.3279E+04  -2.5628E+03  -4.5000E+01
Seg. 8, LAYER  6 SIG1,SIG2,SIG12= -5.0110E+04   2.3279E+04   2.5628E+03   4.5000E+01

Seg. 9, LAYER  1 SIG1,SIG2,SIG12= -2.7167E+04   2.5501E+04   3.9877E+03   4.5000E+01
Seg. 9, LAYER  2 SIG1,SIG2,SIG12= -2.7167E+04   2.5501E+04  -3.9877E+03  -4.5000E+01

Seg.10, LAYER  1 SIG1,SIG2,SIG12= -2.7167E+04   2.5501E+04   3.9877E+03   4.5000E+01
Seg.10, LAYER  2 SIG1,SIG2,SIG12= -2.7167E+04   2.5501E+04  -3.9877E+03  -4.5000E+01

Seg.11, LAYER  1 SIG1,SIG2,SIG12= -2.7167E+04   2.5501E+04   3.9877E+03   4.5000E+01
Seg.11, LAYER  2 SIG1,SIG2,SIG12= -2.7167E+04   2.5501E+04  -3.9877E+03  -4.5000E+01

Seg.12, LAYER  1 SIG1,SIG2,SIG12= -2.7167E+04   2.5501E+04   3.9877E+03   4.5000E+01
Seg.12, LAYER  2 SIG1,SIG2,SIG12= -2.7167E+04   2.5501E+04  -3.9877E+03  -4.5000E+01
```

```
Seg.12, LAYER  3 SIG1,SIG2,SIG12= -2.7167E+04   2.5501E+04   3.9877E+03   4.5000E+01
Seg.12, LAYER  4 SIG1,SIG2,SIG12= -2.7167E+04   2.5501E+04  -3.9877E+03  -4.5000E+01

Seg.13, LAYER  1 SIG1,SIG2,SIG12= -2.7167E+04   2.5501E+04   3.9877E+03   4.5000E+01
Seg.13, LAYER  2 SIG1,SIG2,SIG12= -2.7167E+04   2.5501E+04  -3.9877E+03  -4.5000E+01

Seg.14, LAYER  1 SIG1,SIG2,SIG12= -2.7167E+04   2.5501E+04   3.9877E+03   4.5000E+01
Seg.14, LAYER  2 SIG1,SIG2,SIG12= -2.7167E+04   2.5501E+04  -3.9877E+03  -4.5000E+01

Seg.15, LAYER  1 SIG1,SIG2,SIG12= -4.5894E+04   2.3687E+04   2.8247E+03   4.5000E+01
Seg.15, LAYER  2 SIG1,SIG2,SIG12= -4.5894E+04   2.3687E+04  -2.8247E+03  -4.5000E+01
Seg.15, LAYER  3 SIG1,SIG2,SIG12= -8.9268E+04   2.5987E+04   0.0000E+00   0.0000E+00
Seg.15, LAYER  4 SIG1,SIG2,SIG12= -2.5198E+03   2.1387E+04   6.8741E-05   9.0000E+01
Seg.15, LAYER  5 SIG1,SIG2,SIG12= -2.5198E+03   2.1387E+04   6.8741E-05   9.0000E+01
Seg.15, LAYER  6 SIG1,SIG2,SIG12= -8.9268E+04   2.5987E+04   0.0000E+00   0.0000E+00
Seg.15, LAYER  7 SIG1,SIG2,SIG12= -4.5894E+04   2.3687E+04  -2.8247E+03  -4.5000E+01
Seg.15, LAYER  8 SIG1,SIG2,SIG12= -4.5894E+04   2.3687E+04   2.8247E+03   4.5000E+01

Seg.16, LAYER  1 SIG1,SIG2,SIG12= -2.7167E+04   2.5501E+04   3.9877E+03   4.5000E+01
Seg.16, LAYER  2 SIG1,SIG2,SIG12= -2.7167E+04   2.5501E+04  -3.9877E+03  -4.5000E+01

Seg.17, LAYER  1 SIG1,SIG2,SIG12= -5.0110E+04   2.3279E+04  -2.5628E+03  -4.5000E+01
Seg.17, LAYER  2 SIG1,SIG2,SIG12= -5.0110E+04   2.3279E+04   2.5628E+03   4.5000E+01
Seg.17, LAYER  3 SIG1,SIG2,SIG12= -8.9463E+04   2.5366E+04   0.0000E+00   0.0000E+00
Seg.17, LAYER  4 SIG1,SIG2,SIG12= -1.0757E+04   2.1192E+04   6.2368E-05   9.0000E+01
Seg.17, LAYER  5 SIG1,SIG2,SIG12= -1.0757E+04   2.1192E+04   6.2368E-05   9.0000E+01
Seg.17, LAYER  6 SIG1,SIG2,SIG12= -8.9463E+04   2.5366E+04   0.0000E+00   0.0000E+00

Seg.18, LAYER  1 SIG1,SIG2,SIG12= -4.5894E+04   2.3687E+04  -2.8247E+03  -4.5000E+01
Seg.18, LAYER  2 SIG1,SIG2,SIG12= -4.5894E+04   2.3687E+04   2.8247E+03   4.5000E+01
Seg.18, LAYER  3 SIG1,SIG2,SIG12= -8.9268E+04   2.5987E+04   0.0000E+00   0.0000E+00
Seg.18, LAYER  4 SIG1,SIG2,SIG12= -2.5198E+03   2.1387E+04   6.8741E-05   9.0000E+01
Seg.18, LAYER  5 SIG1,SIG2,SIG12= -2.5198E+03   2.1387E+04   6.8741E-05   9.0000E+01
Seg.18, LAYER  6 SIG1,SIG2,SIG12= -8.9268E+04   2.5987E+04   0.0000E+00   0.0000E+00
Seg.18, LAYER  7 SIG1,SIG2,SIG12= -4.5894E+04   2.3687E+04   2.8247E+03   4.5000E+01
Seg.18, LAYER  8 SIG1,SIG2,SIG12= -4.5894E+04   2.3687E+04  -2.8247E+03  -4.5000E+01

Seg.19, LAYER  1 SIG1,SIG2,SIG12= -2.7167E+04   2.5501E+04   3.9877E+03   4.5000E+01
Seg.19, LAYER  2 SIG1,SIG2,SIG12= -2.7167E+04   2.5501E+04  -3.9877E+03  -4.5000E+01

Seg.20, LAYER  1 SIG1,SIG2,SIG12= -2.7167E+04   2.5501E+04   3.9877E+03   4.5000E+01
Seg.20, LAYER  2 SIG1,SIG2,SIG12= -2.7167E+04   2.5501E+04  -3.9877E+03  -4.5000E+01

Seg.21, LAYER  1 SIG1,SIG2,SIG12= -2.7167E+04   2.5501E+04   3.9877E+03   4.5000E+01
Seg.21, LAYER  2 SIG1,SIG2,SIG12= -2.7167E+04   2.5501E+04  -3.9877E+03  -4.5000E+01

Seg.22, LAYER  1 SIG1,SIG2,SIG12= -5.0110E+04   2.3279E+04  -2.5628E+03  -4.5000E+01
Seg.22, LAYER  2 SIG1,SIG2,SIG12= -5.0110E+04   2.3279E+04   2.5628E+03   4.5000E+01
Seg.22, LAYER  3 SIG1,SIG2,SIG12= -8.9463E+04   2.5366E+04   0.0000E+00   0.0000E+00
Seg.22, LAYER  4 SIG1,SIG2,SIG12= -1.0757E+04   2.1192E+04   6.2368E-05   9.0000E+01
Seg.22, LAYER  5 SIG1,SIG2,SIG12= -1.0757E+04   2.1192E+04   6.2368E-05   9.0000E+01
Seg.22, LAYER  6 SIG1,SIG2,SIG12= -8.9463E+04   2.5366E+04   0.0000E+00   0.0000E+00
```

```
Maximum stress components from BEHX3 (Material type 1):
 0 deg. tension  0.000000E+00
 0 deg. comp.    8.946335E+04
90 deg. tension  2.598729E+04
90 deg. comp.    0.000000E+00
 in-plane shear  3.987729E+03
```

DESIGN MARGINS CORRESPONDING TO THE STARTING DESIGN LISTED
AT THE TOP OF TABLE 3. THESE MARGINS INCLUDE THE EFFECT OF CURING:

```
***** RESULTS FOR LOAD SET NO.   1  ******
 MARGINS CORRESPONDING TO CURRENT DESIGN (F.S.=FACTOR OF SAFETY)
 MARGIN CURRENT
 NO.     VALUE            DEFINITION
  1    2.880E-01 1+0.45*V(1)-1.00*V(2) -1.
  2    3.330E-01  (LOCBUK(1 )/LOCBUKA(1 )) / LOCBUKF(1 )-1; F.S.=  1.30
  3   -1.118E-01  (GENBUK(1 )/GENBUKA(1 )) / GENBUKF(1 )-1; F.S.=  1.00
  4    1.705E-01 (STRM1A(1,2)/STRM1(1,2))/STRM1F(1,2)-1; F.S.=1.00
  5   -5.938E-01 (STRM1A(1,3)/STRM1(1,3))/STRM1F(1,3)-1; F.S.=1.00
  6    5.773E-01 (STRM1A(1,5)/STRM1(1,5))/STRM1F(1,5)-1; F.S.=1.00
Critical margins are in boldface
```

DESIGN MARGINS LISTED IN TABLE 3, FOR WHICH THERE IS NO EFFECT OF CURING:

```
MARGINS CORRESPONDING TO CURRENT DESIGN (F.S.= FACTOR OF SAFETY)
 MARGIN CURRENT
 NO.     VALUE            DEFINITION
  1    2.880E-01  1+0.45*V(1)-1.00*V(2) -1.
  2    2.365E-01  (LOCBUK(1 )/LOCBUKA(1 )) / LOCBUKF(1 )-1; F.S.=  1.30
  3   -1.125E-01  (GENBUK(1 )/GENBUKA(1 )) / GENBUKF(1 )-1; F.S.=  1.00
  4    4.286E+00  (STRM1A(1 ,1 )/STRM1(1 ,1 )) / STRM1F(1 ,1 )-1; F.S.=  1.00
  5    1.753E-01  (STRM1A(1 ,2 )/STRM1(1 ,2 )) / STRM1F(1 ,2 )-1; F.S.=  1.00
  6    2.349E+02  (STRM1A(1 ,3 )/STRM1(1 ,3 )) / STRM1F(1 ,3 )-1; F.S.=  1.00
  7    1.304E+00  (STRM1A(1 ,4 )/STRM1(1 ,4 )) / STRM1F(1 ,4 )-1; F.S.=  1.00
  8    2.299E-01  (STRM1A(1 ,5 )/STRM1(1 ,5 )) / STRM1F(1 ,5 )-1; F.S.=  1.00
Critical margins are in boldface
```

Table 7 Comparison of margins for the nasatruss2 starting design from the GENOPT/BIGBOSOR4 model with no noodles or noodle gaps and from the PANDA2 model for the same configuration.

```
================================================================================

Part 1: GENOPT/BIGBOSOR4 model, no curing:
 MARGIN CURRENT
 NO.     VALUE             DEFINITION
  2    -2.431E-01   (LOCBUK(1 )/LOCBUKA(1 )) / LOCBUKF(1 )-1; F.S.=  1.30
  3    -2.093E-01   (GENBUK(1 )/GENBUKA(1 )) / GENBUKF(1 )-1; F.S.=  1.00
  4     2.410E+00   (STRM1A(1 ,1 )/STRM1(1 ,1 )) / STRM1F(1 ,1 )-1; F.S.=  1.00
  5    -2.418E-01   (STRM1A(1 ,2 )/STRM1(1 ,2 )) / STRM1F(1 ,2 )-1; F.S.=  1.00
  6     1.512E+02   (STRM1A(1 ,3 )/STRM1(1 ,3 )) / STRM1F(1 ,3 )-1; F.S.=  1.00
  7     4.866E-01   (STRM1A(1 ,4 )/STRM1(1 ,4 )) / STRM1F(1 ,4 )-1; F.S.=  1.00
  8    -2.065E-01   (STRM1A(1 ,5 )/STRM1(1 ,5 )) / STRM1F(1 ,5 )-1; F.S.=  1.00
--------------------------------------------------------------------------------

Part 2: PANDA2 model, no curing, no transverse shear deformation (t.s.d.):
 MAR. MARGIN
 NO.  VALUE               DEFINITION
 1 -6.40E-02 Local buckling from discrete model-1.,M=97 axial halfwaves;FS=0.99
16  2.80E-01 buck.(SAND);simp-support general buck;M=2;N=7;slope=0.;FS=0.999
 3  2.41E+00 fibertensn:matl=1,STR,Dseg=6,node=11,layer=5,z=0.0057; MID.;FS=1.
 4 -2.40E-01 fibercompr:matl=1,STR,Dseg=6,node=11,layer=6,z=0.0114; MID.;FS=1.
 5  1.51E+02 transtensn:matl=1,STR,Dseg=3,node=11,layer=3,z=-0.0114; MID.;FS=1.
 6  5.42E-01 transcompr:matl=1,STR,Dseg=6,node=11,layer=5,z=0.0057; MID.;FS=1.
 7 -2.07E-01 inplnshear:matl=1,STR,Dseg=4,node=11,layer=4,z=0.0114; MID.;FS=1.
--------------------------------------------------------------------------------

Part 3: PANDA2 model, no curing, yes transverse shear deformation (t.s.d.):
 MAR. MARGIN
 NO.  VALUE               DEFINITION
 1 -1.70E-01 Local buckling from discrete model-1.,M=97 axial halfwaves;FS=0.99
16 -9.13E-02 buck.(SAND);simp-support general buck;M=2;N=7;slope=0.;FS=0.999
 3  2.41E+00 fibertensn:matl=1,STR,Dseg=6,node=11,layer=5,z=0.0057; MID.;FS=1.
 4 -2.40E-01 fibercompr:matl=1,STR,Dseg=6,node=11,layer=6,z=0.0114; MID.;FS=1.
 5  1.51E+02 transtensn:matl=1,STR,Dseg=3,node=11,layer=3,z=-0.0114; MID.;FS=1.
 6  5.42E-01 transcompr:matl=1,STR,Dseg=6,node=11,layer=5,z=0.0057; MID.;FS=1.
 7 -2.07E-01 inplnshear:matl=1,STR,Dseg=4,node=11,layer=4,z=0.0114; MID.;FS=1.
--------------------------------------------------------------------------------

Part 4: GENOPT/BIGBOSOR4 model, yes curing:
```

American Institute of Aeronautics and Astronautics

```
MARGIN CURRENT
NO.    VALUE              DEFINITION
 2   -2.431E-01  (LOCBUK(1 )/LOCBUKA(1 )) / LOCBUKF(1 )-1; F.S.=  1.30
 3   -2.093E-01  (GENBUK(1 )/GENBUKA(1 )) / GENBUKF(1 )-1; F.S.=  1.00
 4    8.029E+00  (STRM1A(1 ,1 )/STRM1(1 ,1 )) / STRM1F(1 ,1 )-1; F.S.=  1.00
 5   -3.605E-01  (STRM1A(1 ,2 )/STRM1(1 ,2 )) / STRM1F(1 ,2 )-1; F.S.=  1.00
 6   -5.895E-01  (STRM1A(1 ,3 )/STRM1(1 ,3 )) / STRM1F(1 ,3 )-1; F.S.=  1.00
 7   -2.065E-01  (STRM1A(1 ,5 )/STRM1(1 ,5 )) / STRM1F(1 ,5 )-1; F.S.=  1.00
------------------------------------------------------------------------
```

Part 5: PANDA2 model, yes curing, yes transverse shear deformation (t.s.d.):
```
 MAR. MARGIN
 NO.  VALUE                DEFINITION
 1 -1.70E-01 Local buckling from discrete model-1.,M=97 axial halfwaves;FS=0.99
14 -9.13E-02 buck.(SAND);simp-support general buck;M=2;N=7;slope=0.;FS=0.999
 3  8.02E+00 fibertensn:matl=1,STR,Dseg=3,node=11,layer=4,z=-0.0057; MID.;FS=1.
 4 -3.59E-01 fibercompr:matl=1,STR,Dseg=6,node=11,layer=6,z=0.0114; MID.;FS=1.
 5 -5.90E-01 transtensn:matl=1,STR,Dseg=6,node=11,layer=6,z=0.0114; MID.;FS=1.
 6 -2.07E-01 inplnshear:matl=1,STR,Dseg=4,node=11,layer=4,z=0.0114; MID.;FS=1.
========================================================================
```
NOTE 1: The order of the PANDA2 margins has been changed and several PANDA2 margins have been left out of the lists in order to make the comparison between GENOPT/BIGBOSOR4 and PANDA2 predictions easier.

NOTE 2: The "knockdown" for the transverse shear deformation effect in PANDA2 models in which the truss-core sandwich properties are "smeared out" for the computation of general buckling is developed as described in Item No. 807 in the PANDA2 file, ...panda2/doc/panda2.news.

NOTE 3: For the "yes curing" results, the coefficients of thermal expansion and curing delta-temperature are:
alpha1(along fibers)=0.00001, alpha2(normal to fibers)=0.0001, TEMCUR = 200.

NOTE 4: Critical margins are in **boldface**

NOTE 5: In the GENOPT/BIGBOSOR4 model the factor of safety (F.S.) for local buckling is 1.3, whereas in the PANDA2 model the F.S. for local buckling is 1.0.

NOTE 6: In the PANDA2 margins M is the number of axial half-waves over the length, LENGTH = 109 inches, of the cylindrical shell. N is the number of circumferential half-waves over 180 degrees of the circumference of the cylindrical shell.

Table 8 Optimized designs obtained with ILINKS = 0, ILINKS = 2, and ILINKS = 1 for the specific case, nasatruss3, in which the lower bound of THICK(4), the 90-degree layer, is set to 0.00285 inches.

PART 1: ILINKS =0 (These data taken from Table 5) **weight/area=0.006456 lb/in^2**
```
  VALUES OF DESIGN VARIABLES CORRESPONDING TO BEST FEASIBLE DESIGN
 VAR.    CURRENT
 NO.      VALUE                DEFINITION
  1    1.4249E+00  circumferential width of a single module: PITCH
  2    2.8256E-01  circumferential width of the trapezoid crown: BCROWN
  3    5.8772E-01  height of the truss-core sandwich: HEIGHT
  4    6.4605E-02  local radius from base to side of trapezoidal tool: RACUTE
  5    5.0000E-02  local radius from side to crown of trapezoidal tool: ROBTUS
  6    5.7000E-03  layer type thickness: THICK(1 ) ←the +45-degree layers
  7    5.7000E-03  layer type thickness: THICK(2 ) ←the -45-degree layers
  8    5.7000E-03  layer type thickness: THICK(3 ) ←the   0-degree layers
  9    2.8500E-03  layer type thickness: THICK(4 ) ←the  90-degree layers
```

**NOTE: The face sheet laminates in Segments 1, 6, 15, and 18 in Fig. 4 have
      the stacking sequence: [+45, −45, 0, 90, 90, 0 −45, +45]total. Since
      the two adjacent 90-degree plies each have thickness equal to 0.00285
      inches, the truss-core sandwich wall can be fabricated with only a
      single 90-degree ply of thickness 0.0057 inches.**

PART 2: ILINKS = 2 weight/area=0.006204 lb/in^2
```
  VALUES OF DESIGN VARIABLES CORRESPONDING TO BEST FEASIBLE DESIGN
 VAR.    CURRENT
 NO.      VALUE                DEFINITION
  1    1.5470E+00  circumferential width of a single module: PITCH
  2    3.1560E-01  circumferential width of the trapezoid crown: BCROWN
  3    6.2840E-01  height of the truss-core sandwich: HEIGHT
  4    5.0170E-02  local radius from base to side of trapezoidal tool: RACUTE
  5    8.7170E-02  local radius from side to crown of trapezoidal tool: ROBTUS
  6    5.7000E-03  layer type thickness: THICK(1 ) ←the +45-degree layers
  7    5.7000E-03  layer type thickness: THICK(2 ) ←the -45-degree layers
  8    5.7000E-03  layer type thickness: THICK(3 ) ←the   0-degree layers
  9    2.8500E-03  layer type thickness: THICK(4 ) ←the  90-degree layers
```

PART 3: ILINKS = 1 weight/area=0.006385 lb/in^2
```
  VALUES OF DESIGN VARIABLES CORRESPONDING TO BEST FEASIBLE DESIGN
 VAR.    CURRENT
 NO.      VALUE                DEFINITION
```

American Institute of Aeronautics and Astronautics

```
1     1.6300E+00  circumferential width of a single module: PITCH
2     2.8940E-01  circumferential width of the trapezoid crown: BCROWN
3     5.9680E-01  height of the truss-core sandwich: HEIGHT
4     6.0180E-02  local radius from base to side of trapezoidal tool: RACUTE
5     1.0820E-01  local radius from side to crown of trapezoidal tool: ROBTUS
6     5.7000E-03  layer type thickness: THICK(1 ) ←the +45-degree layers
7     5.7000E-03  layer type thickness: THICK(2 ) ←the -45-degree layers
8     5.7000E-03  layer type thickness: THICK(3 ) ←the  0-degree layers
9     2.8500E-03  layer type thickness: THICK(4 ) ←the  90-degree layers
===================================================================================
```

NOTE: The "noodle support" index, ILINKS, is defined in Table 1 and is fully described at Prompt No. 195 in Table 2. See Figs. 26 and 27 for plots of the objective versus design iterations for the models with the "noodle support" index, ILINKS=2 and ILINKS=1, respectively. See Figs. 16 and 17 for the objective and design margins versus design iterations for the model with ILINKS = 0 (noodles do not support the little segments that enclose them).
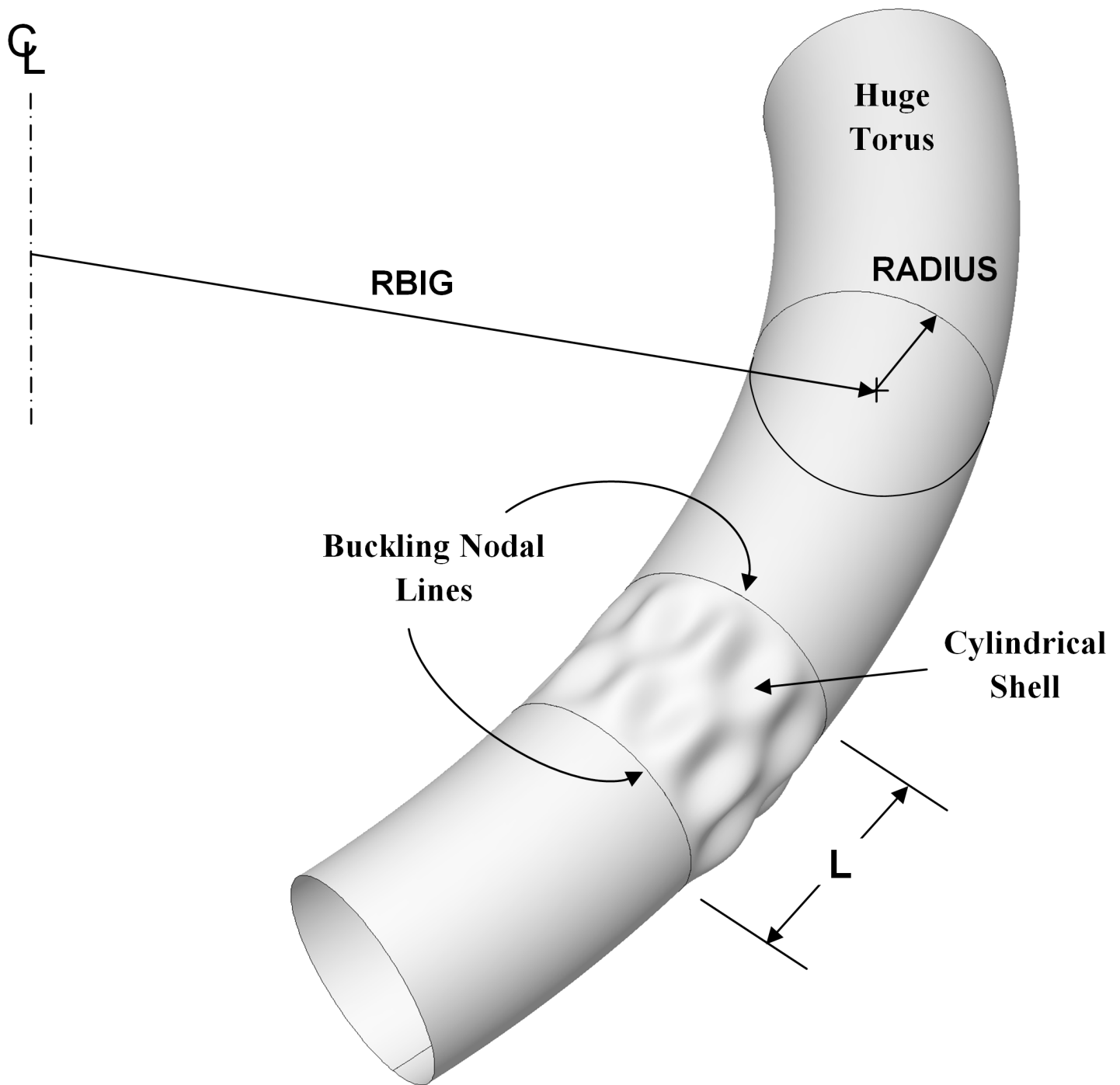
Fig. 1a **Schematic of a "huge torus" model**. For most "huge torus" models, a good choice of RBIG is RBIG = $100 \times L/\pi$. The cylindrical shells studied here have RADIUS = 78.15 inches (inner surface). For the "true prismatic" shell model the kinematic relationships introduced recently into BIGBOSOR4 [8,10] correspond essentially to RBIG = infinity. This figure was created by Robert P. Thornburgh and appears in [8].

American Institute of Aeronautics and Astronautics
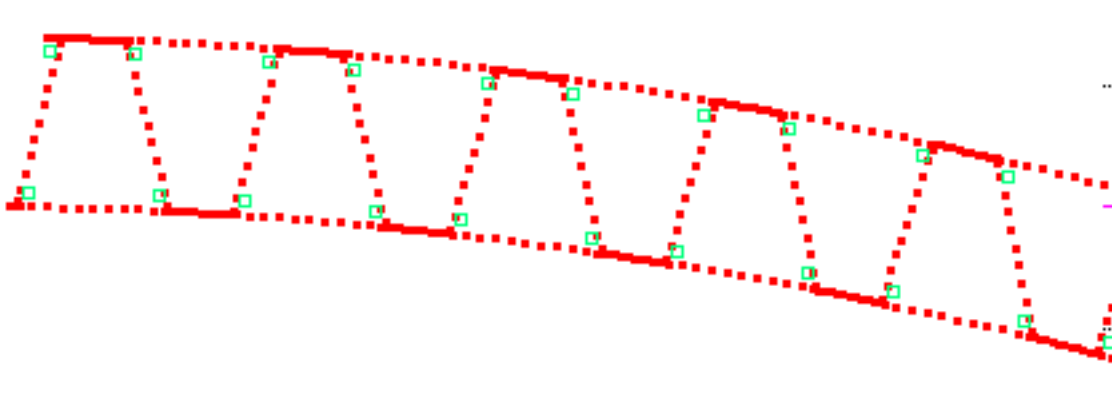
Fig. 1b. Part of the 46-module model used for the prediction of general buckling by GENOPT/BIGBOSOR4. The truss-core sandwich cross section is discretized, and variation of the general buckling displacement in the direction normal to the plane of the paper is trigonometric. The centroid of each noodle is indicated by a small green square. In the general buckling model there are no little curved and flat shell segments that enclose each noodle, as are shown in the next figures that depict various local buckling models. See Figs. 5, 13, 14 for general buckling modes obtained with this type of GENOPT/BIGBOSOR4 model. The segment numbering scheme is for each module is shown in Fig. 6 (top).

Noodle gaps
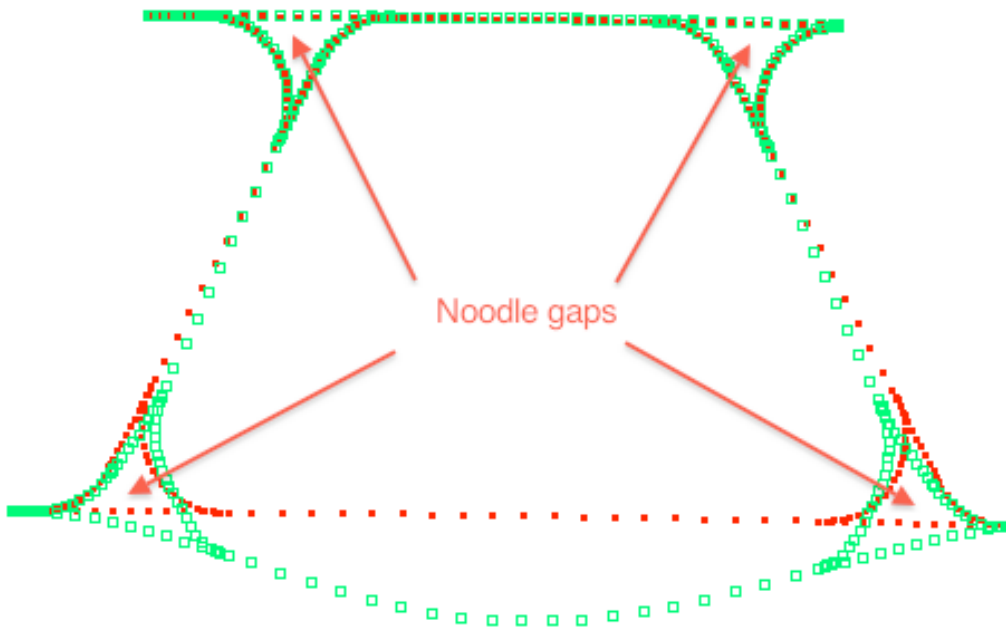
Fig. 1c. Cross section of a single module of the model used for the prediction of local buckling by GENOPT/BIGBOSOR4. In this model the noodles are present (not shown here), but do not support the little shell segments that enclose them. Careful inspection of these little segments, especially those at the bottom of the figure, reveals that they deform in the local buckling mode. This conservative model is generated when the index, ILINKS (defined in Table 1 and fully described at Prompt No. 195 in Table 2) is equal to zero. See Figs. 2, 3, 9 for local buckling modes based on this type of model.

American Institute of Aeronautics and Astronautics
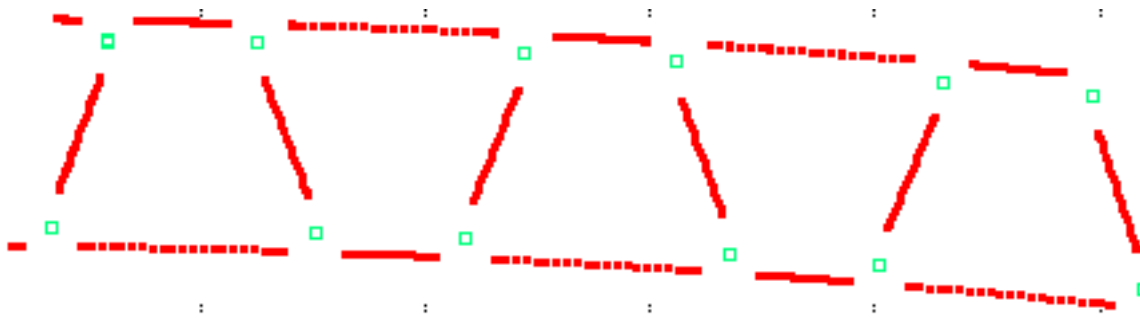
Fig. 1d. Cross section of a three-module model used for the prediction of local buckling by GENOPT/BIGBOSOR4. The centroid of each noodle is indicated by a little green square The support that each noodle provides to the little shell segments that enclose it is represented by rigid links that span the gaps between adjacent web and face sheet shell segments. This model is generated when the index, ILINKS (defined in Table 1 and fully described at Prompt No. 195 in Table 2) is equal to unity. See Fig. 24 for the prediction of local buckling from this type of model.
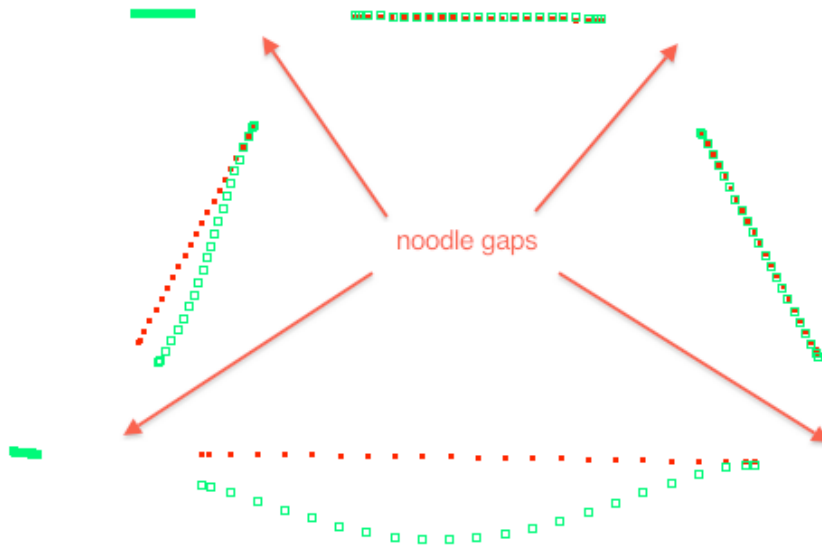
Fig. 1e. The local buckling mode as predicted by a single-module model of the same type as that displayed in Fig. 1d. Notice that the centroid of the noodle gap at the lower left rotates and translates as a rigid body. A similar rotation and translation is prevented at the lower right-hand side of this single-module local buckling model by a clamped boundary condition there. Figure 24 shows how the local buckling load factor converges from above with respect to the number of modules used in the local buckling model with the "noodle support" index, ILINKS = 1. (ILINKS is defined in Table 1 and fully described at Prompt No. 195 in Table 2).
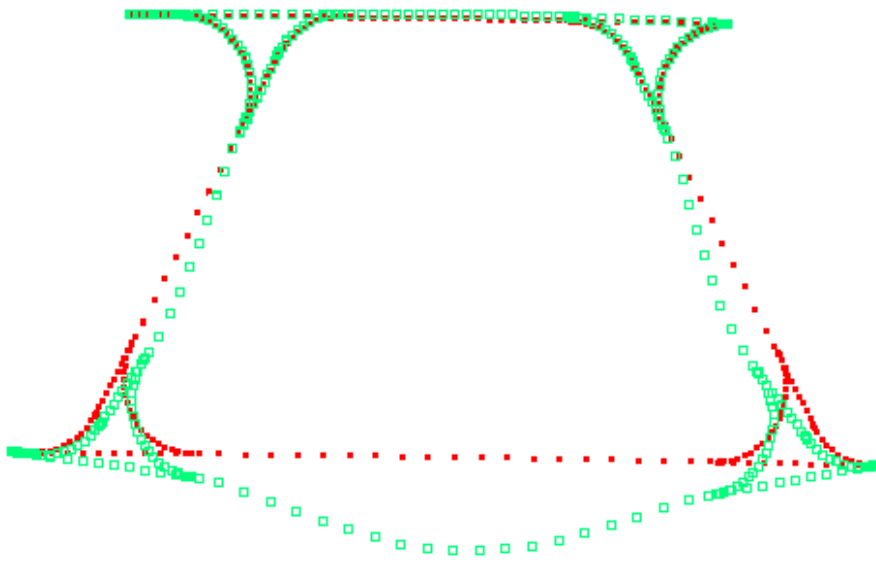
Fig. 1f. Cross section of a single module of the model used for the prediction of local buckling by GENOPT/BIGBOSOR4. In this model the noodles are present (not shown here), and "extra" inner and outer layers are added to each of the little shell segments that enclose each noodle. These "extra" inner and outer layers greatly increase the "hoop" bending stiffnesses of those little shell segments, simulating support of those segments by the enclosed noodles. Careful inspection of these little segments, especially those at the bottom of the figure, reveals that they deform very little in the local buckling mode. (Compare with Fig. 1c.) This model is generated when the index, ILINKS (defined in Table 1 and fully described at Prompt No. 195 in Table 2) is equal to two. Figure 23 shows how the local buckling load factor converges from above with respect to the number of modules used in the local buckling model with the "noodle support" index, ILINKS = 2.

American Institute of Aeronautics and Astronautics
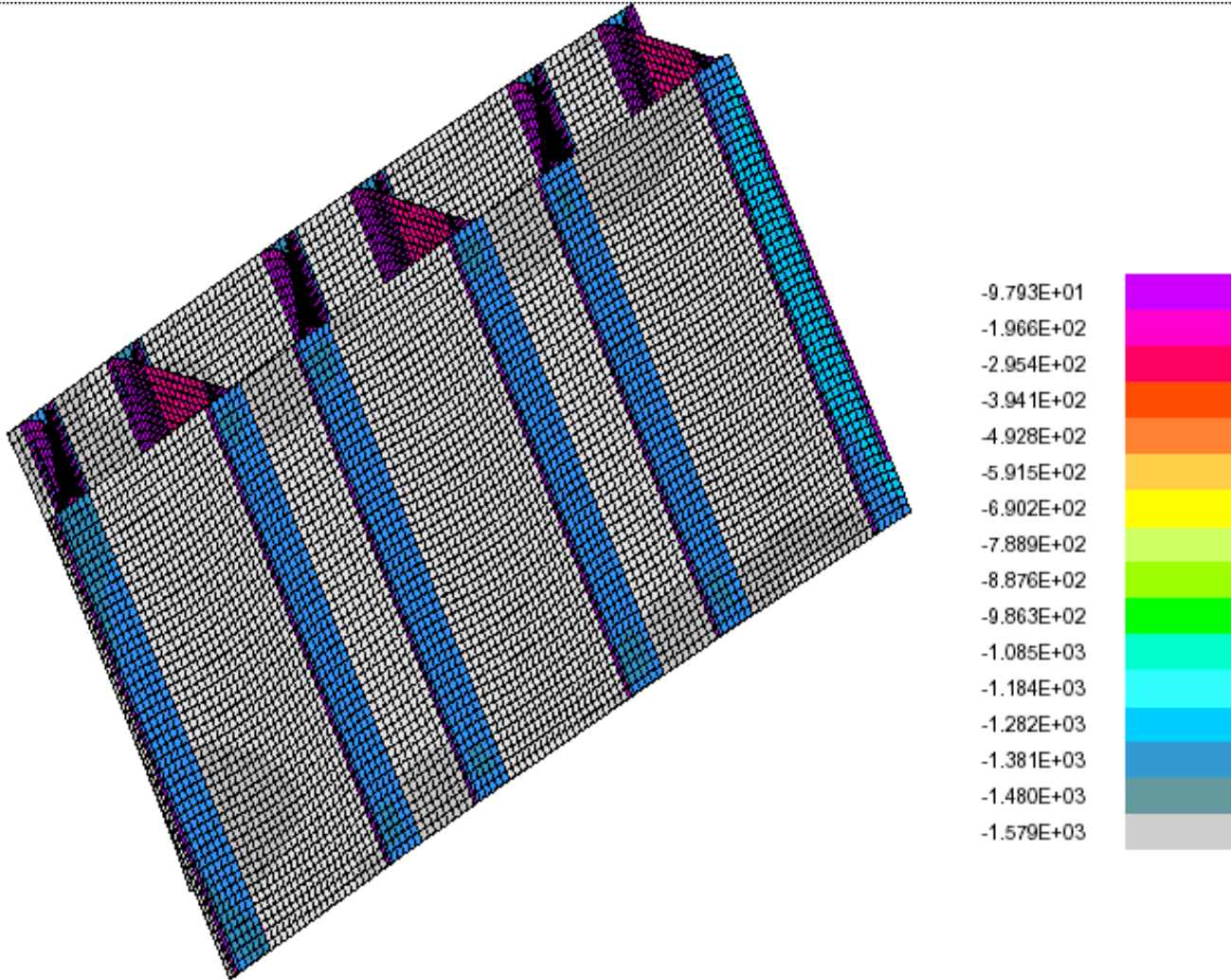
BIGBOSOR4: Nx(seg.1)=-1557.5; Nx(seg2)=-116.61; Nx(seg3)=-1352.4; Nx(seg7)=-233.22 lb/in
PA=1.0; The BIGBOSOR4 segment numbers are shown in Fig. 4
Linear Nx contours from STAGS for the case, "nasatruss2"; 410 elements
STAGS plot of linear prebuckling Nx. Agrees reasonably well with BIGBOSOR4 prediction
Minimum value = -1.57858E+03,   Maximum value = -9.79318E+01

Θ x -35.84
Θ y -13.14
Θ z   35.63

1.133E+00
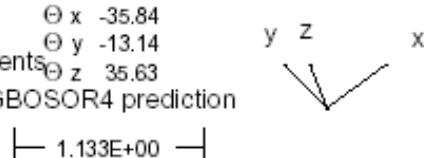
Fig. 1g. Typical membrane pre-buckled state of the truss-core sandwich configuration listed in Table 3 (the "**nasatruss2**" starting design) obtained from uniform end shortening applied to a STAGS model that consists of three modules of the type shown in Fig. 4. The axial compression, N_x (lb/in) in each shell segment is proportional to the axial stiffness of that shell segment. NOTE: STAGS is **not** used for optimization. The purpose of this figure is to emphasize that the pre-buckled state in the GENOPT/BIGBOSOR4 models that are used for optimization of the truss-core sandwich cross section is a **prismatic membrane state**. There is no local bending in the neighborhoods of the edges.
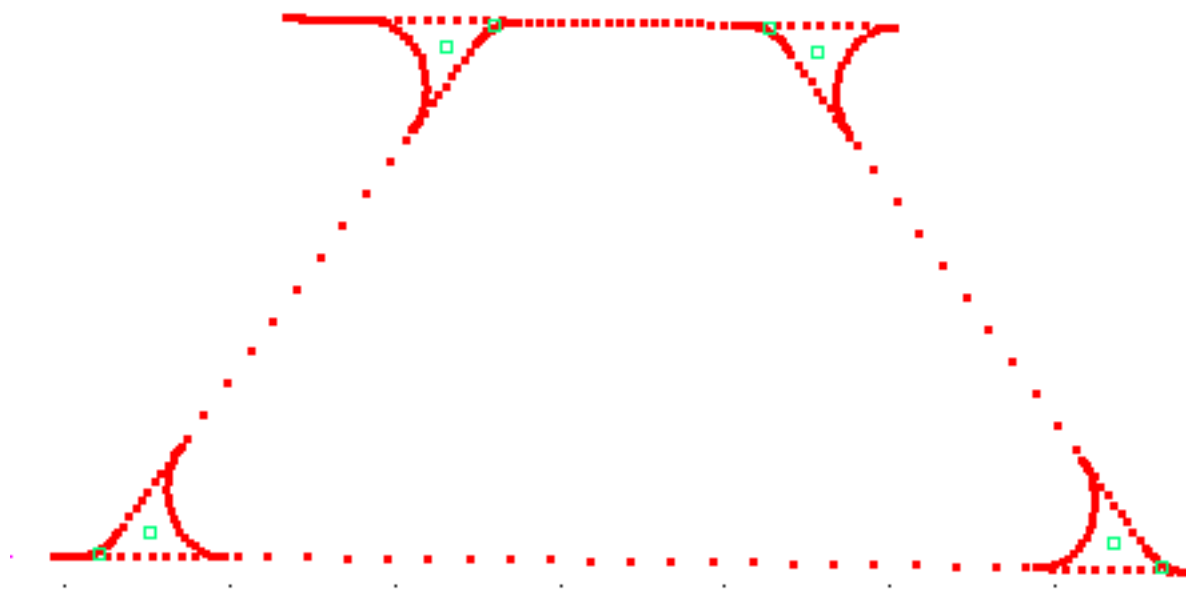
Fig. 2a Discretization of the cross section of a single-module model of the optimized truss-core sandwich wall for the specific case called "**nasatruss2**" (Table 4). This model is used for the **local** buckling analysis. The segment numbering and direction of travel along each segment are shown in Fig. 4. The noodle in each of the four noodle gaps is modeled as two "beams", one of cross-section area, AREA1 (Fig. 7, top), and the other of cross-section area, AREA2 (Fig. 7, bottom). The "beam" of cross-section area, AREA2 is attached to the curved shell segments associated with R_2 (such as Segment 2 in Fig. 4) and the "beam" of cross-section area, AREA1 is attached to the curved shell segments associated with R_1 (such as Segment 5 in Fig. 4). The "beams" are modeled as rings in the huge torus model. The centroids of these rings are indicated in this figure by small green squares. Variation of the local buckling modal displacements in the axial direction (normal to the plane of the paper) is trigonometric. In this local buckling model Segments 1 and 15 (Fig. 4) are shortened in order to prevent local buckling of them. For optimization it is best to use at least three modules in the local buckling model, such as is done in the local buckling model displayed in Fig. 3a.

American Institute of Aeronautics and Astronautics

- — Undeformed; Only one 22-segment module of the type shown in Fig.4 is used here.
—— Deformed; N=number of axial half-waves over the length FACLEN x LENGTH =0.05 x 109 inches

nasatruss2..R,Z_EIGENMODE_1--N_5; eigenvalue=1.3502; one module

Axial Station (inches)

Radius (inches)
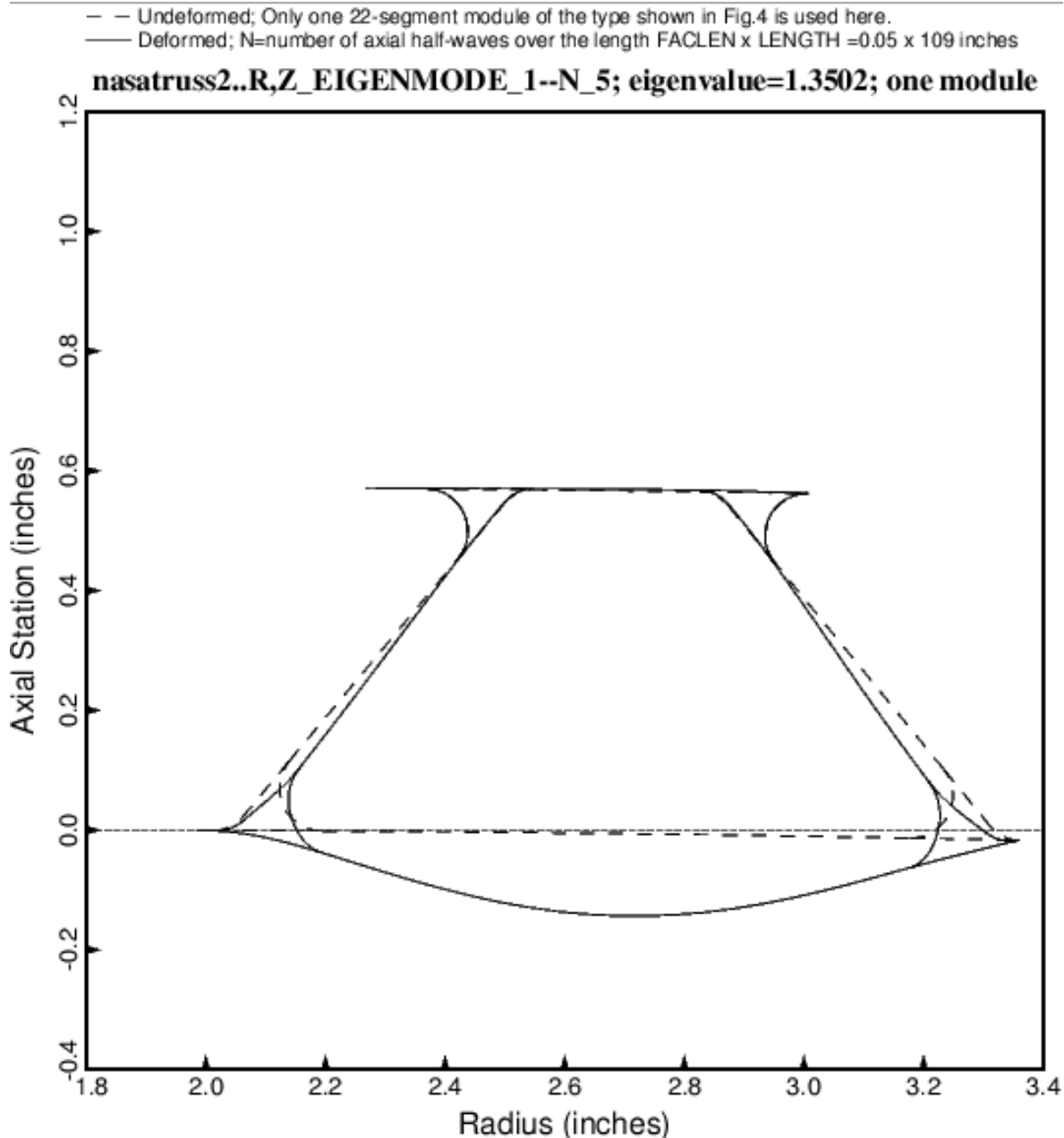
Fig. 2b **A single-module model of the optimized (Table 4) truss-core sandwich shell wall**, showing a local buckling mode shape. The single module used for local buckling consists of 22 BIGBOSOR4 shell segments, numbered as shown in Fig. 4. The local buckling load factor (eigenvalue) is computed in SUBROUTINE BEHX1. **This is an optimized cross-section (Table 4).** The cross-section properties and design margins are listed in Table 4. The quantity N is the number of axial half-waves over the length FACLEN x 109 = 0.05 x 109 inches. FACLEN is one of the input variables established by the GENOPT user. FACLEN is listed in Tables 1 and 2. Segments 1 and 15 are shortened to prevent local buckling there. This figure and Figs. 3a, 3b, and 9 were generated with the "noodle support" index, ILINKS (defined in Table 1 and fully described at Prompt No. 195 in Table 2) equal to 0.

American Institute of Aeronautics and Astronautics

— — Undeformed; Three 22-segment local buckling modules of the type shown in Fig.4 are used.
—— Deformed; N=number of axial half-waves over the length, FACLEN x 100 = 0.05 x 109 inches

nasatruss2..R,Z_EIGENMODE_1--N_5; eigenvalue=1.3102 (BEHX1)
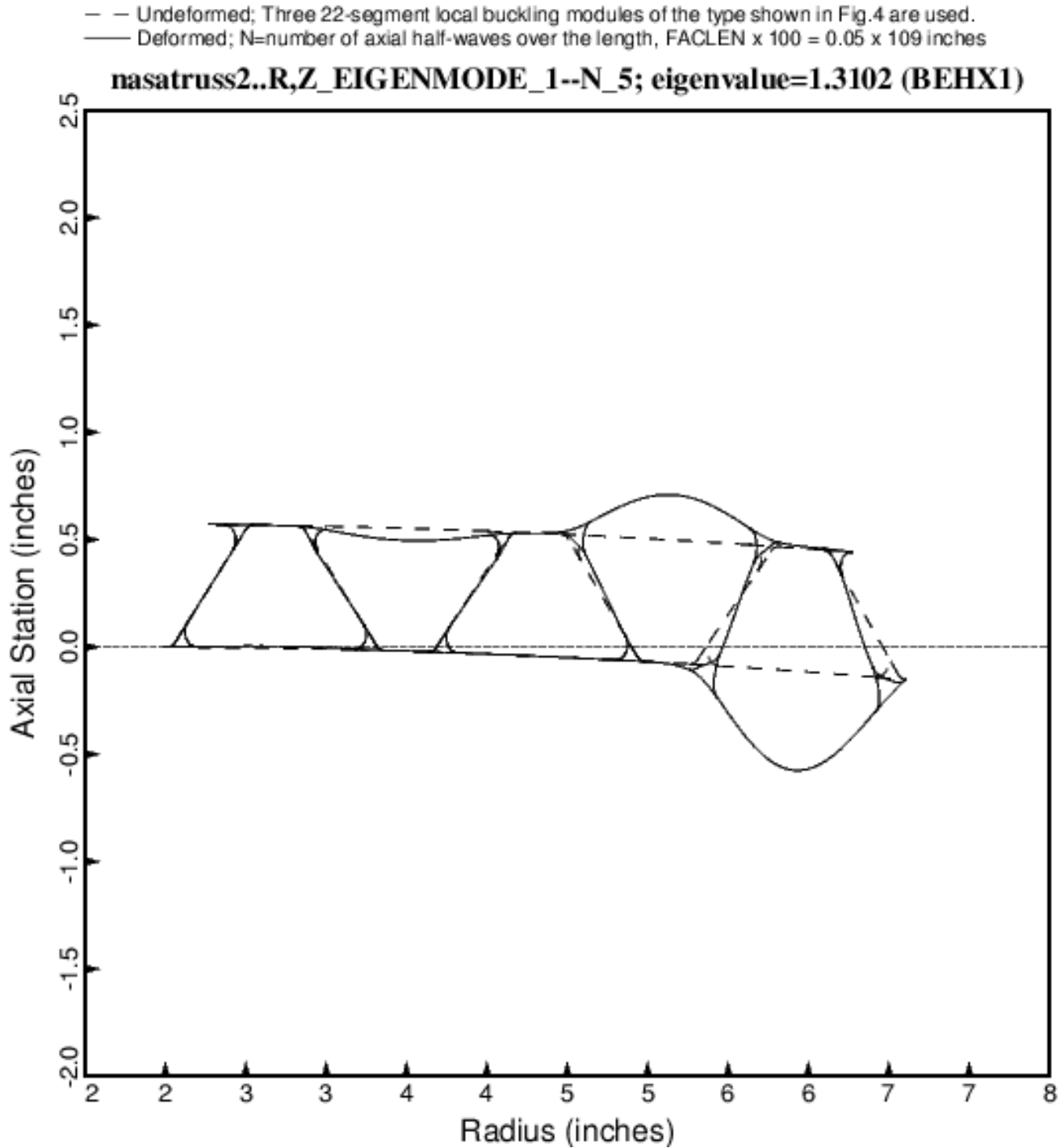
Fig. 3a **A three-module model of local buckling of the optimized (Table 4) truss-core sandwich wall**. Compare with Fig. 2b. The "noodle support" index, ILINKS = 0.

American Institute of Aeronautics and Astronautics

— — Undeformed; N=number of axial halfwaves over the length, FACLEN x LENGTH = 0.05 x 109 inches
—— Deformed; This is a five-module model for the prediction of local buckling

nasatruss2..R,Z_EIGENMODE_1--N_5; eigenvalue=1.3102, 5-module
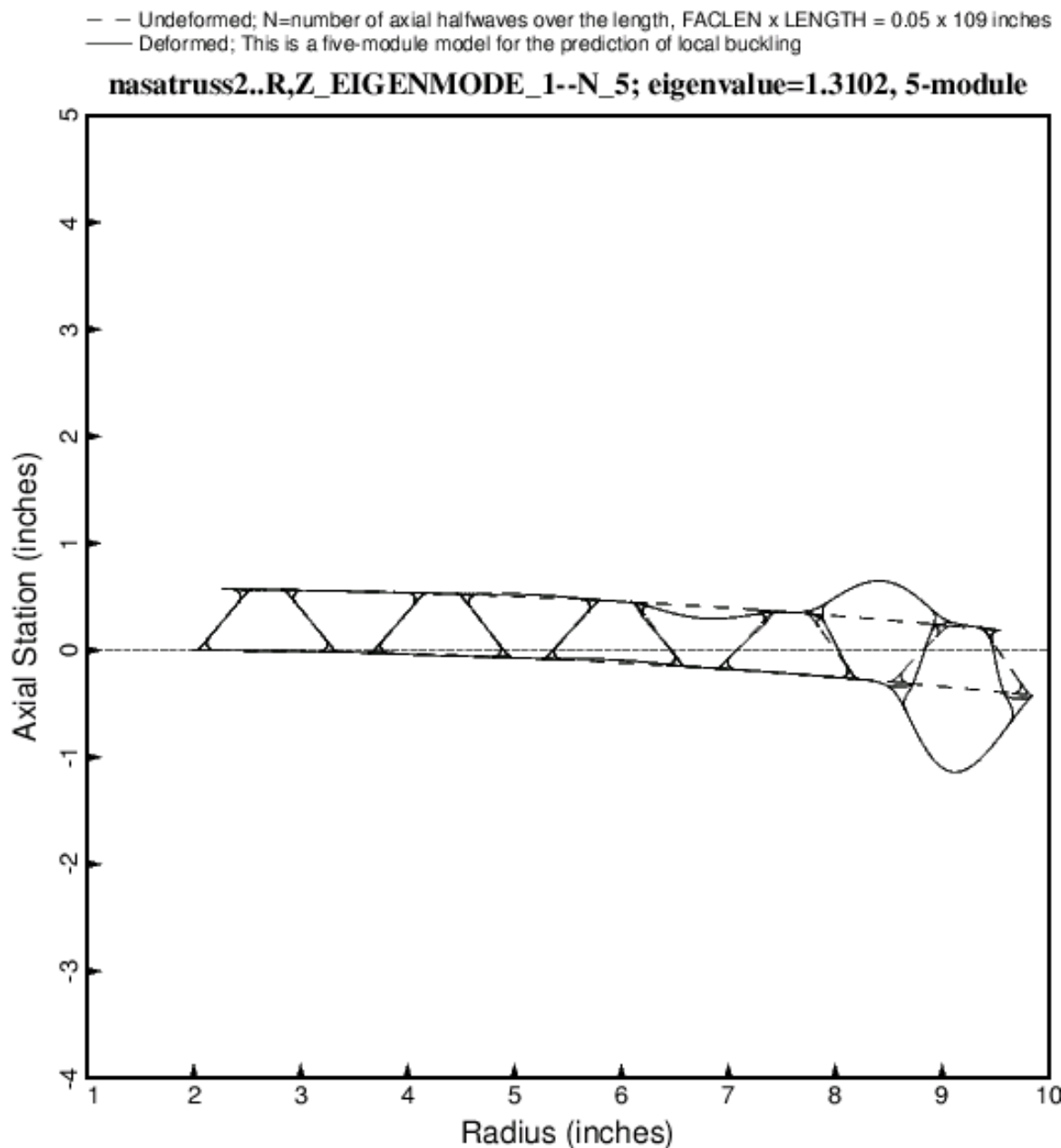
Fig. 3b **A five-module model of the optimized (Table 4) truss-core sandwich shell wall**, showing a local buckling mode shape. This is an optimized cross section. The local buckling load factors from the three-module model and from the five-module model are identical. The three-module model for local buckling is ordinarily used during the optimization process because less computer time is required to find the optimum design with that model than with use of the five-module local buckling model. In the first (left-most) module, Segments 1 and 15 (Fig. 4) are shortened in the radial direction in order to prevent local buckling of those two segments. This holds also for the three-module model displayed in the previous figure and the single-module model displayed in Fig. 2. The "noodle support" index, ILINKS = 0.
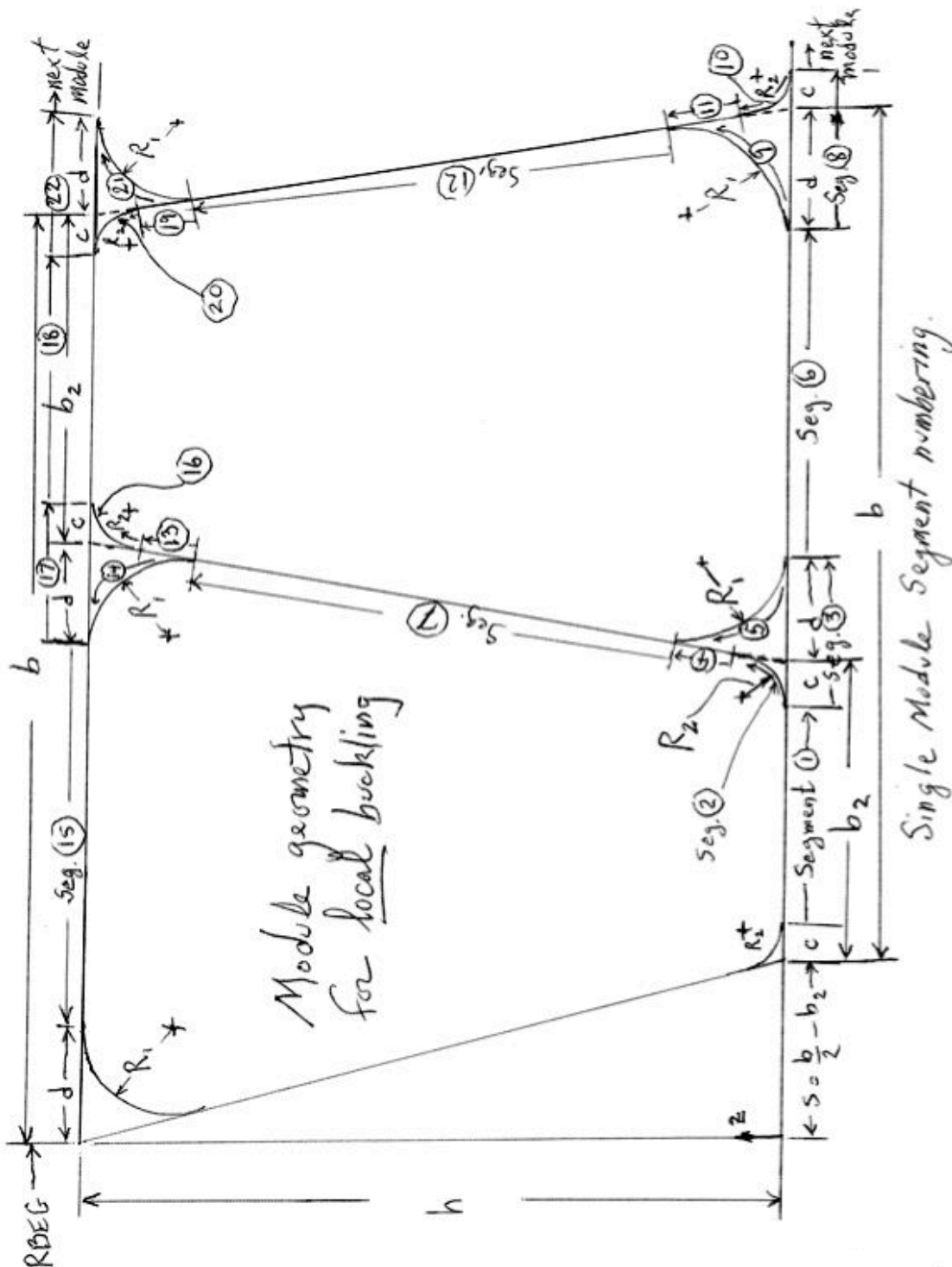
Fig. 4 BIGBOSOR4 model of the 22-segment single-module used for obtaining **local buckling** load factors (eigenvalues) and mode shapes such as those displayed in the previous two figures. This model is also used to determine the stresses in each ply of each laminate.

nasatruss2..R,Z_EIGENMODE_1--N_4; eigenvalue=0.99149 (BEHX2)
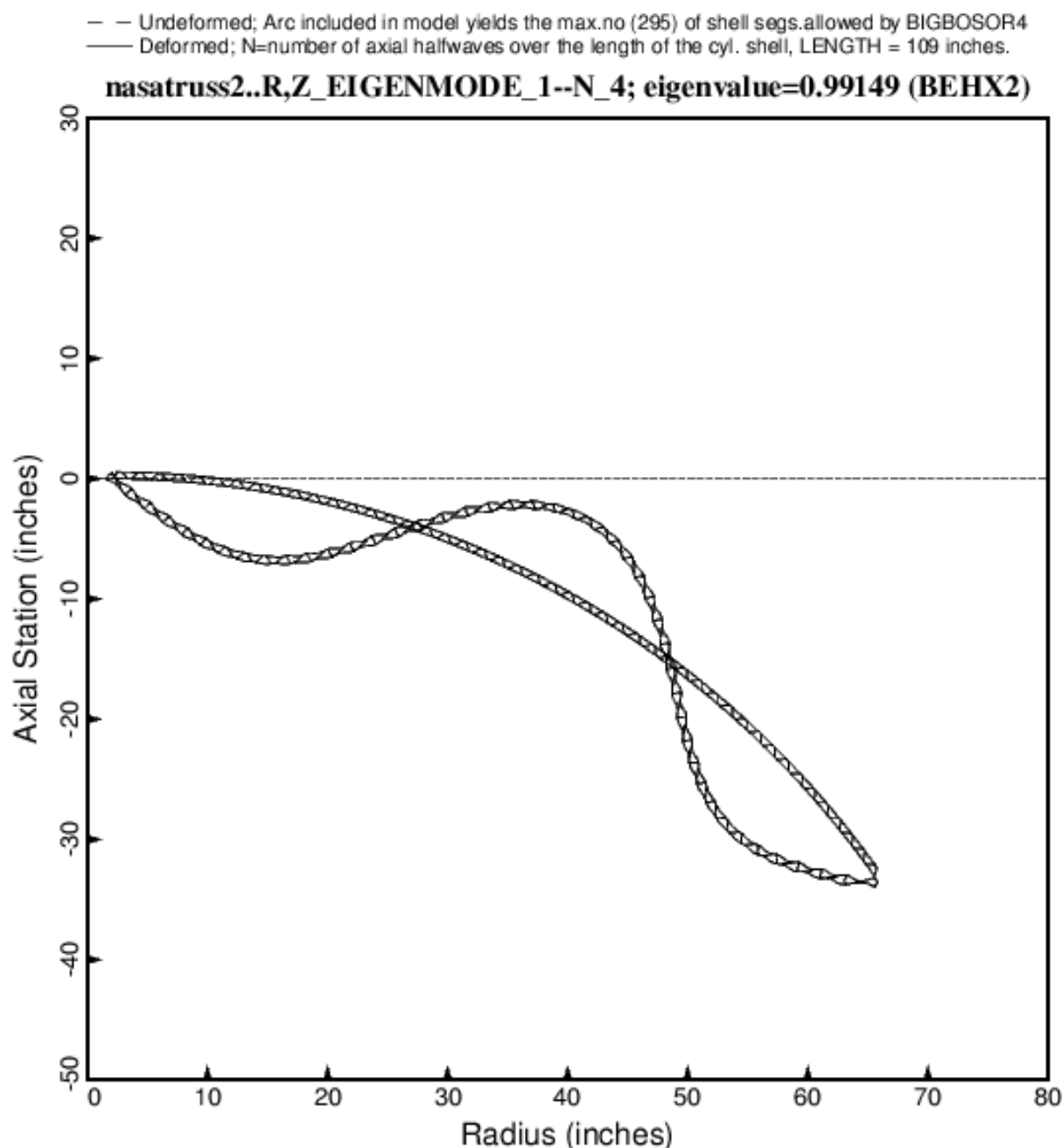
Fig. 5 **A multi-module model of the truss-core sandwich shell wall**, showing a general buckling mode shape. The single module used for general buckling consists of six BIGBOSOR4 shell segments, numbered as shown in the top part of Fig. 6. There are 46 modules in this model. Fig. 1b shows part of the 46-module model used for general buckling. The general buckling load factor is computed in SUBROUTINE BEHX2. **This result is for an optimized truss-core sandwich wall (Table 4)**. The quantity **N** is the number of axial half-waves over the length, 109 inches, of the cylindrical shell. The cross-section properties and design margins of the optimized design are listed in Table 4. The arc shown here is the longest portion of the circumference of the cylindrical shell that can be handled by BIGBOSOR4 for this particular geometry. BIGBOSOR4 presently has an upper limit of 295 shell segments.
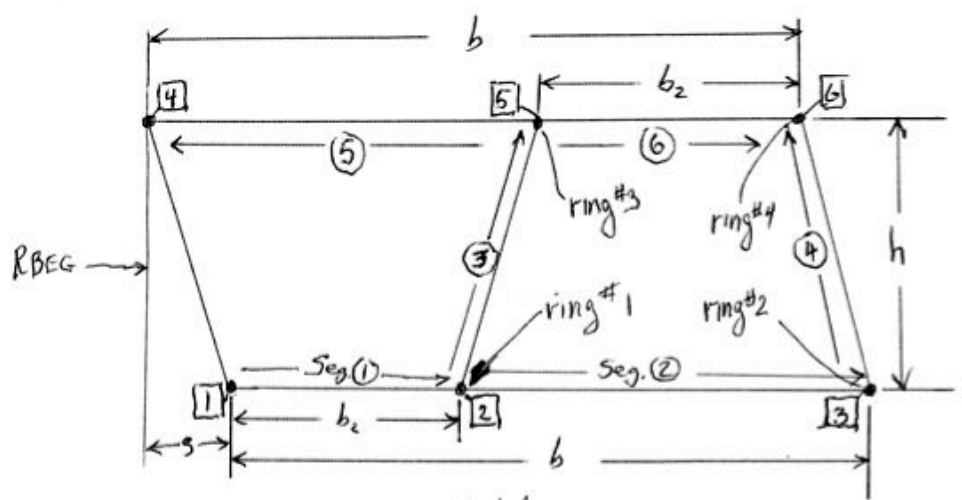
American Institute of Aeronautics and Astronautics
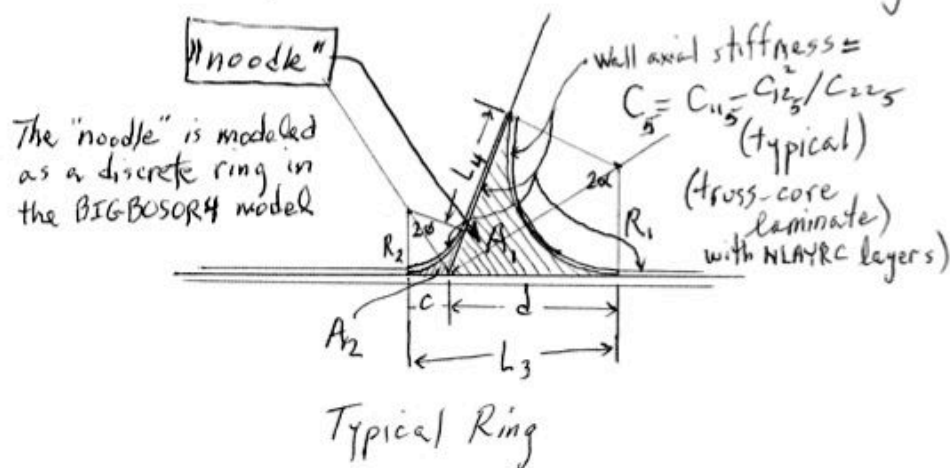
Fig. 6 BIGBOSOR4 shell segment numbering scheme used for a single module of the **general buckling model**. Each "noodle" is modeled as a discrete "ring" (huge torus model shown in Fig. 1a). The "ring" is attached to the truss-core sandwich as indicated in the top part of this figure and with axial stiffness as given in the bottom part. The ring centroid is located at the centroid of the noodle gap shown in the bottom part of this figure. Fig. 1b shows the locations of the noodle centroids in the general buckling model.

The following handwritten equations appear in the figure:

$$S = \frac{b}{2} - b_2$$

$$2\phi = \tan^{-1}(h/s)$$

$$(r_c, z_c) = (r_1, z_1 + R_1)$$

$$(r_2, z_2) = \left[r_1 + d(1 - \cos 2\phi), \; z_1 + d \sin 2\phi\right]$$

$$d = \frac{R_1}{\tan \phi}$$

$$\text{Shaded} \quad AREA1 = R_1 d - \pi R_1^2 \frac{2\alpha}{2\pi}$$

$$\alpha = 90 - \phi$$

$$c = \frac{R_2}{\tan \alpha}$$

$$(r_c, z_c) = (r_1, z_1 + R_2)$$

$$(r_2, z_2) = \left[r_1 + c(1 + \cos 2\phi), \; z_1 + c \sin 2\phi\right]$$

$$\text{Shaded} \quad AREA2 = R_2 c - \pi R_2^2 \frac{2\phi}{2\pi}$$
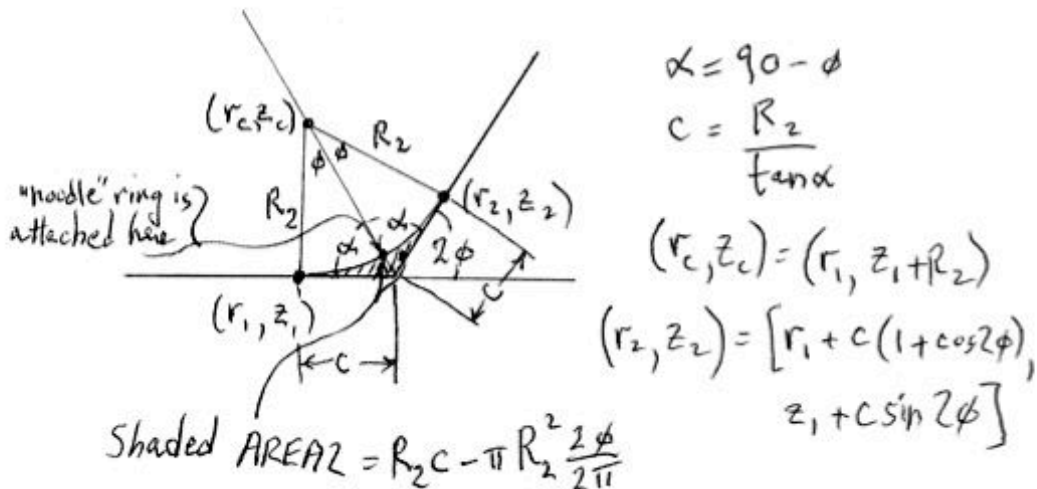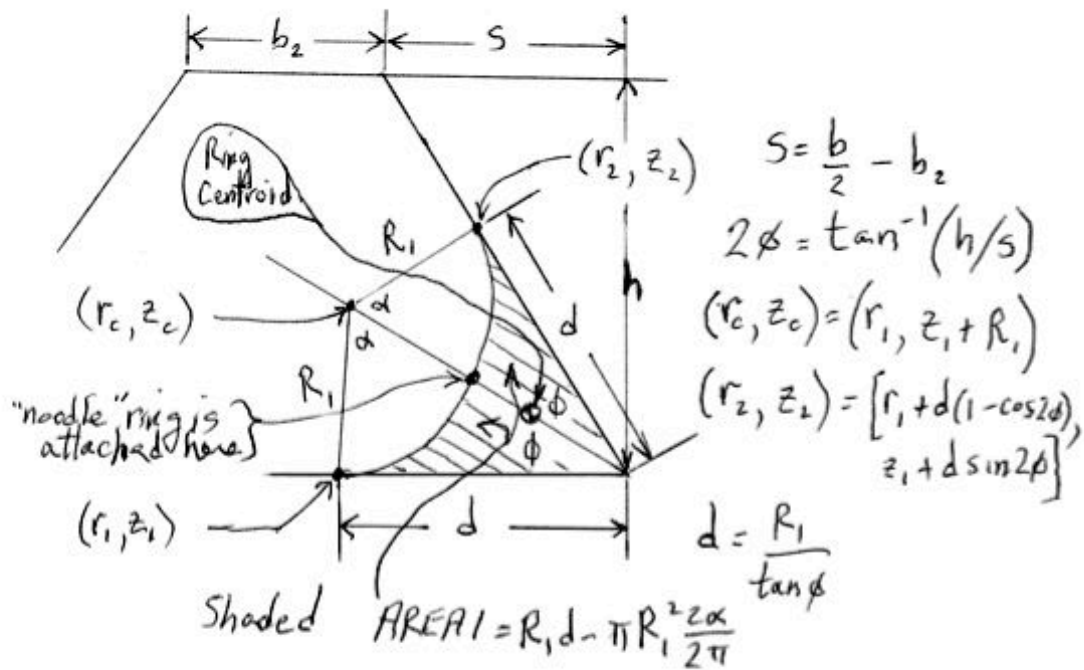
Discrete ring ("noodle") cross section areas.

Fig. 7 How the "noodle" cross-section areas, AREA1 and AREA2, are computed

79

American Institute of Aeronautics and Astronautics
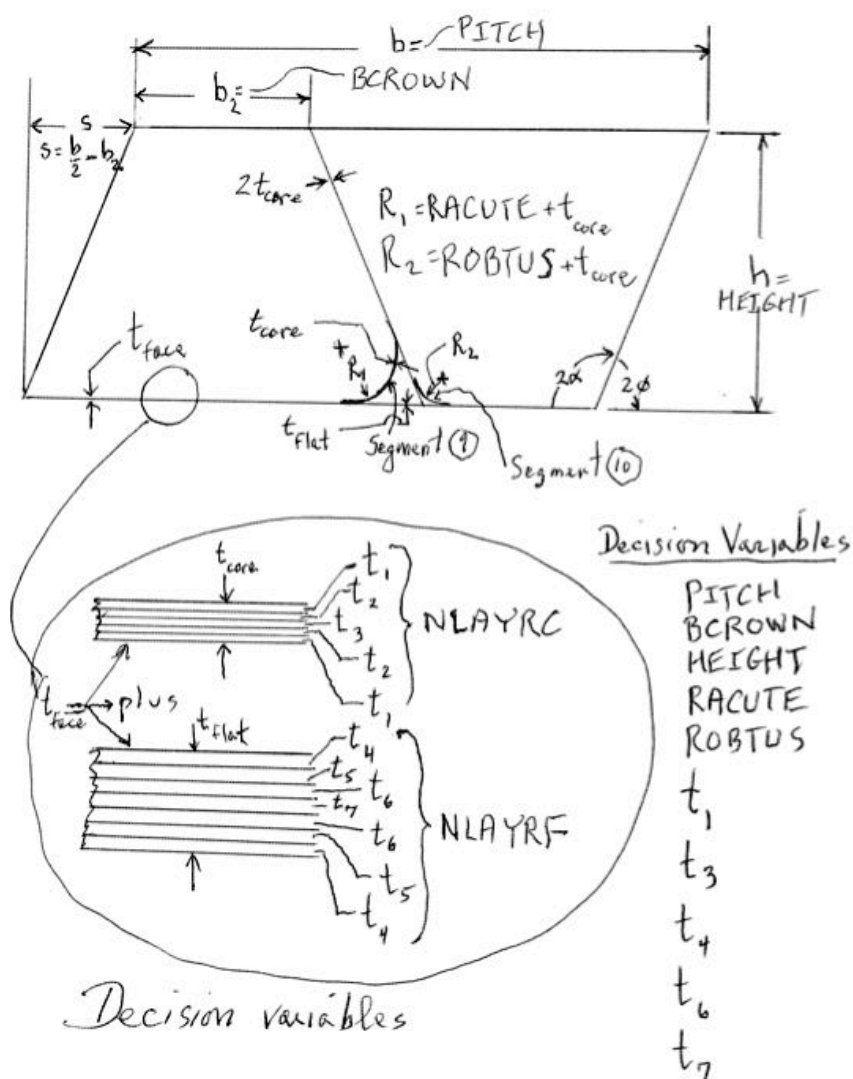
Fig. 8 **Decision variables for a typical specific case** that is a member of the "**trusscomp**" class.. **Note that the composite laminates, NLAYRC ("number of layers in the truss-core laminate") and NLAYRF ("number of layers in each face sheet laminate") are different in this figure from the numbers, NLAYRC and NLAYRF, in the case called** "**nasatruss2**", which one of the specific cases examined in this paper. In the case, **nasatruss2**, NLAYRC = 2 and NLAYRF = 6, and there is only one ply thickness, THICK(1) that is an independent decision variable. The other ply thicknesses in the **nasatruss2** case are all linked to THICK(1), as described in the text. The laminates and decision variables listed in this figure pertain to the specific case called "**test**" in [3], not to the specific case called "**nasatruss2**".

nasatruss2..R,Z_EIGENMODE_1--N_5; eigenvalue=1.6075, 3-modules
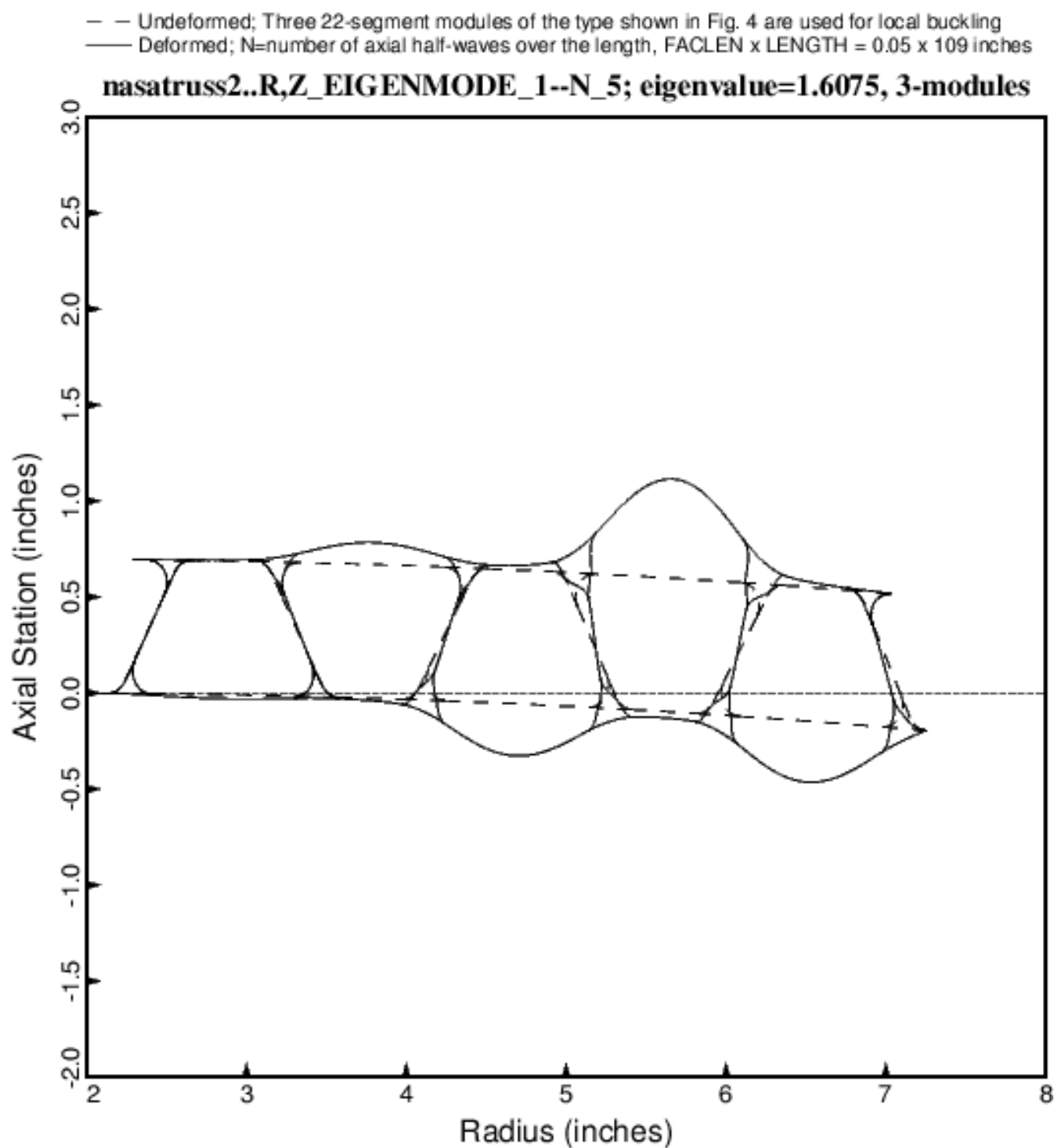
Fig. 9 Specific case called "**nasatruss2**". **Local buckling of the starting design (Table 3) with noodles present**, from three modules of the BIGBOSOR4 22-segment single-module model displayed in Fig. 4. Compare with Fig. 3a, which pertains to the optimized design. The noodles and noodle gaps are included in this model. The quantity **N** is the number of axial half-waves over the length FACLEN x 109 = 0.05 x 109 inches. Segments 1 and 15 (see Fig. 4) are radially shortened in order to prevent local buckling there. The "noodle support" index, ILINKS = 0.

nasatruss2..R,Z_EIGENMODE_1--N_5; eigenvalue=0.98399 (no noodles)
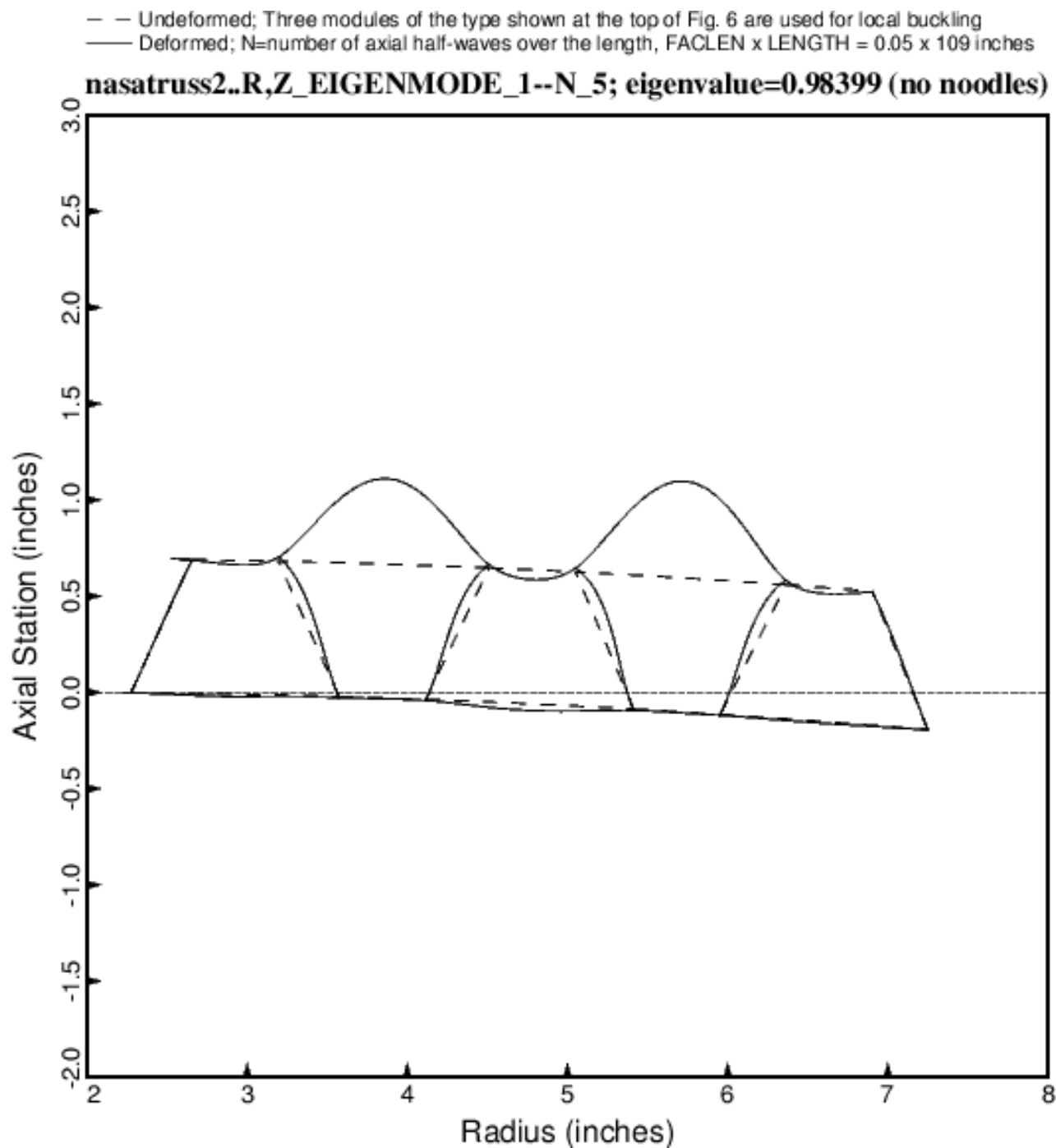
Fig. 10 Specific case called "**nasatruss2**". **Local buckling of the starting design (Table 3) but with no noodles**, from a BIGBOSOR4 three-module, six-segment module of the type displayed at the top of Fig. 6. Compare with Fig. 9, which also pertains to the starting design, but which has noodles and noodle gaps. The presence of noodles and noodle gaps makes a big difference: the local buckling load factor cited here being 0.98399, whereas that cited in Fig. 9 for the same design being 1.6075. Segments 1 and 15 (see Fig. 4) of the first module (left-most module) are radially shortened in order to prevent local buckling in those two segments.

nasatruss2..R,Z_EIGENMODE_2--N_100; eigenvalue=0.946322 (no noodles
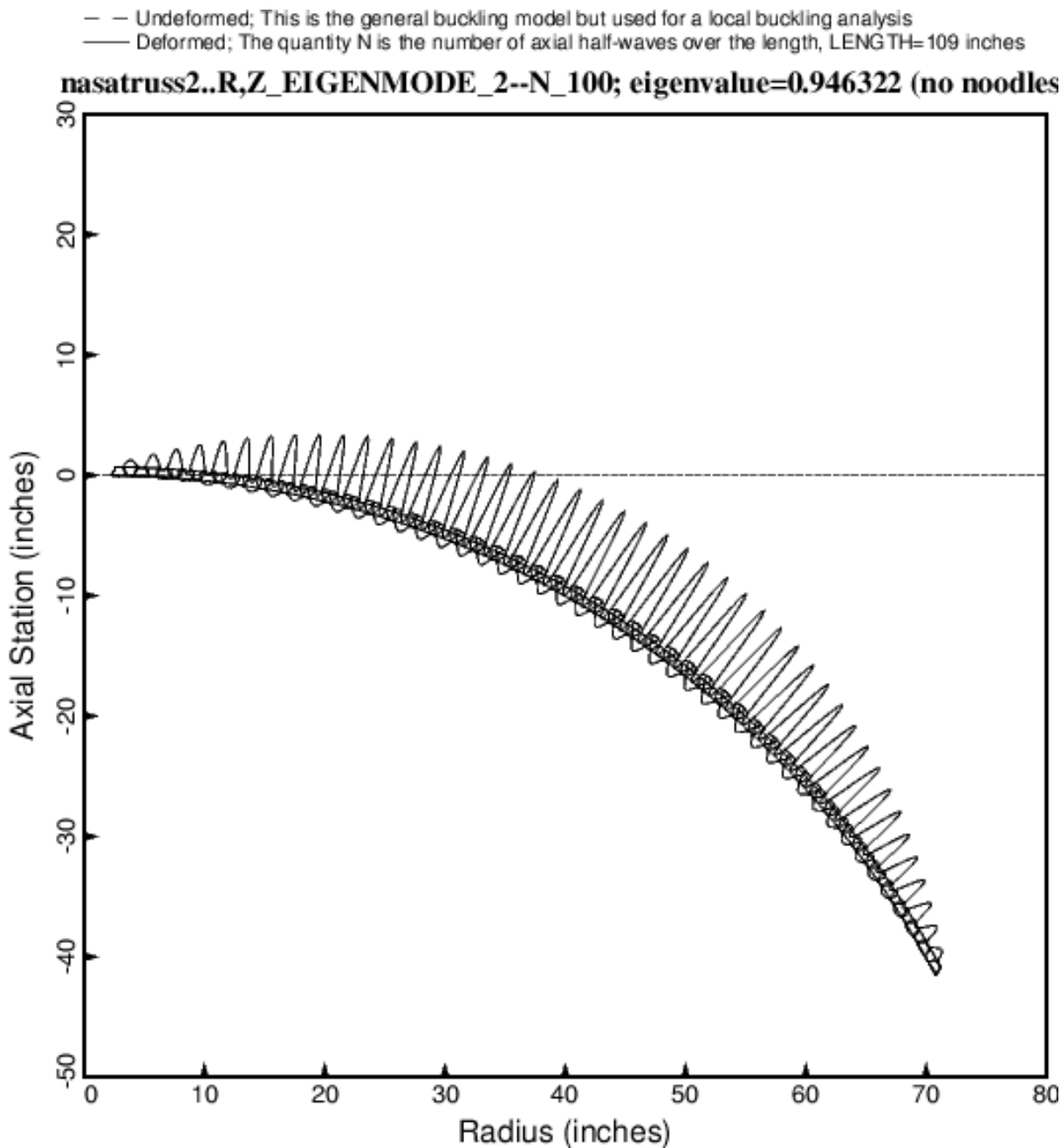
Fig. 11 Specific case called "**nasatruss2**". **Local buckling of the starting design (Table 3) but with no noodles**, from the same BIGBOSOR4 model as that used for general buckling (Fig. 14). Compare with Fig. 10, which also pertains to the starting design and has no noodles. With no noodles present, the three-module model (Fig. 10) and the multi-module model (this figure) yield local buckling load factors that are reasonably close to one another; the local buckling load factor cited in this figure is 0.946322 and that cited in Fig. 10 is 0.98399. The local buckling mode shown here corresponds to the second eigenvalue for N = 100 axial half-waves. The first eigenvalue is associated with an edge buckling mode (not shown here) at the right-most end of the arc that is of no interest in this study, since it cannot occur in an actual complete (360-degree) closed cylindrical shell.
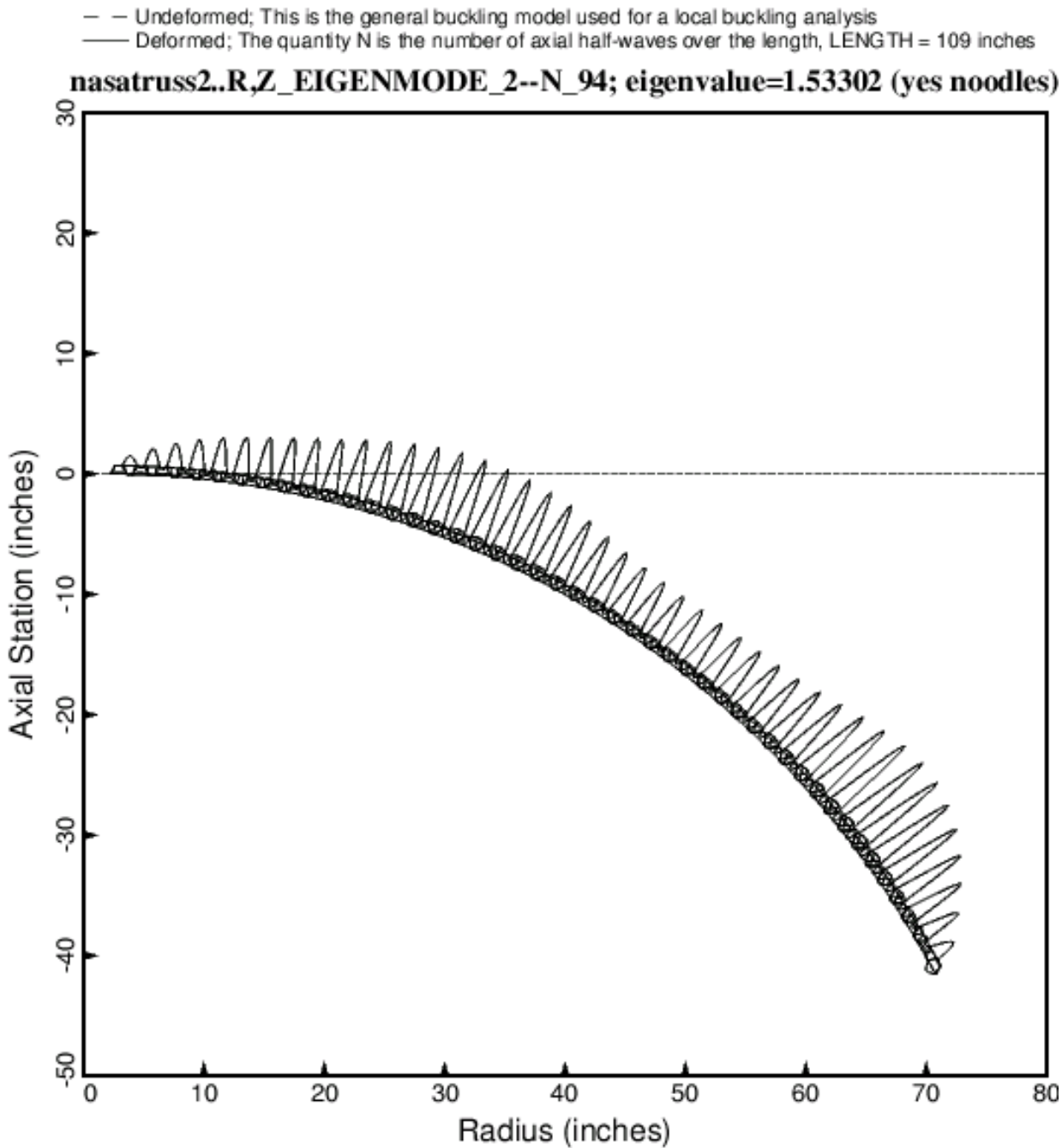
Fig. 12 Specific case called "**nasatruss2**". **Local buckling of the starting design (Table 3) with noodles present**, from the same BIGBOSOR4 model as that used for general buckling (Fig. 13). Compare with Fig 11, which also pertains to the starting design but with no noodles. With noodles present, the three-module model (Fig. 9) and the multi-module model (this figure) yield local buckling load factors that are quite different; the buckling load factor cited in this figure is 1.53302, whereas that cited in Fig. 9 is 1.6075. Both models have noodles, but only the model shown in Fig. 9 has noodle gaps. Hence, the noodle gaps raise the local buckling load factor by about 5 percent with the conservative "noodle support" index, ILINKS = 0.

nasatruss2..R,Z_EIGENMODE_1--N_3; eigenvalue=0.88751 (BEHX2)
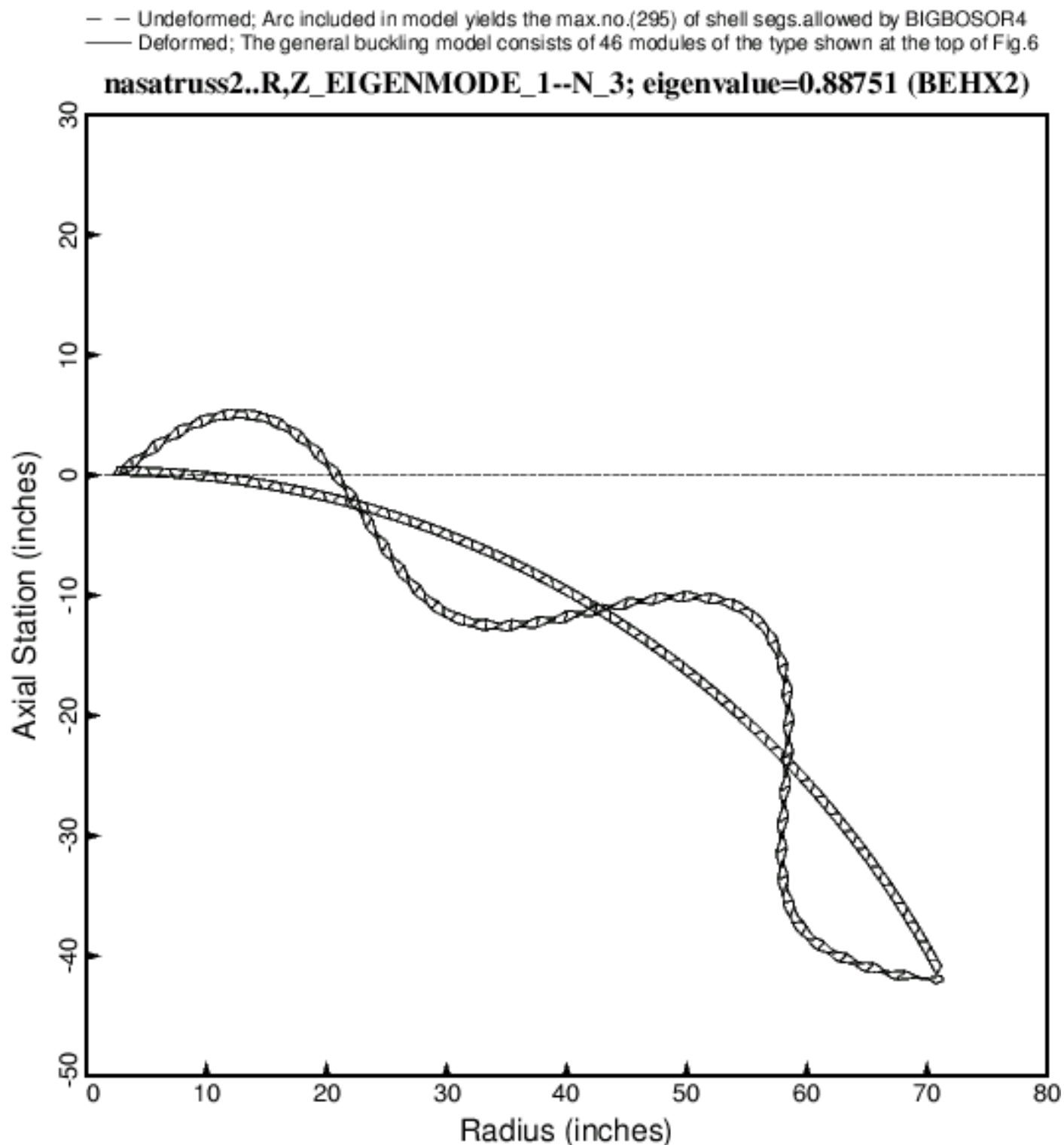
Fig. 13 Specific case called "**nasatruss2**". **General buckling of the starting design (Table 3) with noodles present**. Compare with Fig. 5, which pertains to the optimized design with noodles present. The quantity **N** is the number of axial half-waves over the length, 109 inches, of the cylindrical shell.

American Institute of Aeronautics and Astronautics

nasatruss2..R,Z_EIGENMODE_1--N_3; eigenvalue=0.79071 (no noodles)
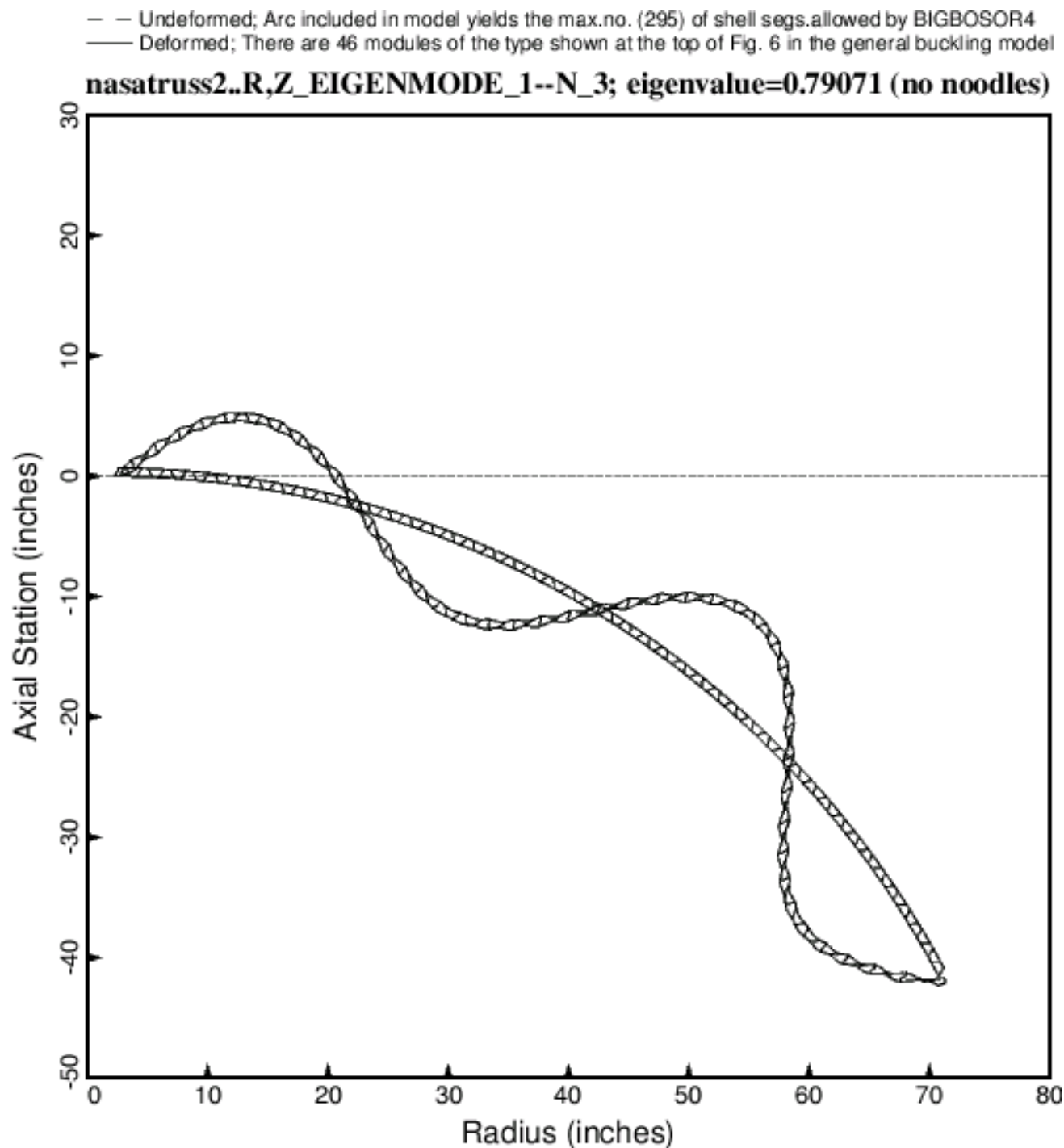
Fig. 14 Specific case called "**nasatruss2**". **General buckling of the starting design (Table 3) with no noodles.** Compare with Fig. 13, which pertains to the starting design with noodles present. The noodles increase the general buckling load factor by about 11 per cent, from 0.79071 cited in this figure to 0.88751 cited in Fig. 13. The quantity **N** is the number of axial half-waves over the length, 109 inches, of the cylindrical shell. The locations of the noodle centroids in the general buckling model are shown in Fig. 1b.

American Institute of Aeronautics and Astronautics
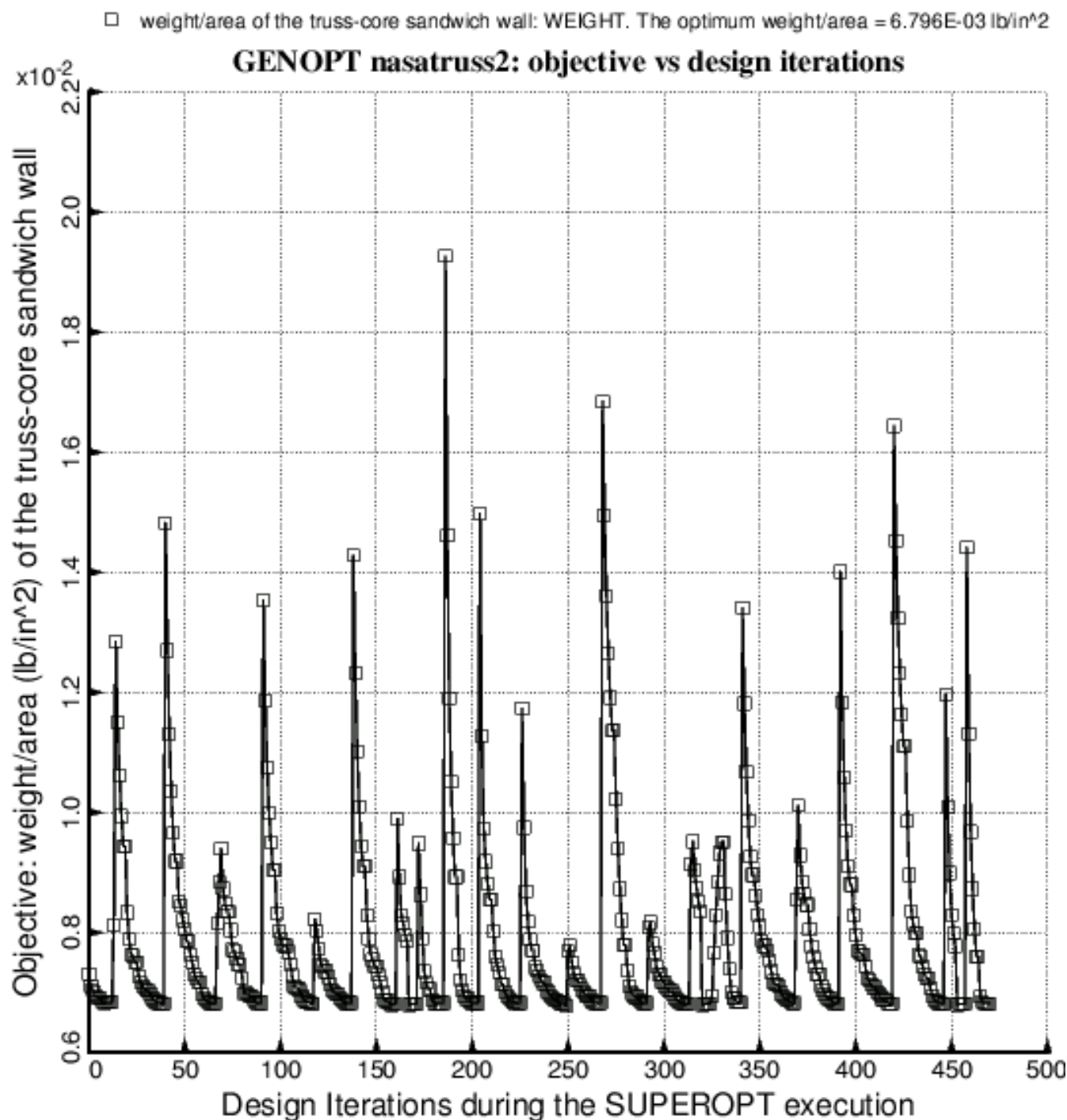
Fig. 15 Specific case called "**nasatruss2**". **Evolution of the objective** (weight/area) during an execution of SUPEROPT. About 48 hours of computer time on the LINUX workstation in the first author's office were required for this computer run. The design at Iteration 0 is the starting design listed in Table 3. The optimum design is that listed in Table 4. Each "spike" in this plot corresponds to a new "starting" design, which is obtained by a random process mostly consistent with linking and inequality relationships [4D, 4L].

American Institute of Aeronautics and Astronautics
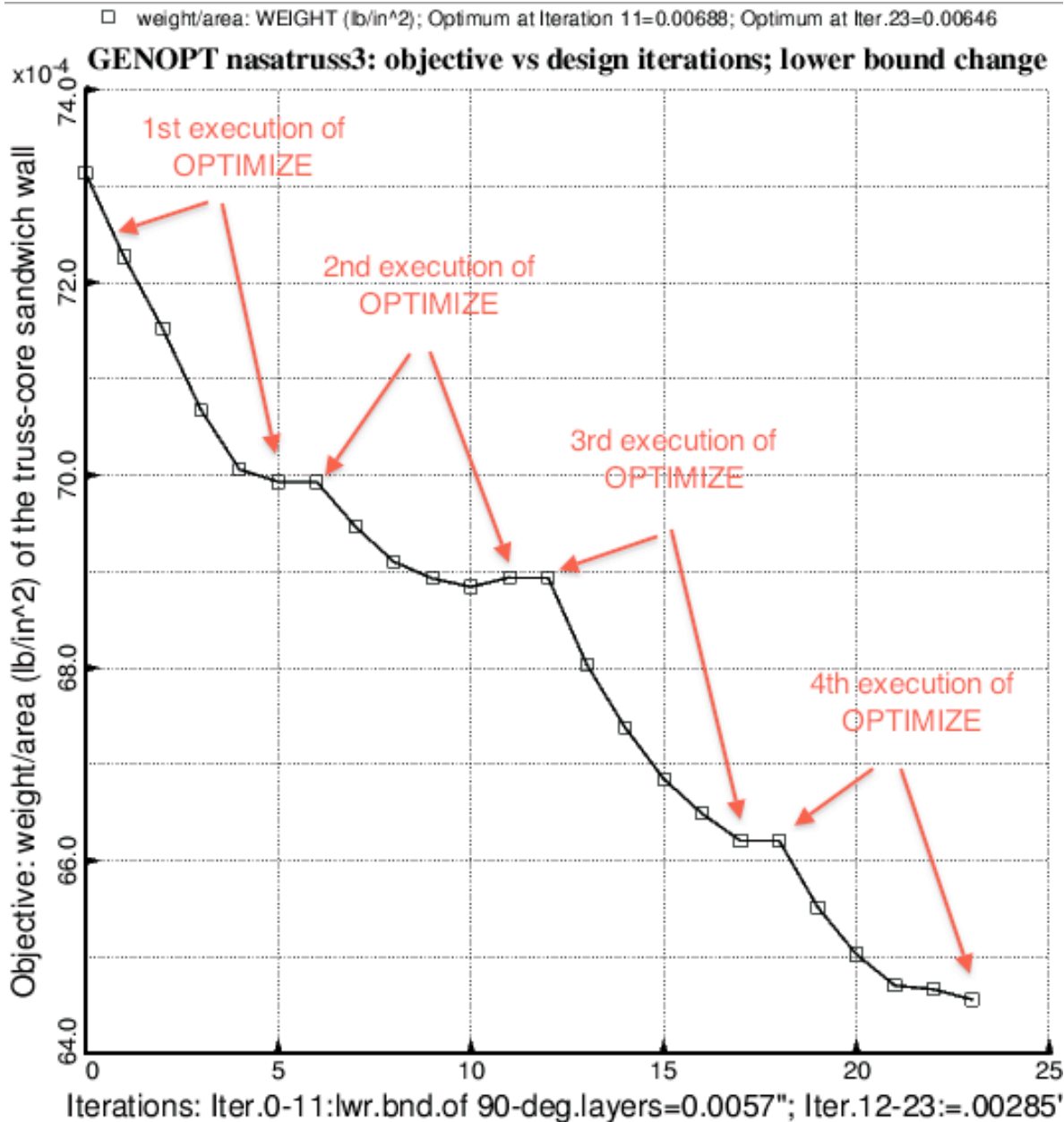
Fig. 16. **Evolution of the objective** (weight/area) for the specific case, "**nasatruss3**" during four executions of OPTIMIZE [3,6]. The design at Iteration 0 is the starting design listed in Table 3. The design at Iteration 11 is the optimum design listed in Table 4. At Iteration 11 the lower bound of the thickness of each 90-degree ply was changed from 0.0057 inches to 0.00285 inches. The 90-degree plies always occur in adjacent pairs at or near the mid-surface of the face sheet laminates. The optimum design at Iteration 23 is that listed in Table 5. At the final optimum design the thickness of each 90-degree ply is at the new lower bound, 0.00285 inches. Since 90-degree layers always occur in pairs, the optimized truss-core sandwich cylindrical shell can be fabricated with only one 90-degree ply of thickness 0.0057 inches instead of the two adjacent 90-degree plies each of thickness 0.00285 inches listed in Table 5.

American Institute of Aeronautics and Astronautics
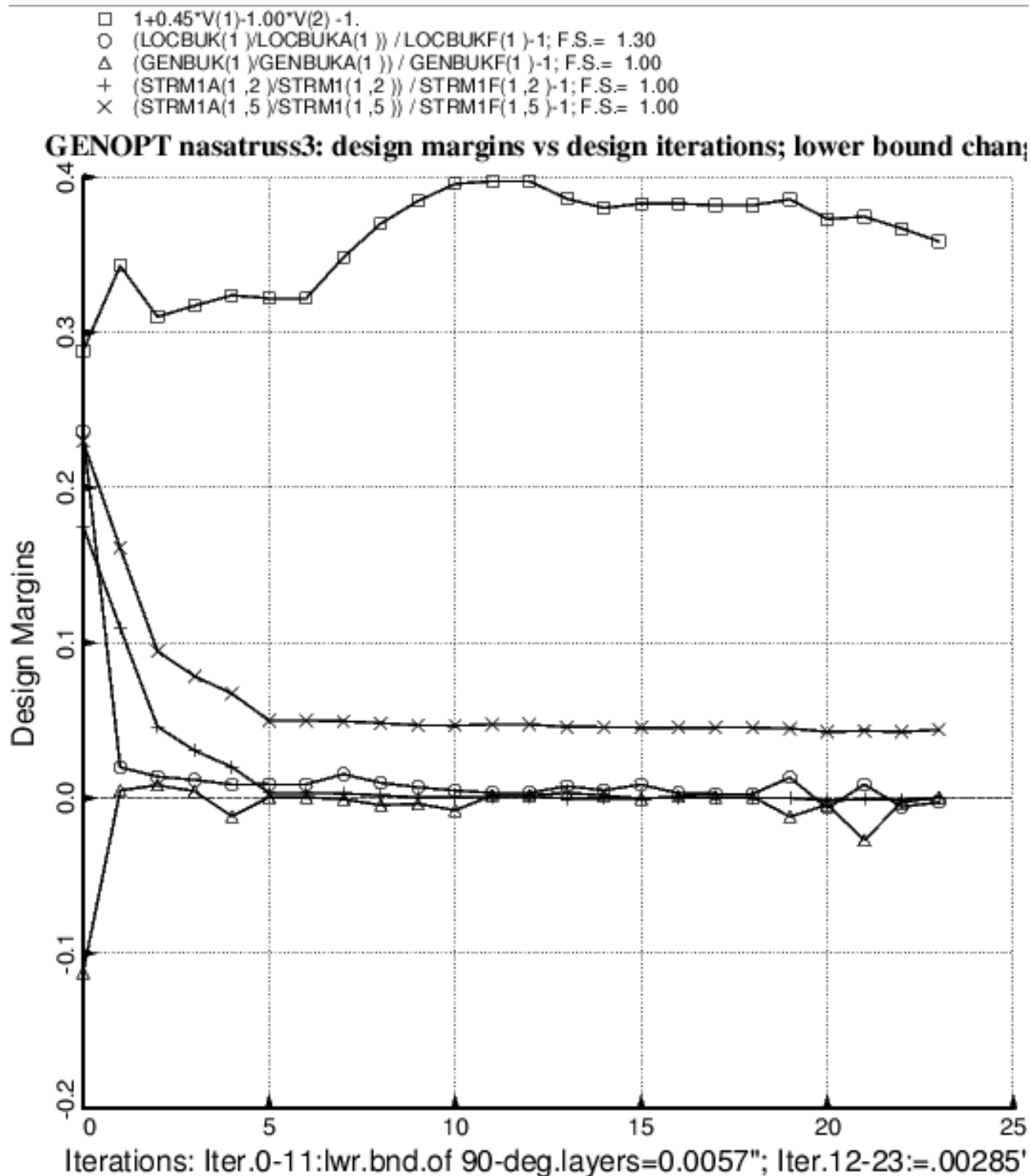
Fig. 17 **Evolution of the design margins** for the specific case, "**nasatruss3**", during the same four executions of OPTIMIZE [3,6] as those for which the objective is displayed in the previous figure. For most of this process four of the five margins listed in the legend are critical. The optimum design at Iteration 11 is that listed in Table 4. The optimum design at Iteration 23 is that listed in Table 5.

Typical noodle gap with noodle line of attachment to face sheet shown as a black beam "unit". The eccentricity of the beam centroid with respect to the line of attachment is not shown.
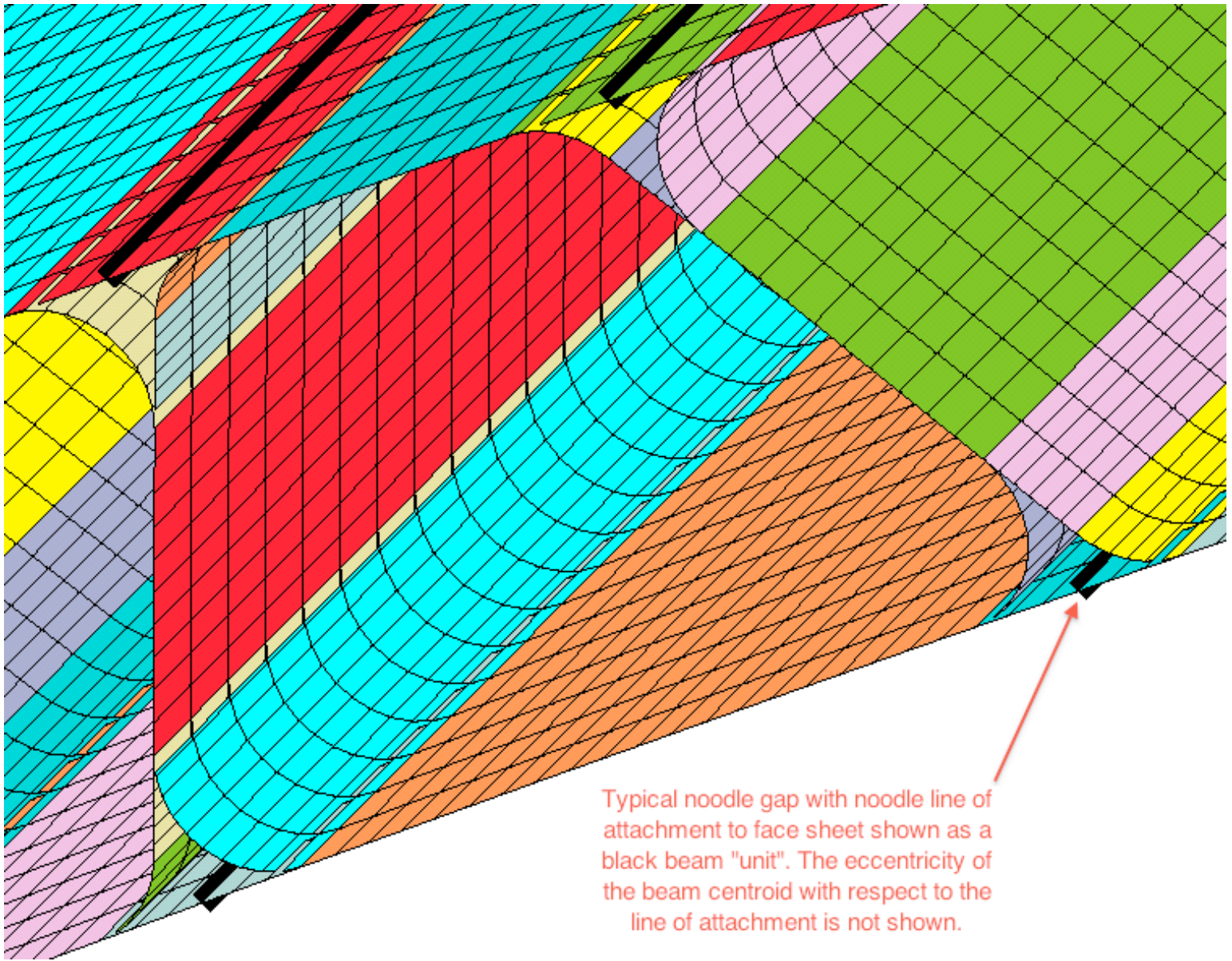
Fig. 18 "**nasatruss2**" starting design (Table 3). **Close-up view of a STAGS finite element model of one of the local buckling modules.** Each shell unit is shown in a different color. The black "units" represent the noodles. Unfortunately, STAGS does not show the eccentricity of the noodle centroid with respect to its attachment point of the face sheet. However, this eccentricity is present and accounted for in the STAGS model. The STAGS input file, ***.inp**, is automatically created by the generic GENOPT/BIGBOSOR4 case called **"trusscomp"**. Comparisons between results from GENOPT/BIGBOSOR4 and general purpose computer programs such as STAGS [15-18] are provided in [1].
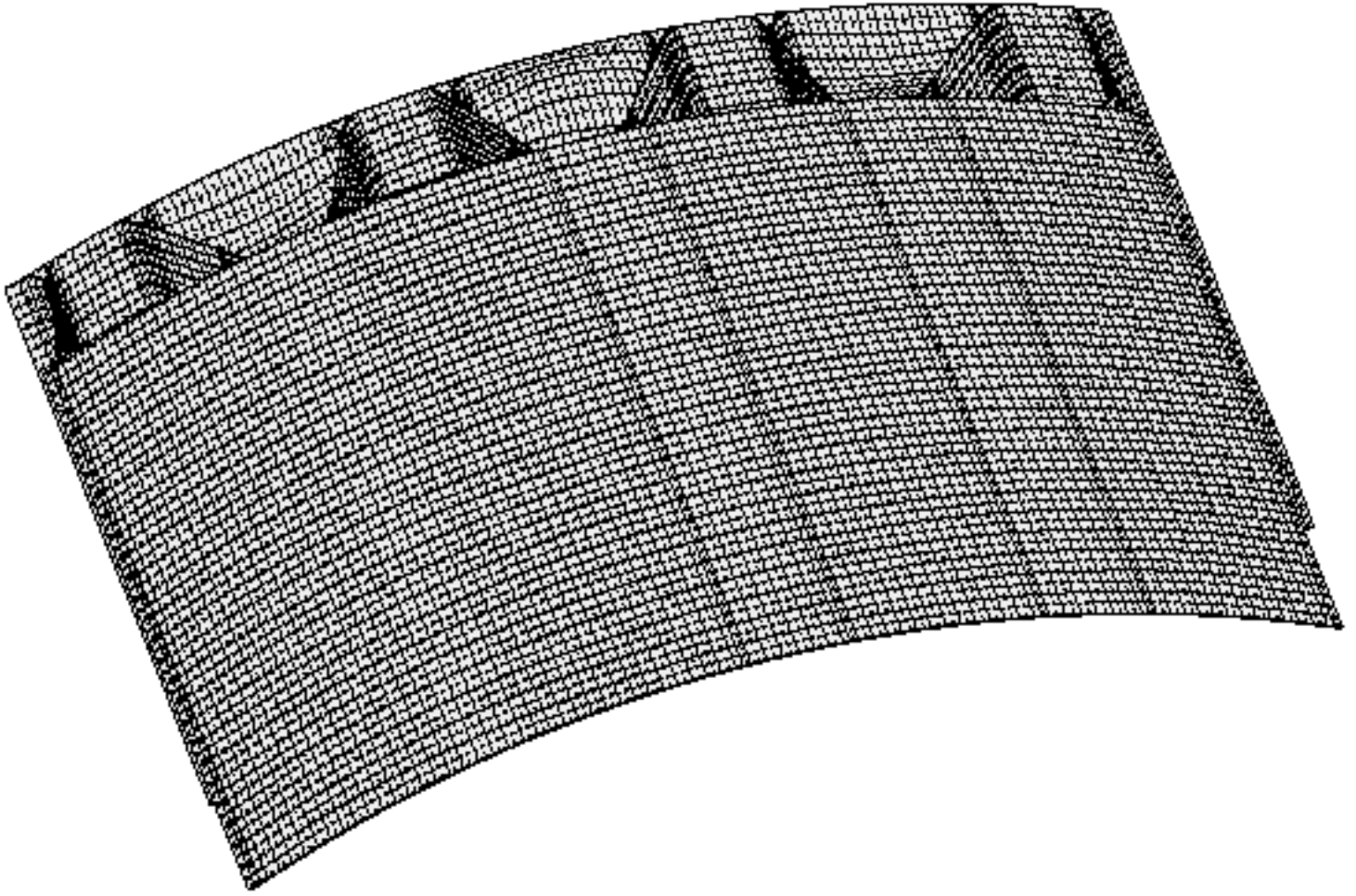
Fig. 19 A typical local buckling mode from a STAGS model of part of the axially compressed truss-core sandwich cylindrical shell. The axial length included in this model is FACLEN x LENGTH = 0.05 x 109 = 5.45 inches. Four 22-segment modules of the type shown in Fig. 4 are included in this particular local buckling model. "Noodles" and "noodle gaps" are included in this model. The STAGS 480 finite element is used for the shell segments and the STAGS 928 finite elements are used for the "noodles", which are treated as discrete stringers located in the "noodle gaps" (Fig. 18). This particular STAGS model has a much smaller radius (7.815 inches) than the radius (78.15 inches) of the cylindrical shell that is the subject of the rest of this paper. The much smaller radius is used in this figure so that the reader can easily see that the STAGS model for local buckling includes the overall curvature of the cylindrical shell. The axial compression is applied by uniform end shortening in such a way that the pre-buckled state of the shell is uniform axial compression withz only very small localized edge effects that do not affect the buckling behavior (Fig. 1g).
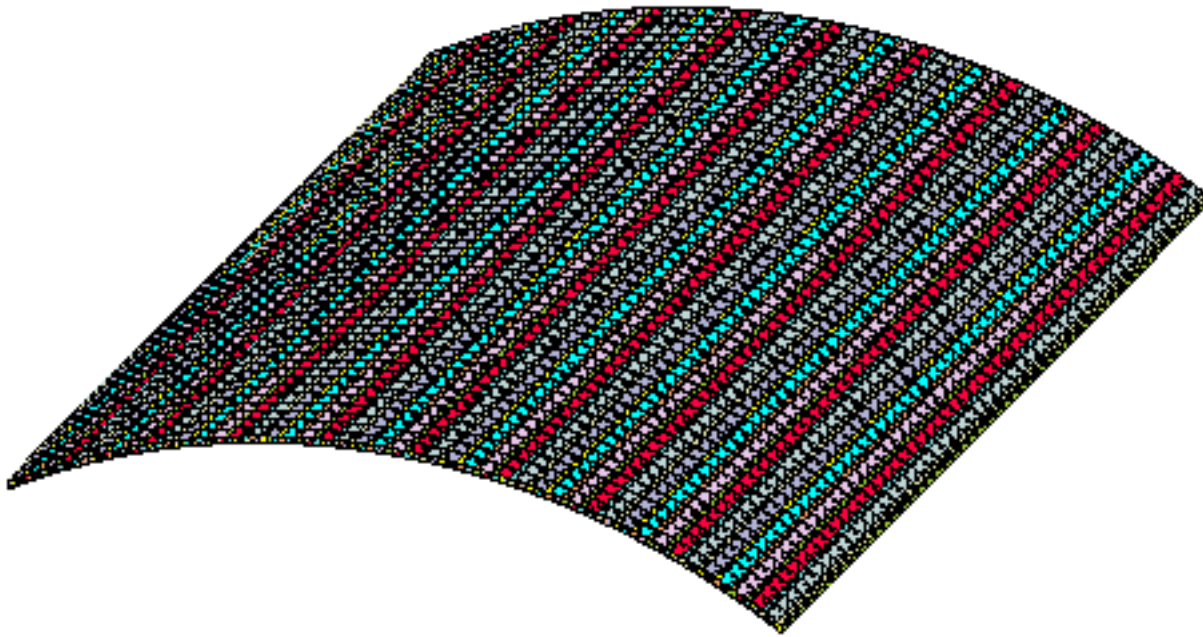
Model geometry, all units
STAGS model with 276 shell units

Θ x   24.00
Θ y -22.00
Θ z   30.00

Fig. 20a. "**nasatruss2**" starting design (Table 3). STAGS model for obtaining general buckling load factors and mode shapes. As seen in the next figure this model includes the two face sheets and truss-core webs, but does not include the "noodle gaps" such as those displayed in Fig. 18. The "noodles" are included as discrete stringers that are attached at the intersections of the truss-core webs with the two face sheets and with the noodle centroids located eccentrically as shown in the BIGBOSOR4 model displayed in Fig. 1b. STAGS 480 finite elements are used for the shell segments and STAGS 928 finite elements are used for the "noodles". Each module of this STAGS model is analogous to the six-segment GENOPT/BIGBOSOR4 module displayed at the top of Fig. 6. See detail in Fig. 20b.

American Institute of Aeronautics and Astronautics
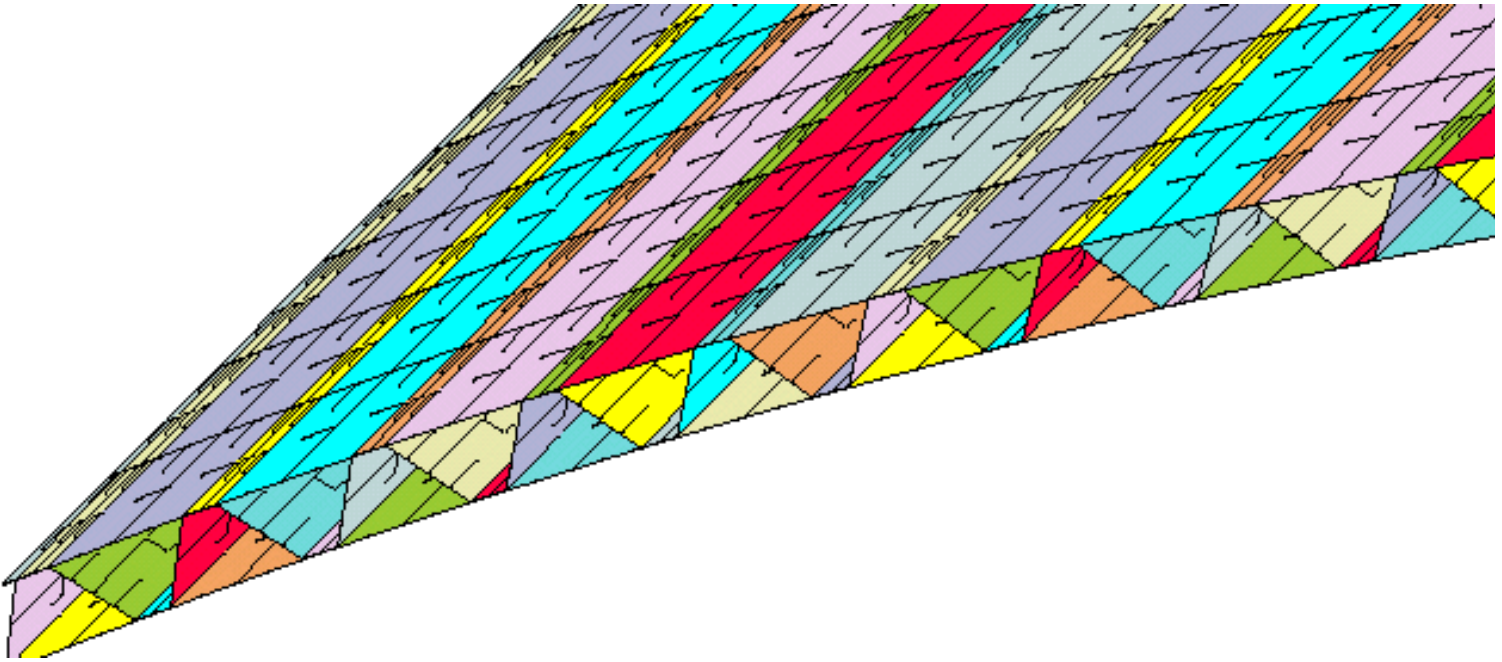
Fig. 20b "**nasatruss2**" starting design (Table 3). Detail from the lower left-hand corner of the previous figure. This model has two 480 finite elements (NCOLSG = 5) across the width of each of the six segments in each module of the 46-module general buckling model. A single module in this STAGS multi-module model is analogous to the GENOPT/BIGBOSOR4 module shown at the top of Fig. 6.

American Institute of Aeronautics and Astronautics
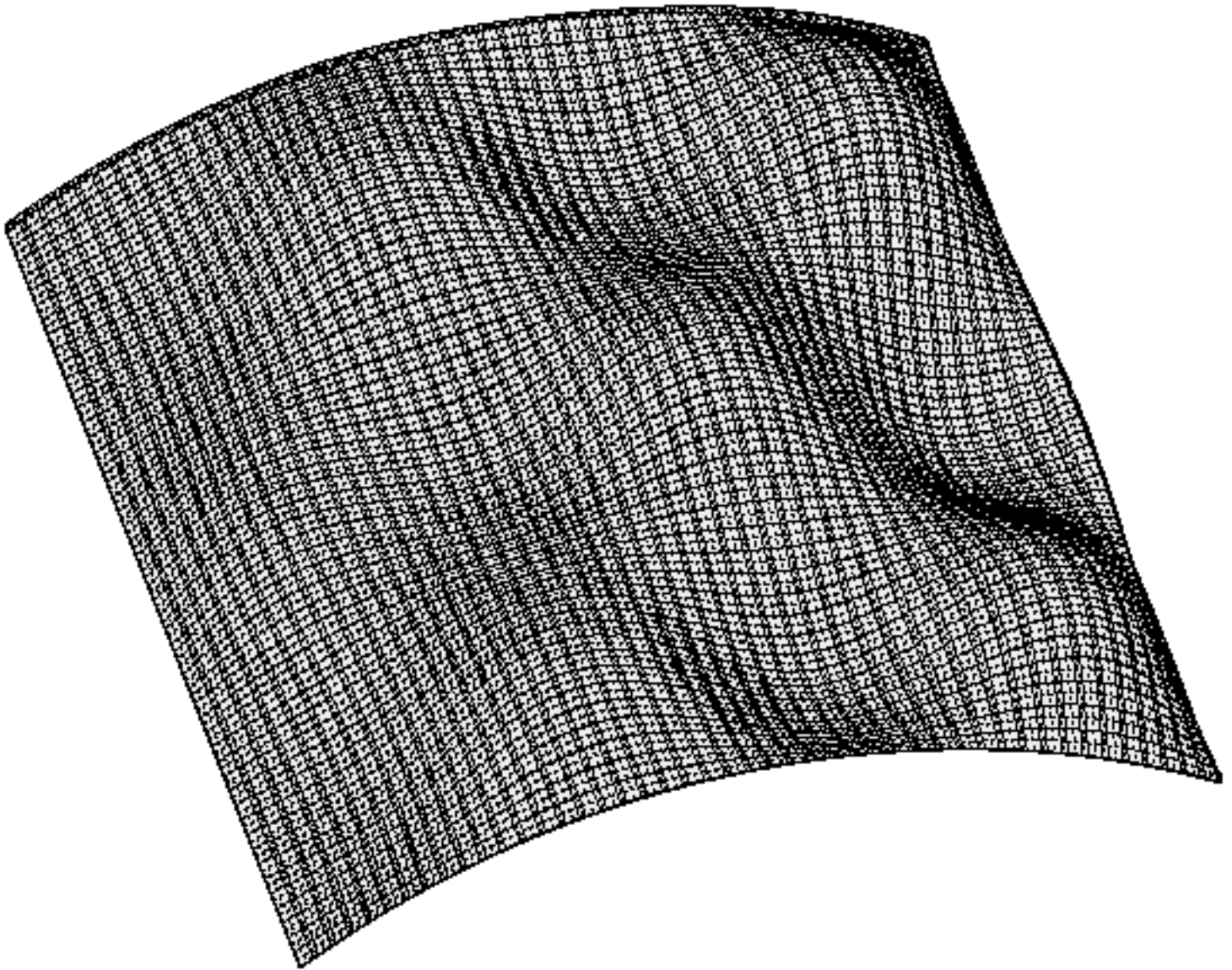
Fig. 21 "**nasatruss2**" starting design (Table 3). A general buckling mode from the STAGS model displayed in the previous two figures. The STAGS 480 finite element is used for the shell segments, and the STAGS 928 finite element is used for the noodles, which are represented as discrete stringers. The noodles are not shown in this figure.

American Institute of Aeronautics and Astronautics
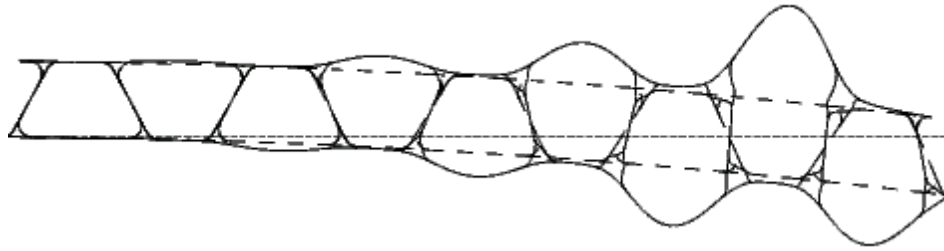
(a) EFNOOD = 0.0 lb/in^3 ; ILINKS = 0; eigenvalue=1.6074, N = 5 axial half-waves over 5.45 inches

(b) EFNOOD = 10^4 lb/in^3; ILINKS = 0; eigenvalue=1.6687, N = 5 axial half-waves over 5.45 inches
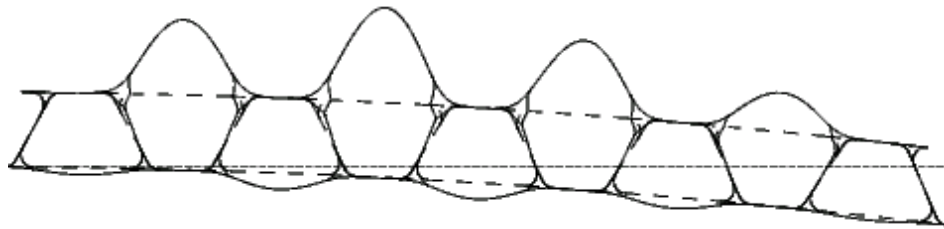
(c) EFNOOD = 10^5 lb/in^3; ILINKS = 0; eigenvalue=1.9577, N = 6 axial half-waves over 5.45 inches
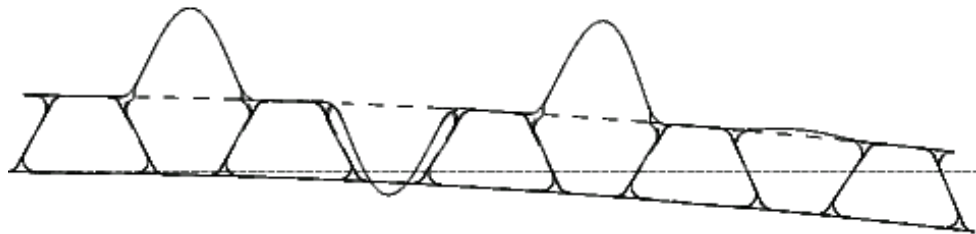
(d) EFNOOD = 10^6 lb/in^3; ILINKS = 0; eigenvalue=2.4481, N = 7 axial half-waves over 5.45 inches
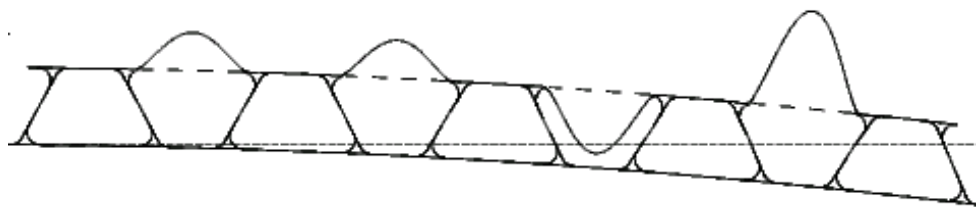
(e) EFNOOD = 10^7 lb/in^3; ILINKS = 0; eigenvalue=2.9035, N = 7 axial half-waves over 5.45 inches

Fig. 22 continued on next page.

Fig. 22 (continued)
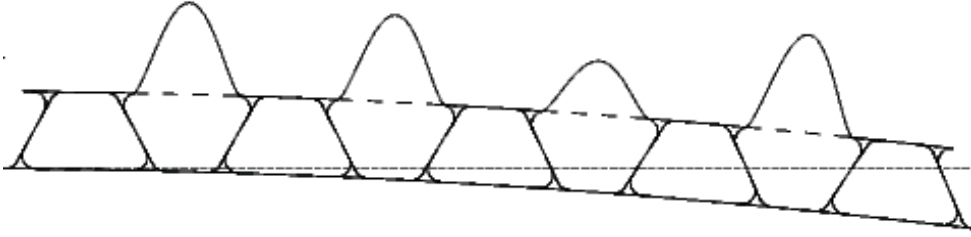
(f) EFNOOD = 10^8 lb/in^3; ILINKS = 0; eigenvalue=3.2400, N = 8 axial half-waves over 5.45 inches
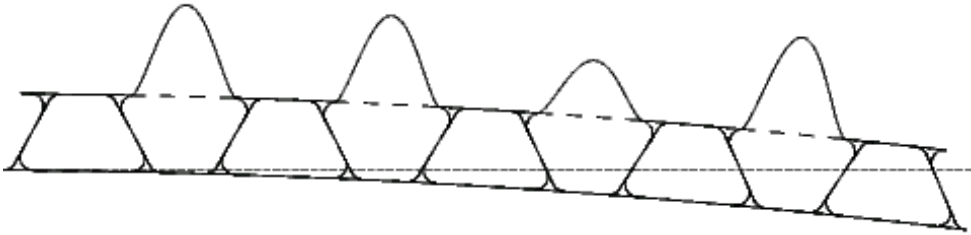
(g) EFNOOD = 10^9 lb/in^3; ILINKS = 0; eigenvalue=3.4328 N = 8 axial half-waves over 5.45 inches
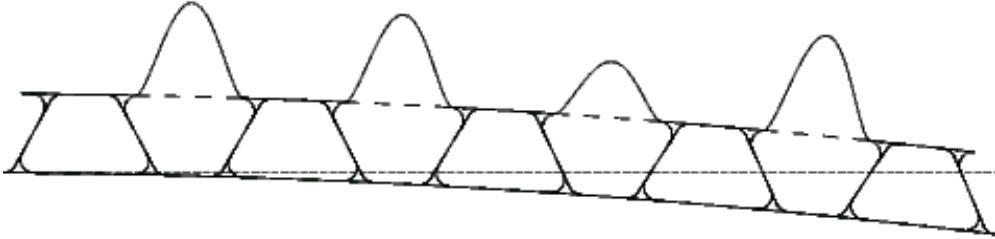
(h) EFNOOD = 10^{10} lb/in^3; ILINKS = 0; eigenvalue=3.56910, N = 8 axial half-waves over 5.45 inches
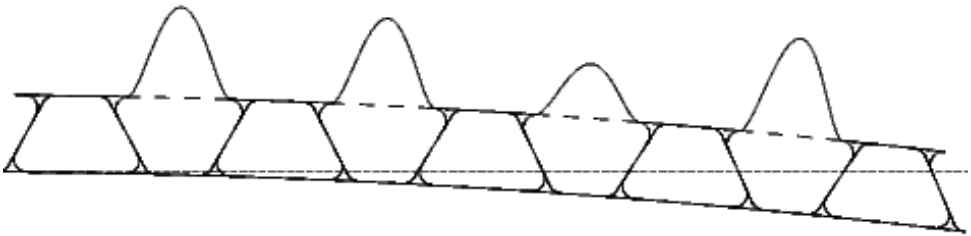
(i) EFNOOD = 10^{11} lb/in^3; ILINKS = 0; eigenvalue=3.7699, N = 8 axial half-waves over 5.45 inches

Fig. 22 "**nasatruss2**" starting design (Table 3). Effect of noodle elastic foundation stiffness, EFNOOD on the prediction of local buckling from the GENOPT/BIGBOSOR4 model including "noodles" and "noodle gaps". Five 22-segment modules of the type displayed in Fig. 4 are used for this local buckling analysis. Notice that in Fig. 22(a) the elastic foundation stiffness, EFNOOD, is zero. Fig. 22(a) corresponds to the same structure as is displayed in Fig. 9. Figure 22(a) has five 22-segment modules, whereas the model shown in Fig. 9 has three modules. EFNOOD represents connection of the little segments that enclose each noodle to ground via an elastic foundation instead of being connected to each other. Therefore this model is unconservative. Notice that convergence with respect to EFNOOD is very slow. Round-off error may affect the predictions for high values of EFNOOD.
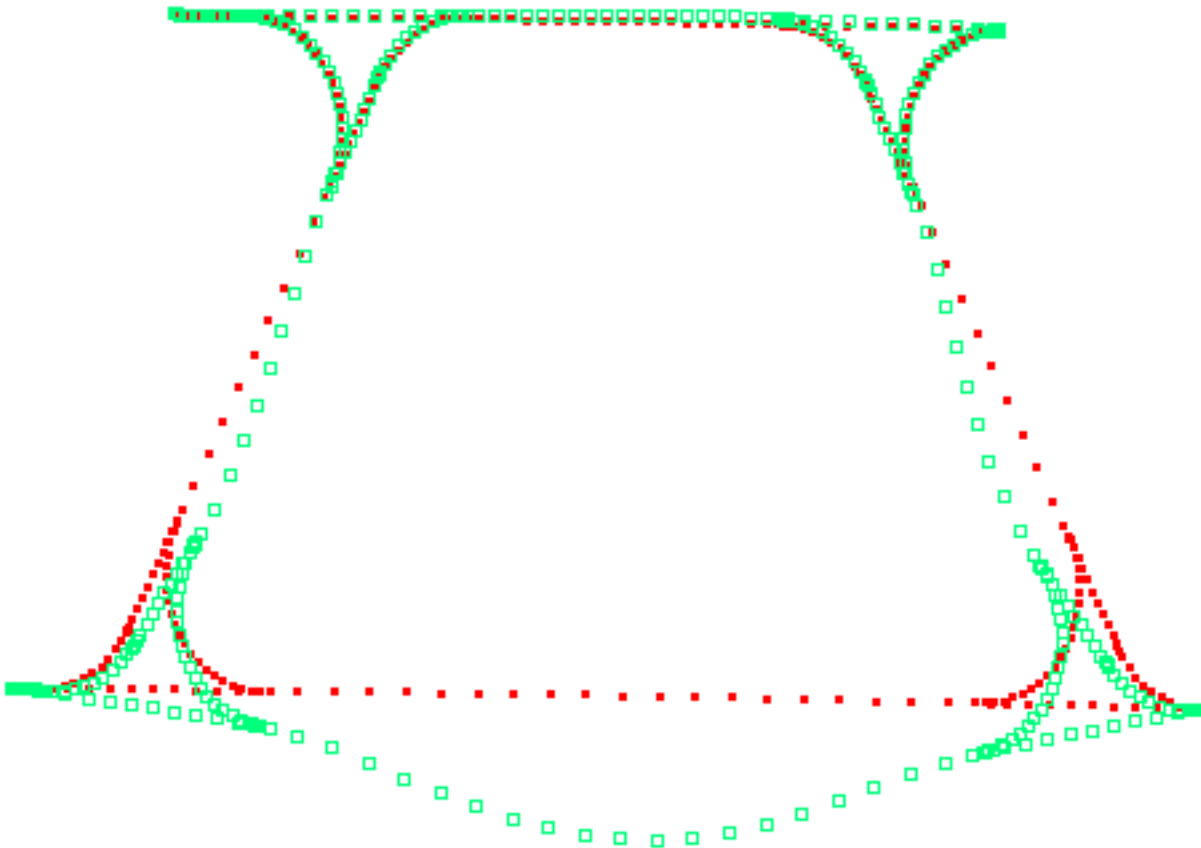
Fig. 23(a) A one-module local buckling model with ILINKS = 2; eigenvalue=2.8218; there are 6 or 7 axial half-waves over the axial length, FACLEN x LENGTH = 0.05 x 109 = 5.45 inches
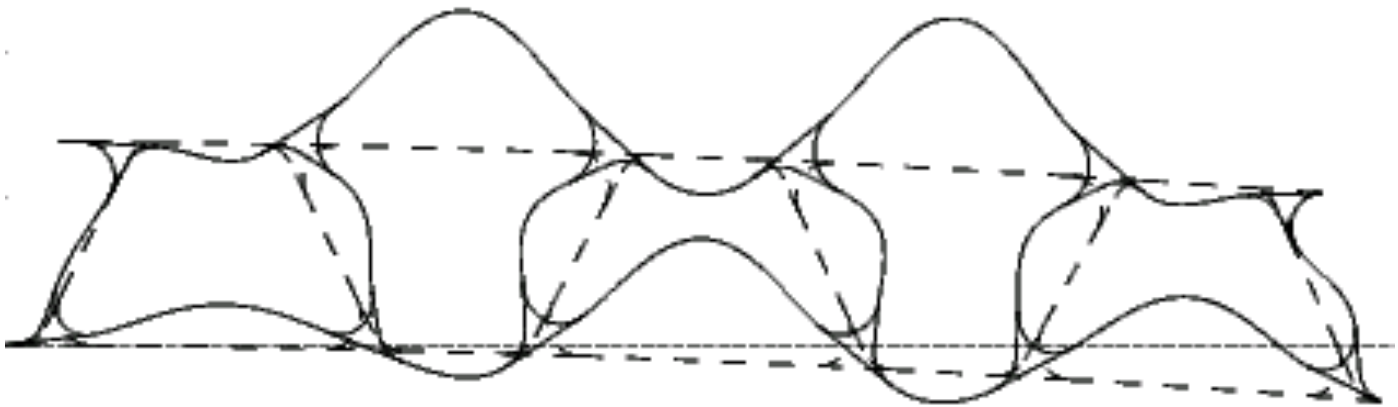
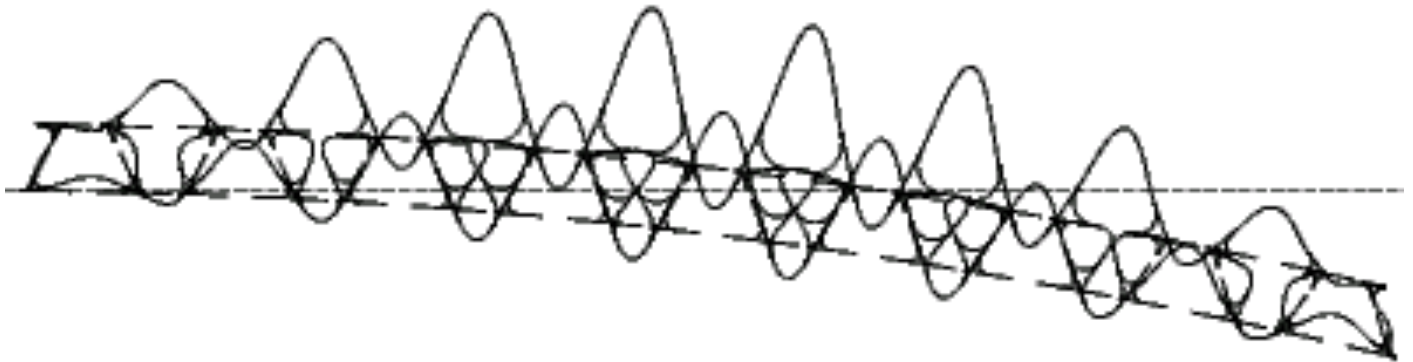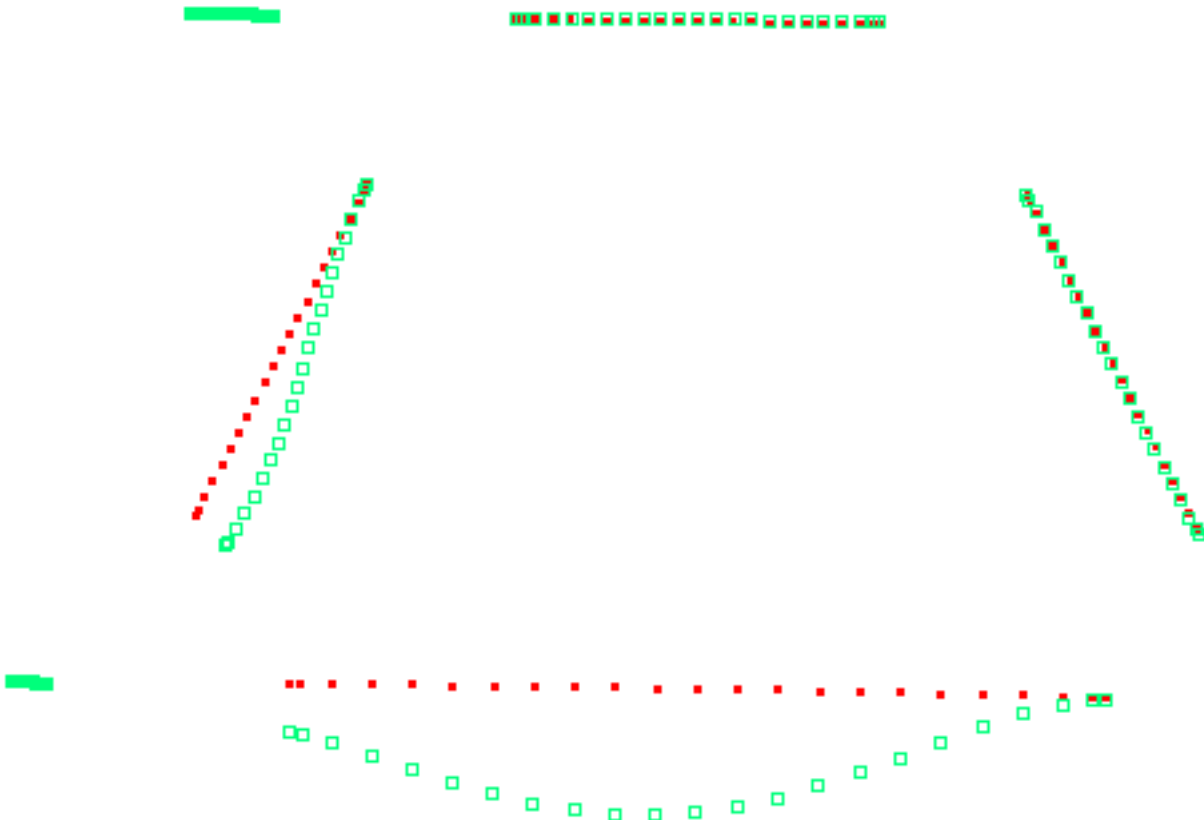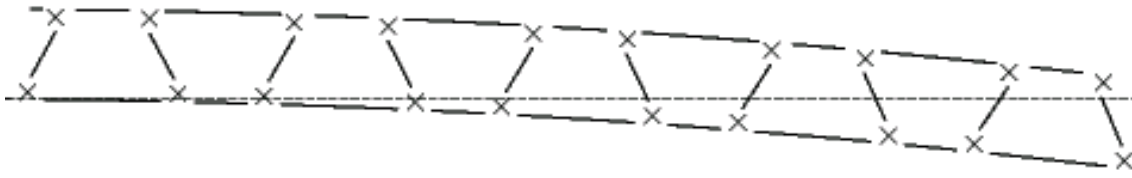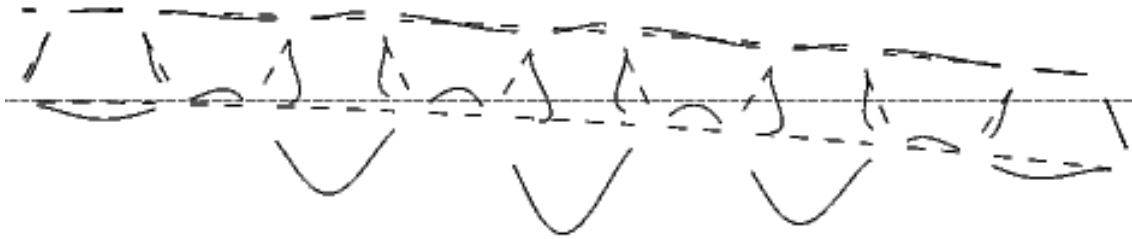(b) A three-module local buckling model with ILINKS = 2; eigenvalue=2.4562; 6 axial half-waves over 5.45"

Fig. 23 (continued)
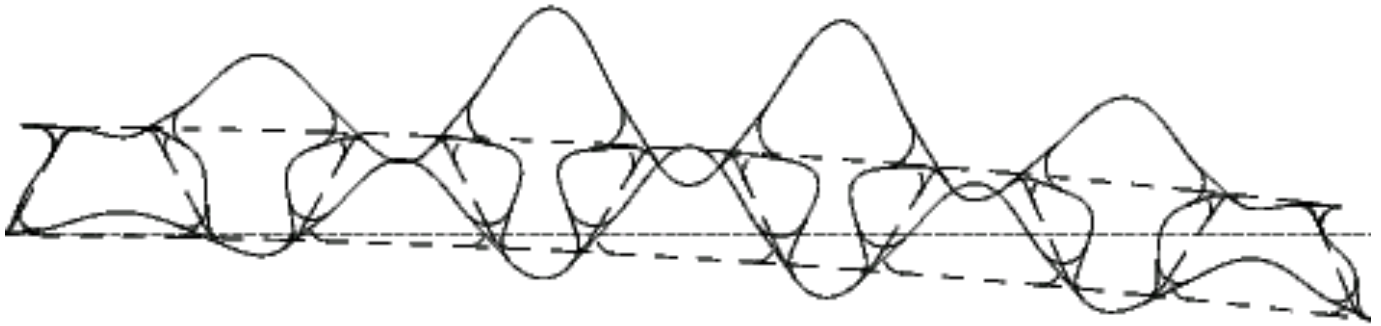
(c) A five-module local buckling model with ILINKS = 2; eigenvalue=2.3887; 5 axial half-waves over 5.45"
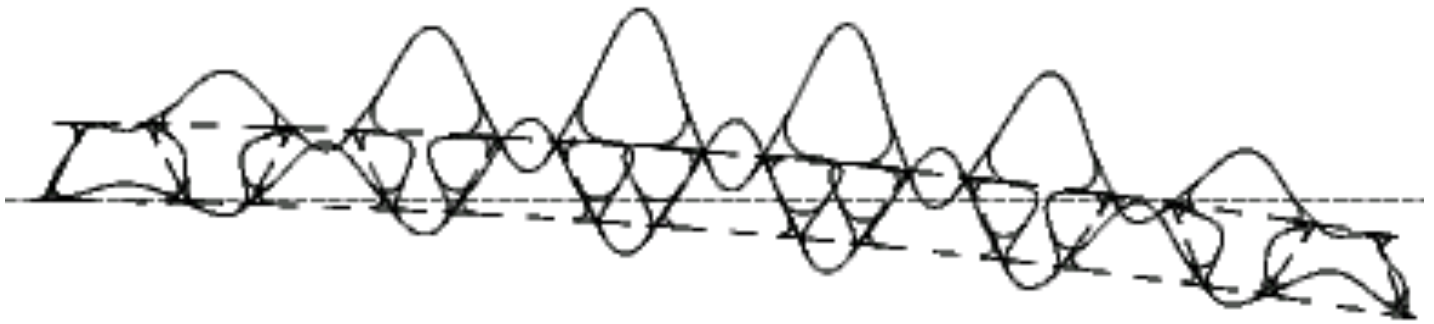
(d) A seven-module local buckling model with ILINKS = 2; eigenvalue=2.3672; 5 axial half-waves over 5.45"

(e) A nine-module local buckling model with ILINKS = 2; eigenvalue=2.3583; 5 axial half-waves over 5.45"

Fig. 23 "**nasatruss2**" starting design (Table 3). A BIGBOSOR4 local buckling model with use of the "noodle support" index, ILINKS = 2. The little shell segments that enclose each noodle are given a very high 90-degree (meridional) bending stiffness in order to simulate the effect of each noodle supporting the little shell segments that surround it.

Fig. 24(a) A one-module local buckling model with ILINKS = 1; eigenvalue=3.0518; there are 7 or 8 axial half-waves over the axial length, FACLEN x LENGTH = 0.05 x 109 = 5.45 inches

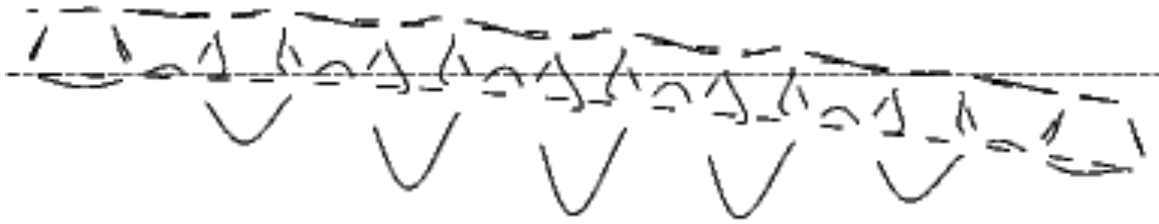(b) A three-module local buckling model with ILINKS = 1; eigenvalue=2.4736; 6 axial half-waves over 5.45"

Fig. 24 (continued)

(c) A five-module BIGBOSOR4 local buckling model with the use of ILINKS = 1. The "X"s represent the noodle centroids. There are discontinuities (gaps) between every shell segment in this and the other BIGBOSOR4 ILINKS = 1 models displayed in this figure.

(d) A five-module local buckling model with ILINKS = 1; eigenvalue=2.3701; 5 axial half-waves over 5.45"

(e) A seven-module local buckling model with ILINKS = 1; eigenvalue=2.3461; 5 axial half-waves over 5.45"
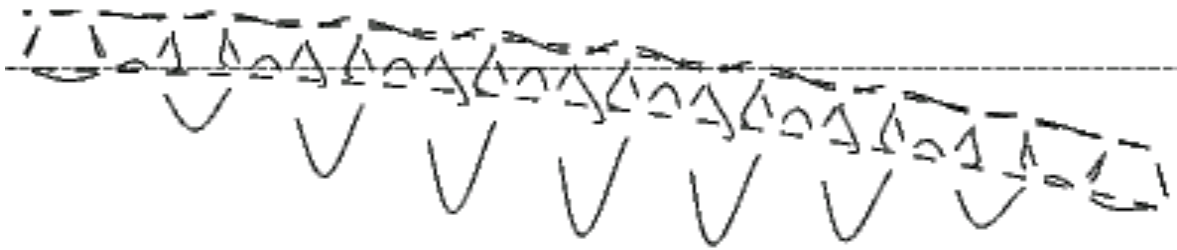
(f) A nine-module local buckling model with ILINKS = 1; eigenvalue=2.3369; 5 axial half-waves over 5.45"

Fig. 24 "**nasatruss2**" starting design (Table 3). Local buckling from the BIGBOSOR4 "rigid links" (ILINKS=1) models. Note that where local buckling occurs there exists significant rigid body rotation of the noodle gaps. Compare with Fig. 22(a), for which the shell segments are continuous and for which no support is provided by the noodle to the little shell segments that enclose the noodle. Compare with Fig. 22 in which the noodle support is simulated by an elastic foundation and with Fig. 23 in which the noodle support is simulated by greatly increased hoop bending stiffness of the little segments that enclose each noodle.
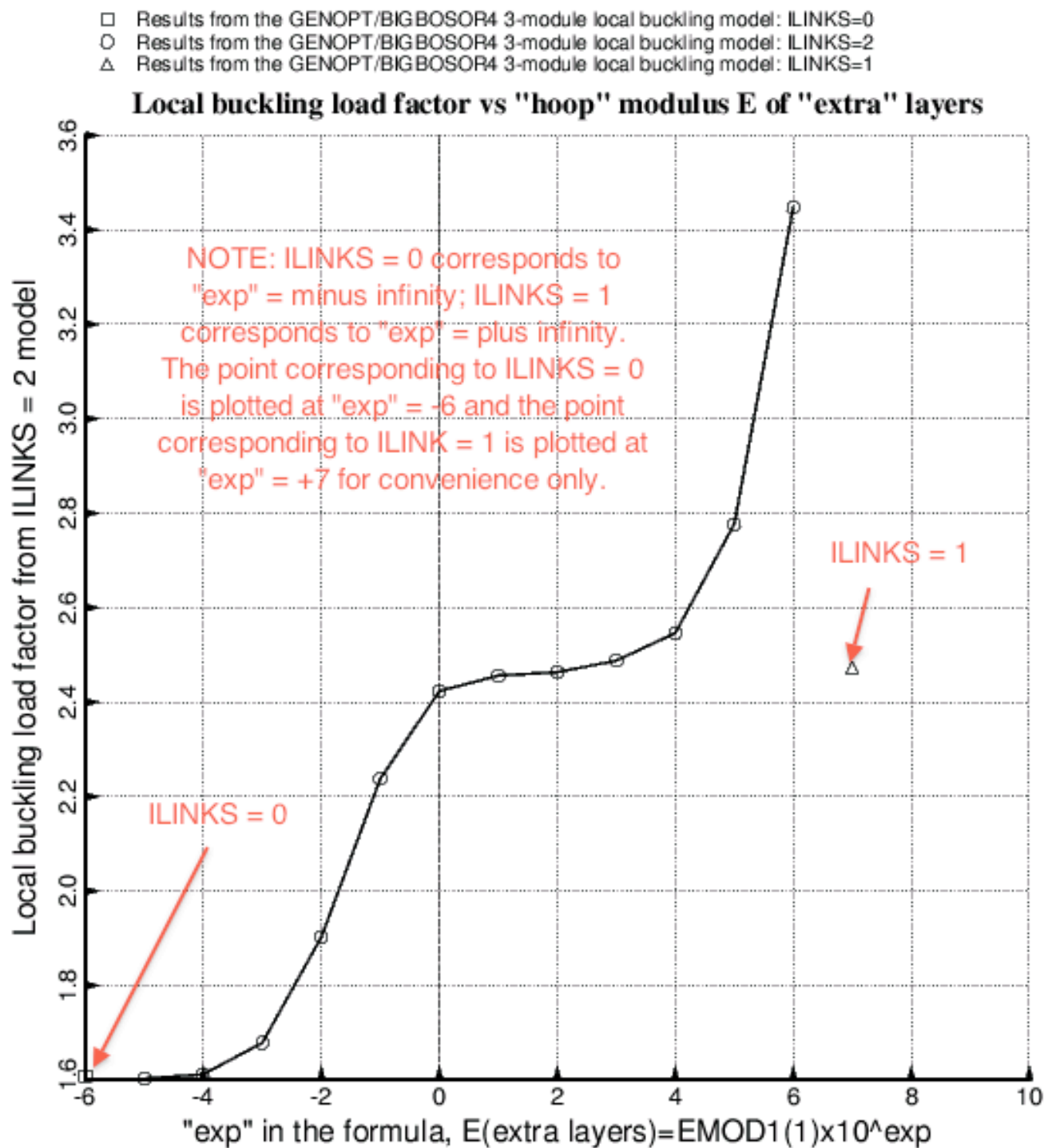
American Institute of Aeronautics and Astronautics

Fig. 25 "**nasatruss2**" starting design (Table 3). Local buckling load factor from the ILINKS = 2 model (Fig. 23) as a function of the "hoop" modulus, E, of the "extra" inner and outer layers that are applied to the little shell segments that enclose each noodle in order to simulate the support that noodle provides for those little shell segments. Three modules (Fig. 23b) are used in the local buckling model to obtain the local buckling load factors plotted here.
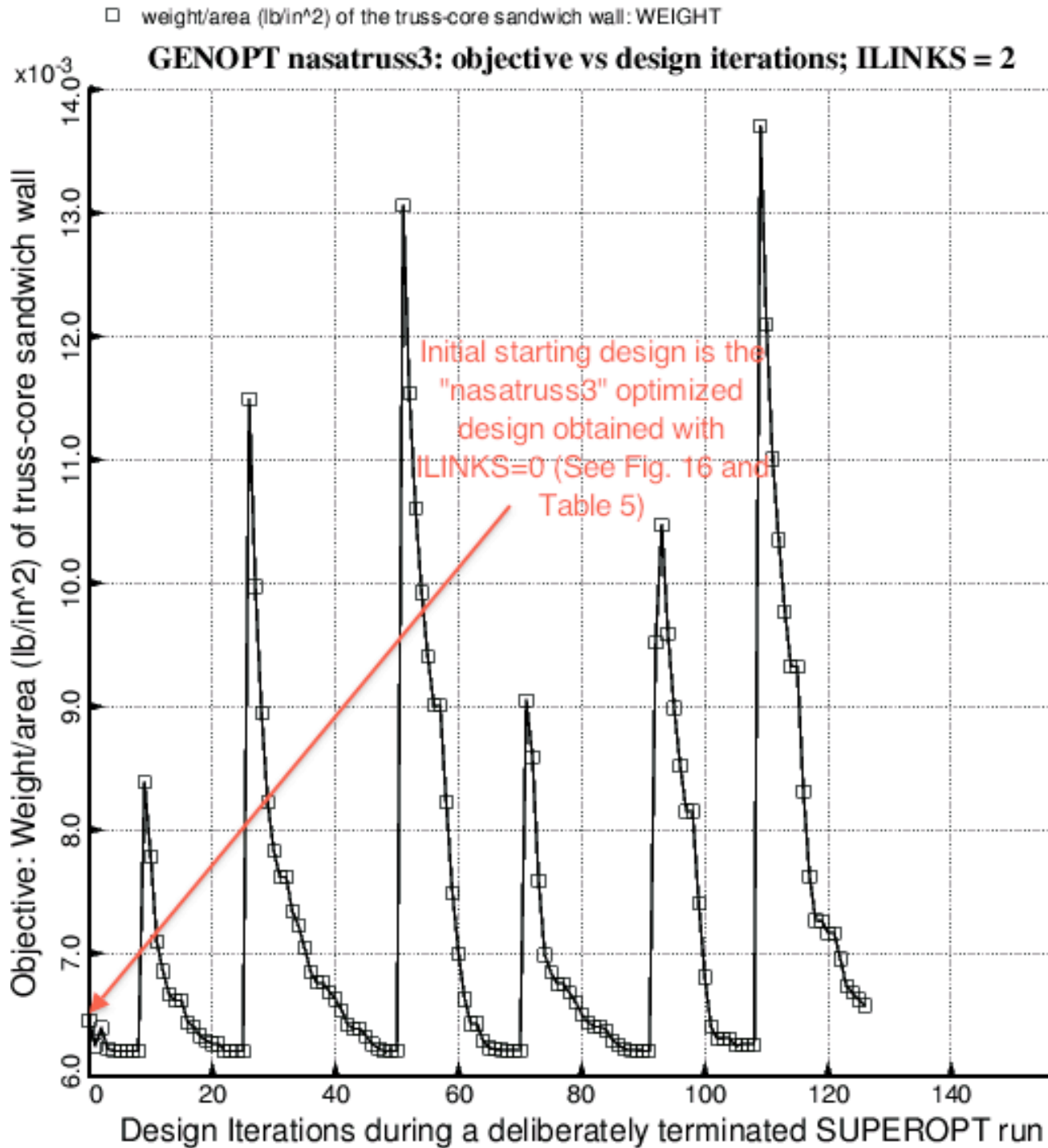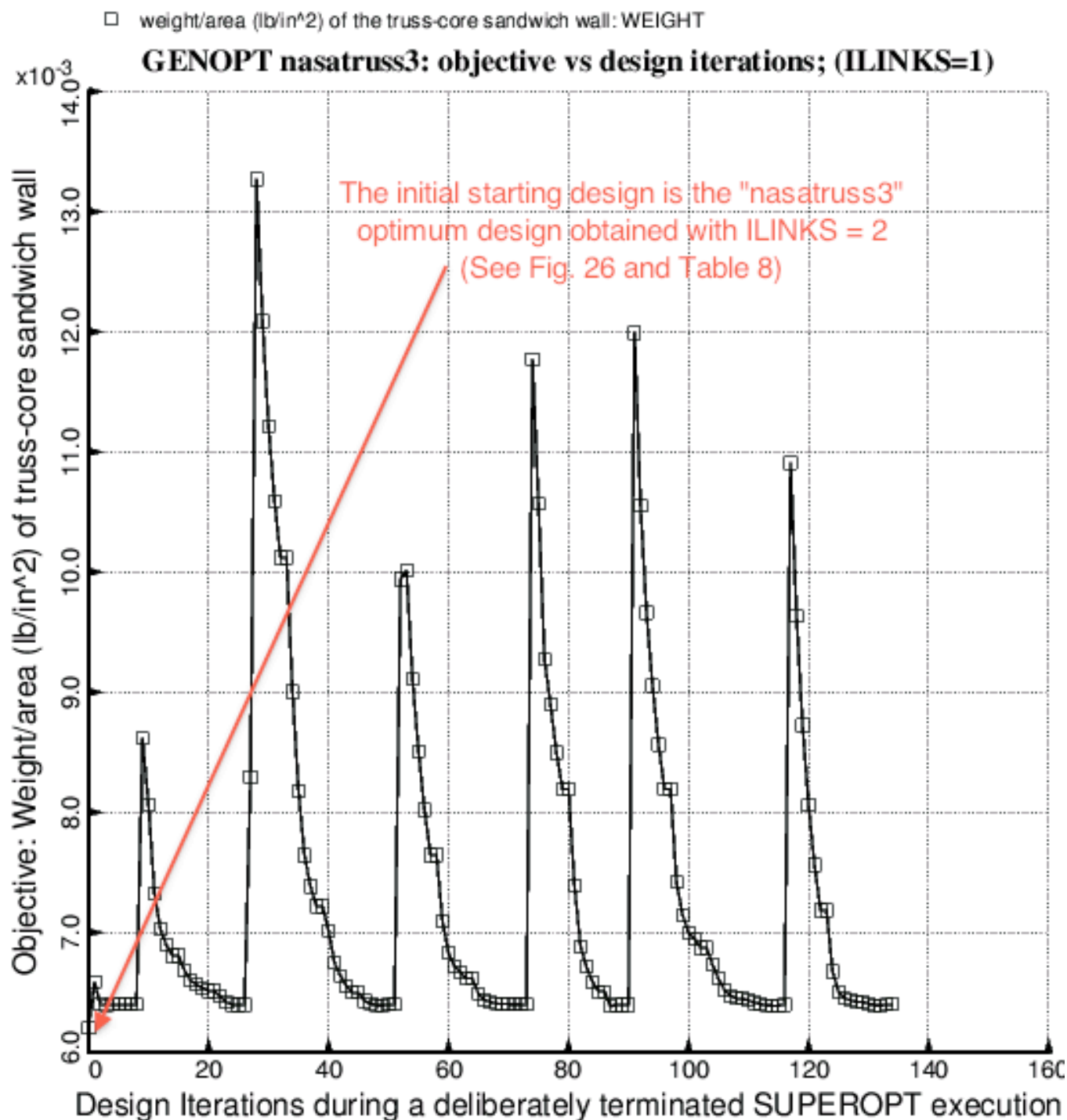
Fig. 26 Optimization of the specific case called "**nasatruss3**" with the use of ILINKS = 2. The SUPEROPT run was deliberately terminated in order to save calendar time. The optimized weight/area = 0.006204 lb/in^2, is only about 4 per cent lower than the optimized weight obtained with the more conservative ILINKS = 0 model.

American Institute of Aeronautics and Astronautics

Fig. 27 Optimization of the specific case called "**nasatruss3**" with the use of ILINKS = 1. The SUPEROPT run was deliberately terminated in order to save calendar time. The optimized weight/area = 0.006385 lb/in^2, is only 1.1 per cent lower than the optimized weight obtained with the more conservative ILINKS = 0 model.
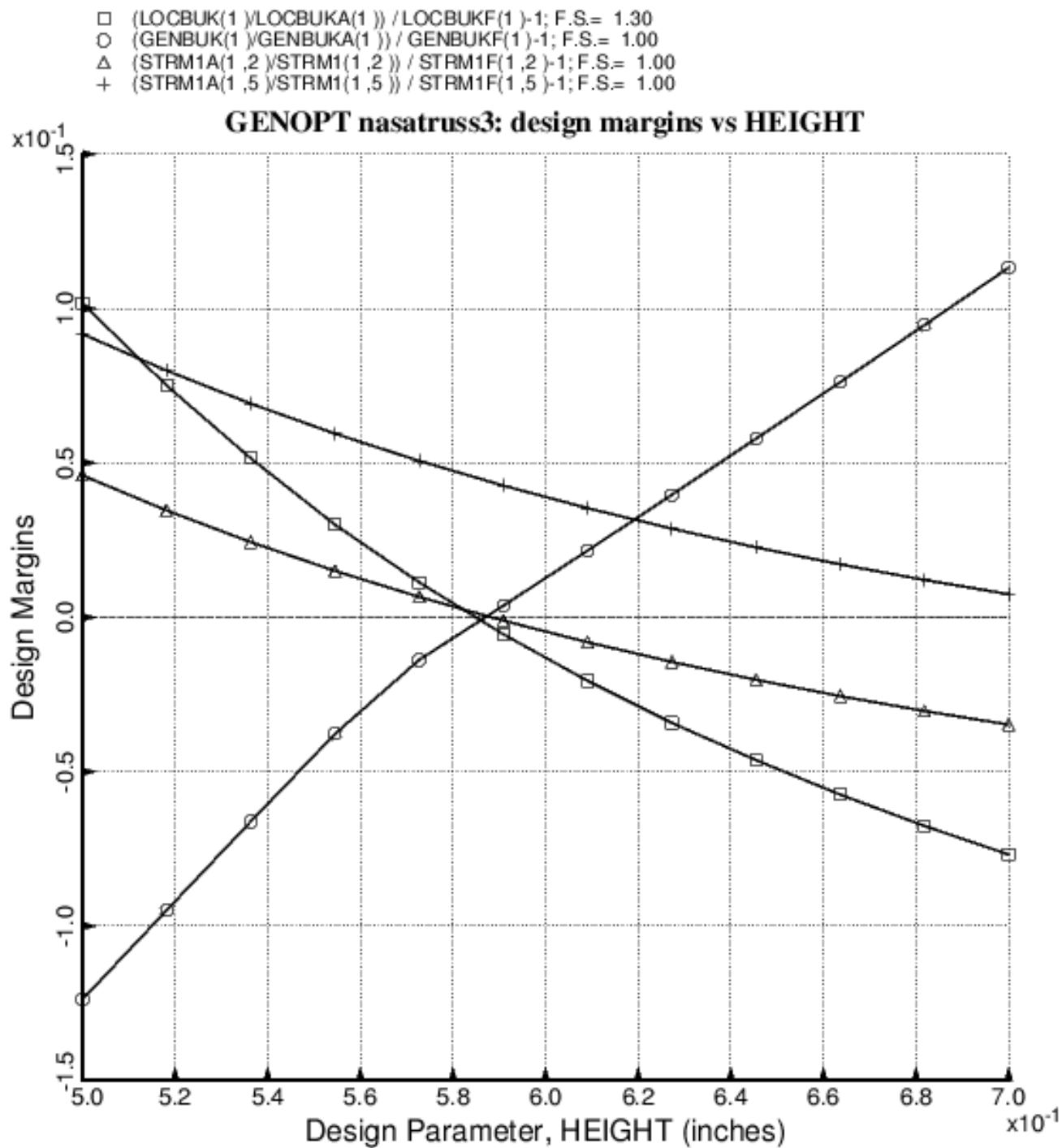
American Institute of Aeronautics and Astronautics

Fig. 28 Sensitivity of the optimized "**nasatruss3**" design with respect to the height, HEIGHT, of the truss-core sandwich wall. The optimum design, listed in PART 1 of Table 8, was obtained with the "noodle support" index, ILINKS = 0 (noodles do NOT support the little shell segments that enclose them). At the optimum design, HEIGHT = 0.58772 inches.

American Institute of Aeronautics and Astronautics